NUMERICAL MODELLING OF INELASTIC BEHAVIOR OF REINFORCED CONCRETE ELEMENTS CONSIDERING CRACKS AND BOND

by

A. MURAT TÜRK

B.S. in C.E., Bogaziçi University, 1991

Submitted to the Institute for Graduate Studies in Science and Engineering in partial fulfillment of the requirements for the degree of

Master of Science

in

Civil Engineering

Bogaziçi University

1993

ACKNOWLEDGEMENTS

I wish to express my appreciation and gratitude to Prof. Dr. Cengiz Karakoç for his helpful discussions, criticisms and suggestions.

I am grateful to Prof. Dr. Özal Yüzügüllü and Doç. Dr. Turan Özturan for their valuable remarks and recommendations.

I am grateful to Orhun Köksal for providing research materials and helpful suggestions.

I express my deep gratitude and special thanks to my family for their confidence, support and patience.

ABSTRACT

During the last 25 years, the use of the finite element method in structural engineering area has provided a powerful tool for engineers that has very wide applicability. This method also can be applicable to reinforced concrete members and structures. To be able to use finite element method for the concrete, the behavior of concrete must be modelled numerically, considering concrete cracking, tension stiffening, multiaxial material characteristics, interface behavior, bond properties and other effects. In this study, interface behavior of concrete is studied and a finite element program is developed. Aggregate interlock mechanism that is the concrete to concrete interface shear transfer mechanism, is studied using Gambarova-Karakoç formulations. A new concept, shear retention factor which is supposed to take account of the reduction of the shear stiffness of concrete elements by cracking, is analyzed and by making use of the Karakoç formulations, an original formulation is proposed. The results of the analysis performed in this study are compared with the experimental results obtained by various researchers.

ÖZET

Son 25 yılda büyük gelişme gösteren sonlu elemanlar metodu yapı mühendisliği alanında çok geniş uygulama sahası bulmuştur. Özellikle lineer olmayan bir malzeme olan betonarmede bu metod etkili biçimde kullanılabilmektedir. Fakat metodun hassas sonuçlar vermesi gerçek malzeme davranışının modellenmesi ile mümkün olabilir.

Bu çalışmada betonarme kirişler, dikdörtgen elemanlar kullanılarak ve beton ile çelik arasındaki aderans dikkate alınarak sonlu elemanlar metodu ile incelenmiştir. Bunun yanında çatlamış betonun kesme kuvveti aktarımı için Gambarova - Karakoç formülleri kullanılmıştır. Ayrıca kesme rijitliğini bir katsayı ile çarparak azaltma ilkesine dayanan kavram incelenmiş ve karşılaştırmalı analiz yapılmıştır.

TABLE OF CONTENTS

LIST OF FIGURES

LIST OF SYMBOLS

B	Crack stiffness matrix
$B_{nn}, B_{nt}, B_{tn}, B_{tt}$	Crack stiffness matrix coefficients
D	Elastic stiffness matrix
D_{cr}	Stiffness matrix of cracked concrete
D_{max}	Maximum aggregate size
E	Elastic tangent modulus
E_0	Initial elastic tangent modulus
E_{sec}	Secant elastic modulus at the maximum
E_1, E_2	Elastic tangent modulus in the principal stress directions
F	Flexibility matrix of uncracked concrete
f_c'	Maximum compressive strength of concrete
f_t'	Tensile strength of concrete
G	Elastic shear modulus
G^{cr}	Shear modulus of cracked concrete
K	Global stiffness matrix of a system
k_h, k_v	Bond slip moduli in horizontal and vertical directions
N	Normal force
p	Reinforcement ratio
r	Ratio of tangential displacement to normal displacement
S	Slip between concrete and reinforcement
s	Smeared crack spacing
t	Thickness of an element
T	Transformation matrix
V	Shear force
α	Principle stress ratio
β	Shear retention factor
δ_n, δ_t	Tangential and normal displacements
ε_{cu}	Maximum strain value of concrete
ε_0	Initial strain value

ε_{ic}	Equivalent uniaxial strain of the maximum stress value
$\varepsilon_{nn}, \varepsilon_{nt}, \varepsilon_{tn}, \varepsilon_{tt}$	Averaged strains of cracked concrete
ε_u	Maximum compressive strain for concrete
ε_{max}	Maximum strain of steel
γ^{cr}	Shear strain of the cracked concrete
σ_1, σ_2	Principal stresses
σ_{ic}	Maximum compressive stress
$\sigma_{nn}^c, \sigma_{nt}^c$	Normal and shear stresses across crack
υ	Poisson's ratio

I. INTRODUCTION

I.1. GENERAL

The developments in the computer technology during the last few decades have provided new design tools for the structural engineer. At the same time, the construction industry has undergone an evolution characterized by the construction of large scale and sophisticated structures. Special attention must be paid to structural safety because any structural failure or even local damage may give rise to many problems for community, both spatially and temporally. The use of conventional techniques proves to be no longer sufficient. To overcome such problems, much more sophisticated methods have been developed.

Recent research, so far, has focused on the development of realistic constitutive laws for concrete and also reinforced concrete. The primary purpose of these attempts was to implement the numerical models into finite element programs. One of the important objects of the research concerns the in-plane shear transfer, across the existing cracks in concrete. Interface shear transfer provides a vital contribution to the capacity of structures. There is still a lack of knowledge about the triaxial behavior with regard to shear forces in cracked concrete. The main reason is that shear loading leads to complicated physical mechanisms such as multiaxial stress conditions with inclined crack formation in the beams or walls, interlocking of cracks, rotation of cracks, dowel action and reduced bond resistance of reinforcing bars.

Interface shear transfer mechanisms can be divided into two parts as concrete-to-concrete (aggregate interlock) and concrete-to-reinforcement mechanisms (dowel action).

The basic aim of this study is to present a unified approach for the numerical modelling of inelastic behavior of concrete. This approach is incorporated in a finite element analysis and through a computer program in which special provision is made for interface shear transfer mechanisms especially aggregate interlock mechanism and bond interaction between concrete and steel.

I.2. LITERATURE REVIEW

The behavior of concrete depends on its compound, casting, loading type, loading history, time and cracking. The investigations carried out until now show that all of the proposed models have certain deficiencies. Most widely used failure envelope was developed by Kupfer and Gerstle (1) according to the results of series of tests conducted by themselves. Furthermore, an idealized model on equivalent strain concept is proposed by Darwin and Pecknold (2). The model based on several experimental results conducted by Karson and Jirsa. L. Cedolin and others (3) developed a triaxial failure envelope for concrete under short term and monotonic loading using their experimental results.

Some of the important interface shear models for concrete are proposed by Fardis and Büyüköztürk (4), Bazant and Gambarova (5), Gambarova and Karakoç (6), Walraven (7). These models were developed due to the test results of Paulay and Loeber (8), Daschner (9).

Using the results of the theoretical and experimental studies on concrete, many constitutive models have been developed. By making use of these models, some complex nonlinear finite element packages were written. Available nonlinear computer analysis methods for structural concrete forms may be distinguished from each other by structural discretization, adopted constitutive laws and the prestressing modelling.

Ngo and Scordelis (10) published the first paper on finite element analysis of reinforced concrete structures. Nonlinear analysis of reinforced concrete elements using finite element method have been published by Cervenka(11), Valliopan and Doolan (12), Yüzügüllü and Schnobrich (13), Cedolin and Dei Poli (14) and many others.

One of the advantages of using the finite element method for the investigation of the behavior of reinforced concrete elements is that it gives a wide range of information from a single computer analysis such as normal and shear stress distribution, tensile forces in reinforcing steel, forces in bond-link elements, principal stresses.

I.3. OBJECT AND SCOPE

Modelling of the interface shear transfer (aggregate interlock) mechanisms as means of transferring shear stresses along preformed cracks has great importance in determining the stiffness chacteristics of reinforced concrete.

Many mathematical models have been developed during last twenty years period to characterize the real stress-strain behavior and the failure criteria of the concrete under multiaxial stress states. All of these analytical models have certain inherent advantages and disadvantages which depend on their particular application.

Three primary factors, namely, aggregate interlock of cracked concrete, bond mechanism between steel and concrete, dowel action of reinforcing steel affect the nonlinear behavior of concrete subjected to shear.

In this study, inelastic behavior of concrete is studied using aggregate interlock mechanism and local bond mechanism while dowel action mechanism being disregarded. While these mechanisms are being studied, a comparative study is conducted using a finite element computer program. Furthermore, some important concepts such as shear retention factor, path dependency in cracked concrete are studied.

II. MATERIAL MODELS

II.1. NUMERICAL MODELLING OF CONCRETE

There are several models for defining the complicated stress-strain behavior of concrete under various stress states.

Experimental results show that concrete behaves in a highly nonlinear manner under uniaxial compression. Figure 2.1.1 shows a typical stress-strain relationship subjected to uniaxial compression. This stress-strain curve is linearly elastic up to 30 per cent of the maximum compressive strength. Above this point, the curve increases gradually up to approximately 70-90 per cent of the maximum compressive strength. Immediately after the peak value, this stress-strain curve descends. This part of the curve is termed softening. After the curve descends, crushing failure occurs at an ultimate strain ε_{cu}. A numerical expression has been developed by Hognestad (15) which treats ascending part as a parabola and the descending portion as a straight line. This expression can be given as:

for $0<\varepsilon<\varepsilon'_0$:

$$\frac{\sigma}{\sigma_{cu}} = 2\frac{\varepsilon}{\varepsilon'_0}\left(1-\frac{\varepsilon}{2\varepsilon'_0}\right) \qquad (2.1)$$

for $\varepsilon'_0<\varepsilon<\varepsilon'_0$

$$\frac{\sigma}{\sigma_{cu}} = 1-0.15\left(\frac{\varepsilon-\varepsilon'_0}{\varepsilon_{cu}-\varepsilon'_0}\right) \qquad (2.2)$$

Equivalent uniaxial strain concept for any stress has been developed so as to assess, at any stage, degradation of stiffness and strength of plain concrete and also to allow the actual biaxial stress-strain curves to be extracted from such uniaxial curves. This concept provides a method of separating the Poisson effect from the cumulative strain.

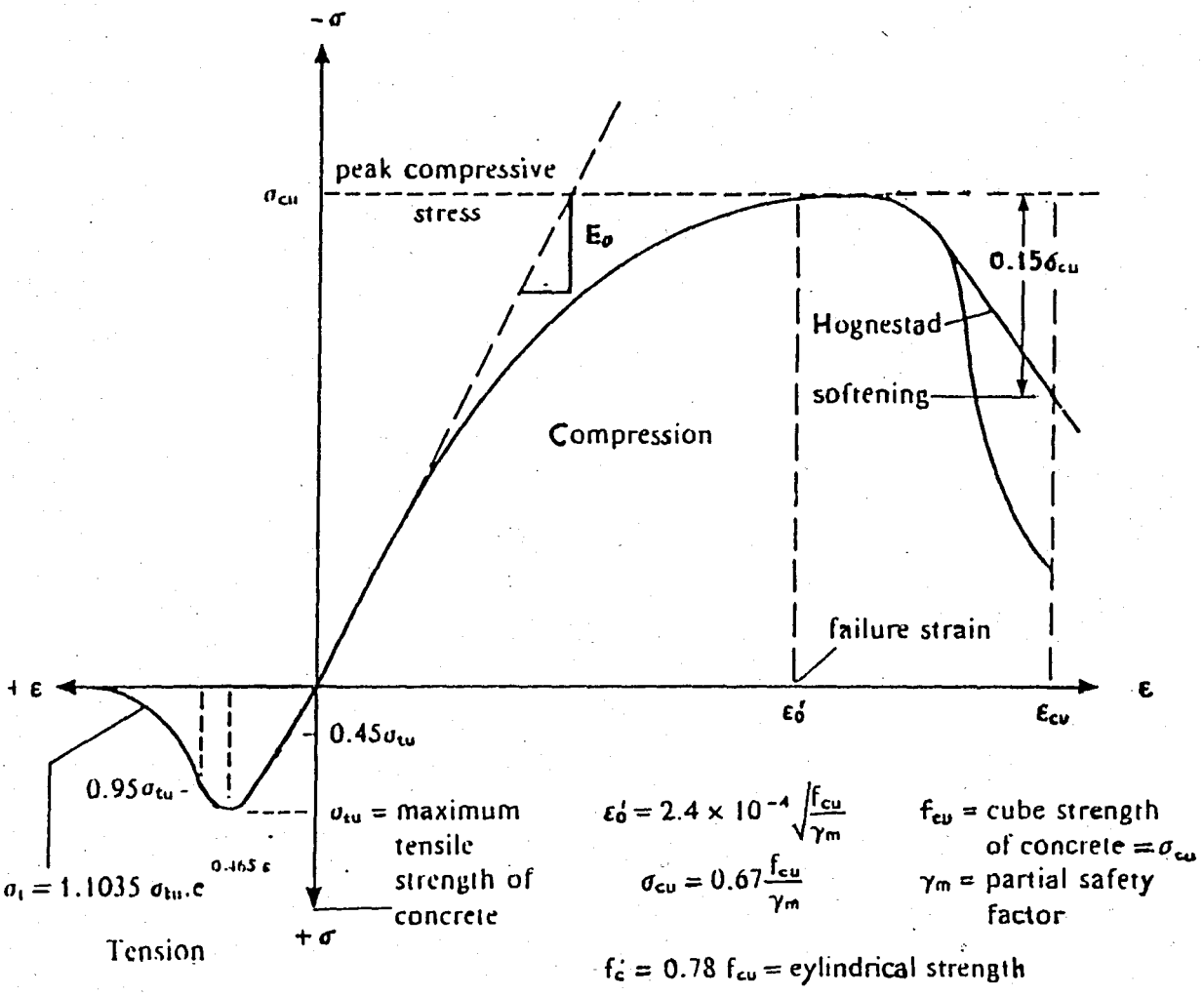

FIGURE 2.1.1 Typical uniaxial stress-strain curve for concrete(26)

Figure 2.1.2 shows the equivalent uniaxial strain ε_{ie} for considering the concrete as a linear material. The value of ε_{ie} for nonlinear part is written as

$$\varepsilon_{ie} = \sum d\varepsilon_{ie} = \sum \frac{\Delta\sigma_i}{E_{ti}} \qquad (2.3)$$

where $d\varepsilon_{ie}$ and $d\sigma_i$ are, respectively, differential changes in stress and equivalent uniaxial strain in the *i*th direction.Σ is for all load increments and E_{ti} is the tangent modulus in the *i*th direction.

The widely used function for the simulation of stress-strain curves for concrete under biaxial stress states is based on a direct extension of Saenz's equation in compression. Saenz(16) selected curves for compressive loading and has defined them numerically as:

$$\sigma_{cn} = \sigma_i = \frac{\varepsilon_{io} E_0}{1 + (\frac{E_0}{E_{sec}} - 2)\frac{\varepsilon_{io}}{\varepsilon_0} + (\frac{\varepsilon_{io}}{\varepsilon_0})^2} \qquad (2.4)$$

E_0 :Tangent modulus of elasticity at the beginning.
E_s : Secant modulus at the point of maximum compressive stress.
ε_{ie} : Equivalent uniaxial strain at the maximum stress.

Saenz's curve is particularly useful because the initial slope and the values of peak stress and corresponding strain can be entered as independent variables. (Figure 2.1.3)

Some investigators have attempted to evaluate concrete strength under biaxial compression, biaxial tension, biaxial tension-compression or under any combination of loads. The value of the maximum compressive stress σ_{cu} is a function of the principle stress ratio $\alpha=\sigma_1/\sigma_2$, the uniaxial compressive strength f_c' and the strain at the peak uniaxial stress ε_c. The value of the maximum stresses in the two principle directions σ_{1c} and σ_{2c} can be obtained from the biaxial strength envelope modified by Kupfer and Gerstle (1). (Figure 2.1.4)

For the biaxial compression region Kupfer and Gerstle found the closely estimated strength envelope for $\sigma_1 \geq \sigma_2$ such as :

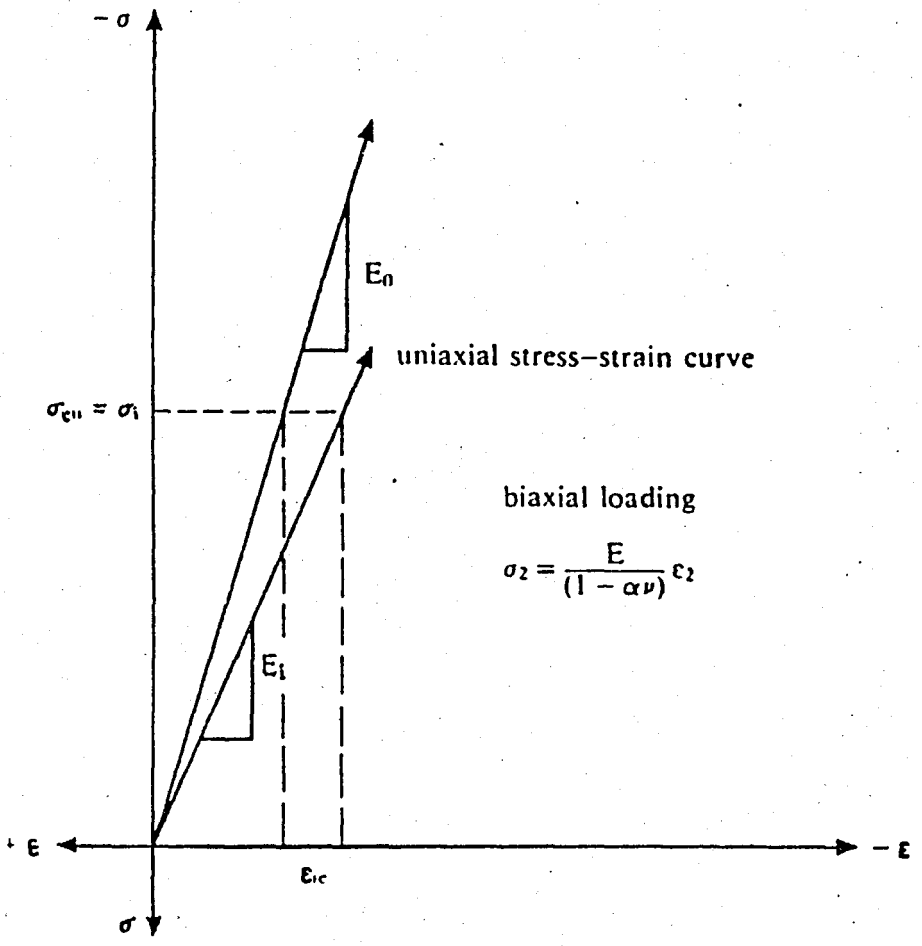

FIGURE 2.1.2 Stress-strain curve and equivalent strain(26)

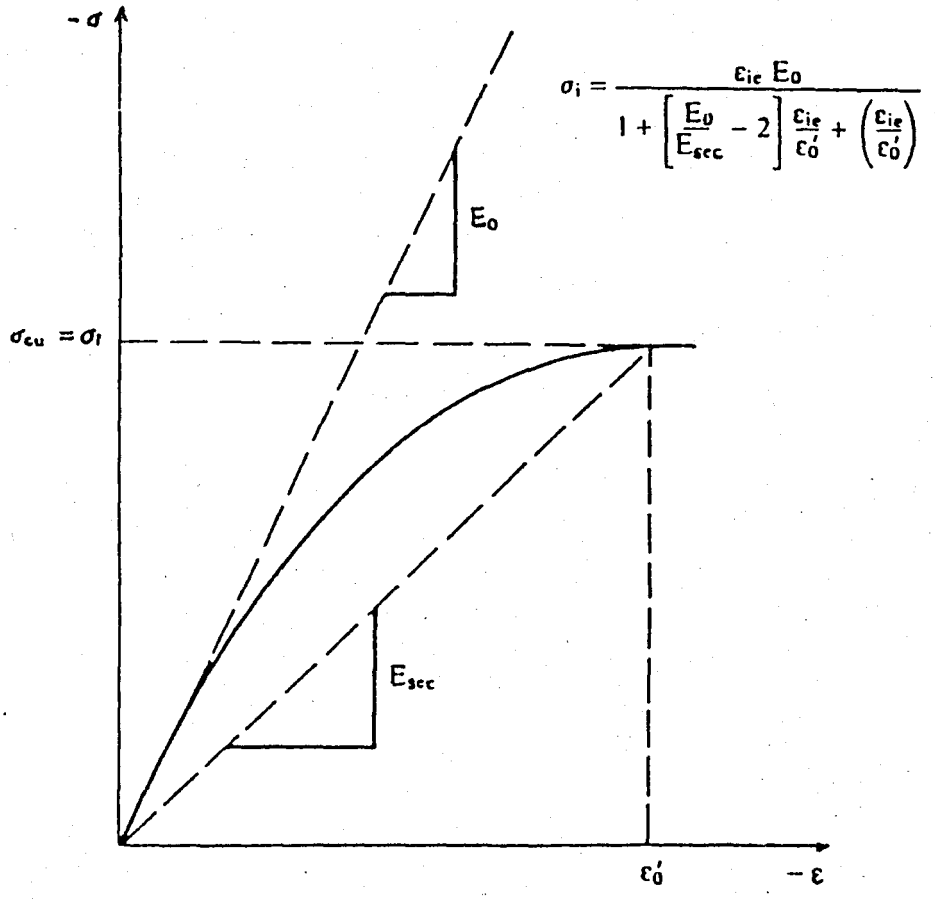

FIGURE 2.1.3 Equivalent uniaxial stress-strain curve(16)

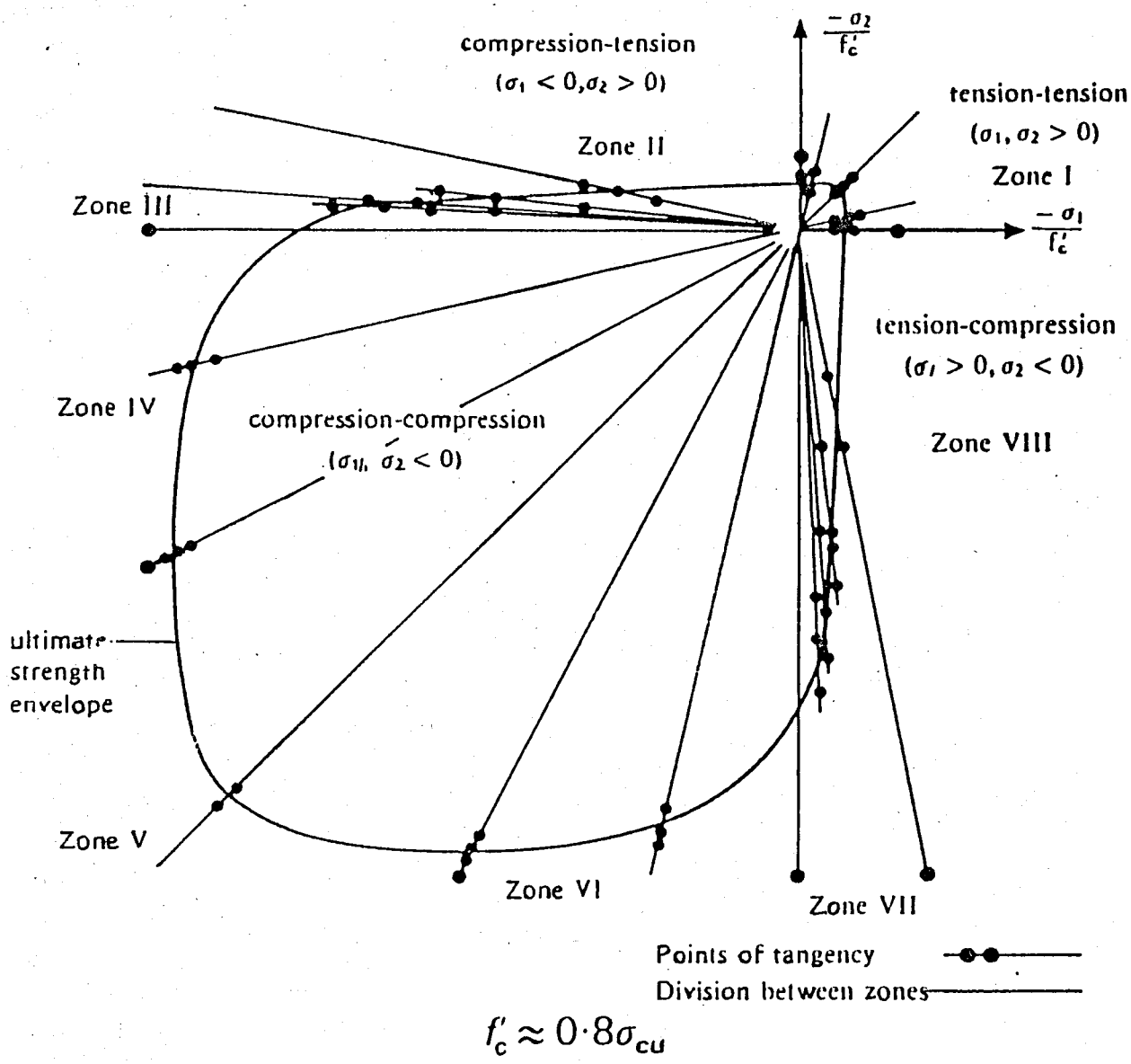

FIGURE 2.1.4 Simulation of a typical biaxial state curve (26)

$$\left(\frac{\sigma_1}{f_c'}+\frac{\sigma_2}{f_c'}\right)^2-\frac{\sigma_2}{f_c'}-3.65\frac{\sigma_1}{f_c'}=0 \qquad (2.5)$$

The boundaries for four regions can be obtained easily from the curve. Failure occurs when non-dimensionalised stress lies outside the failure envelope. Throughout the analysis, tensile stresses are considered to be positive and compressive stresses to be negative. For tensile failure, it is assumed that the load may be carried in the direction of the crack and may not be transferred across crack. For the case of compressive failure, it is assumed that no load may be carried in any direction.(Figure 2.1.5)

This model is suitable for the application to planar problems such as beams, deep beams, shear walls, panels and thin shells where the stresses are mainly biaxial.

II.2. NUMERICAL MODELLING OF STEEL

In this study, the steel reinforcement is taken as uniaxial bar elements. For steel elements, an ideal elastoplastic behavior is assumed.

The modulus of elasticity of steel and maximum strain are taken as $E=2.10^6$ kg/cm^2 and $\varepsilon_{max}=0.01$

After yield point, the behavior is modeled by using a line with a little inclination in order to prevent some problems which may arise during calculations.

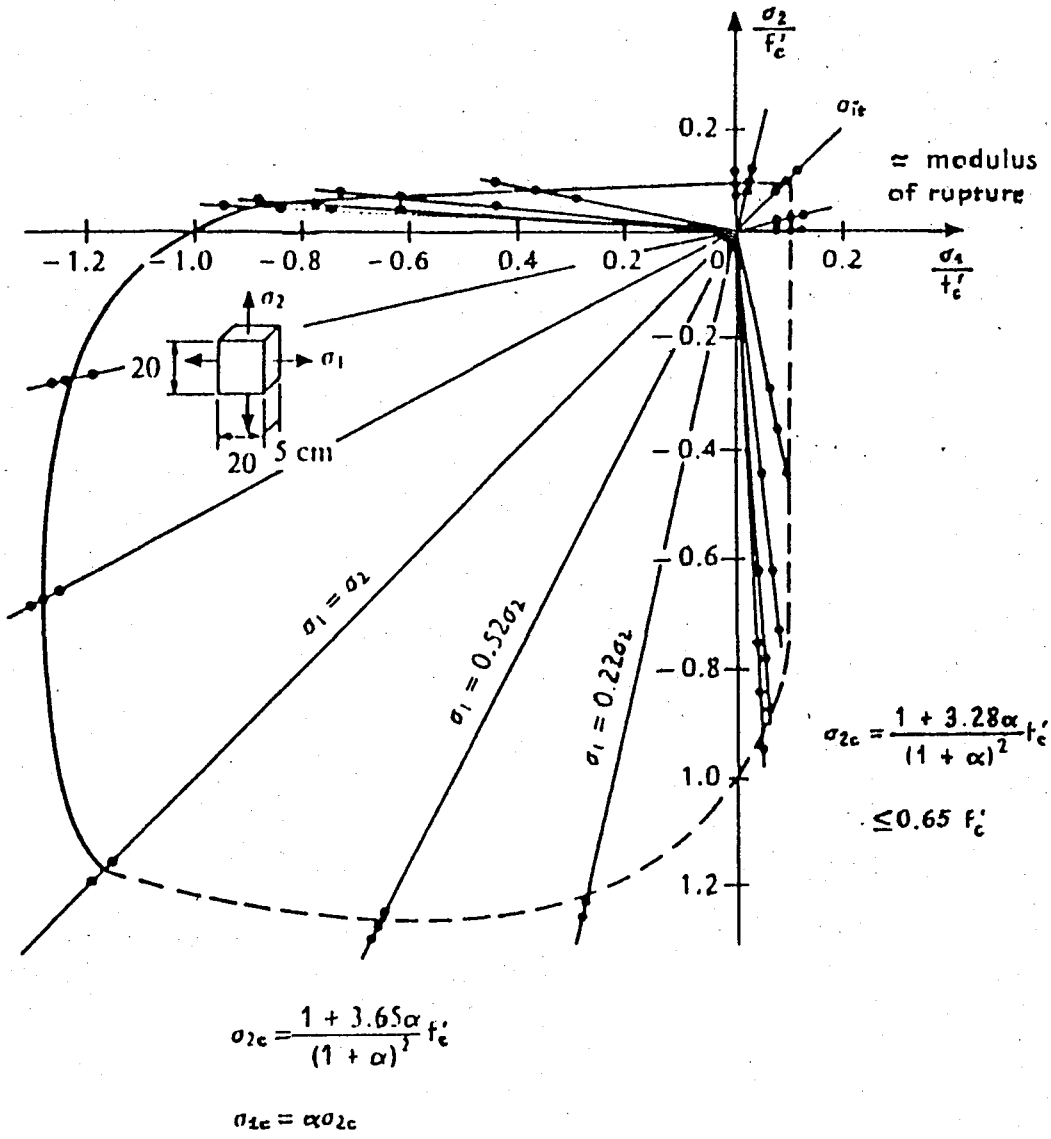

FIGURE 2.1.5 Biaxial stress state strength (1)

II.3. NUMERICAL MODELLING OF BOND

Much work has been carried out on the bond between concrete and steel. This phenomenon still remains as one of the most difficult topics in the study of concrete. It is found that the bond between concrete and steel is due to the combination of chemical adhesion, bearing action and friction. For a small slip, there will be an adhesion surface between the concrete and steel, resistance to slip is given by the shear strength of the fine particles of concrete filling the ribs of the steel. When some slip occurs, the adhesion will be zero. Bearing action is caused by the ribs of the bars or prestressing cables in contact with concrete. Slip takes place when the concrete surrounding the reinforcement bars or cables is crushed. At the failure of the structure, bond generally depends on the friction at the failure surface. This friction is destroyed when large slip occurs. The bond-slip relationship is vital for bonded members subjected to incremental and ultimate loads.

The main variables which might affect bond between concrete and steel are:

(a) concrete mix, temperature and humidity;
(b) the age of concrete;
(c) the tensile and compressive strength at test;
(d) bar type, embedment length and concrete cover;
(e) the loading speed and repeated loadings.

One of the important bond stress-slip models is Ngo-Scordelis model (10). This model is simple and easily applicable to the finite element programs. Figure 2.3.1 shows a two dimensional linkage element to be incorporated into a finite element analysis. The springs are denoted by k_h and k_v respectively. The value of k_h can be given by

$$k_h = \frac{d\sigma_b}{dS} \tag{2.6}$$

where k_h is the slope of the local bond slip curve, $d\sigma_b$ is the incremental bond stress and dS is the incremental local slip.

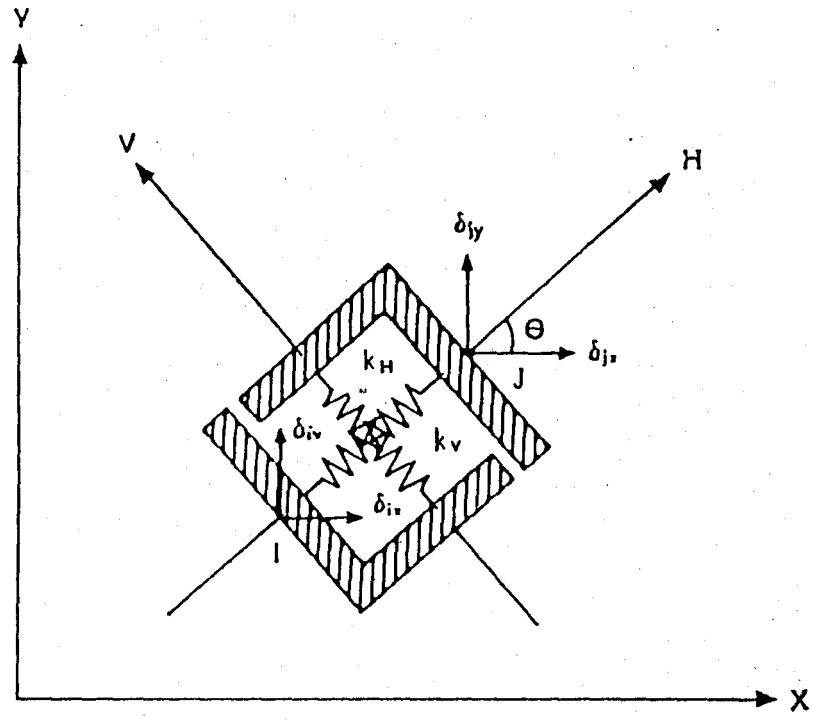

FIGURE 2.3.1 Two dimensional bond linkage element (10)

III. MODELLING OF CRACKED CONCRETE

III.1. GENERAL

Concrete behavior has some important nonlinearities regarding both uncracked concrete and cracked concrete. Concrete in tension is modelled as a linear elastic strain softening material. The principal stresses and their directions are computed initially in uncracked concrete. If the maximum principal stress for some reason exceeds the limit value, a crack is assumed to occur in a plane perpendicular to this stress. After this, the material behavior in this zone of concrete becomes orthotropic. The local material axes in the given zone coincide with the principal stress directions. If one of these directions is fixed, the procedure is known as 'fixed crack approach'. If the principal material axes is rotated to coincide with the principal stress and strain directions, the model is known as 'rotating crack model'. In this study, fixed crack approach is used.

It is the fact that cracked concrete transmits a significant amount of shear because of roughness along each two surfaces. The shear transfer mechanism is 'aggregate interlock' which depends on the aggregate size and grading and accompanied with crack dilatancy which is the coupling between the tangential displacement and normal displacement along crack surface.(Figure 3.1.1.a,b,c)

Some steps of formulation for cracking can be written as:

(a) The direct tensile stress cannot be supported in the direction normal to the cracks when crack occurs.

(b) The opposite faces of a crack opening in a normal direction will interlock when they are subjected to a parallel differential movement. As a result, restraint of movement and volume changes will cause forces which will only be transmitted across the crack. With large crack widths, these surfaces would completely separate and the aggregate interlock becomes no longer present. If the strain across the crack is positive, the crack is considered open and rigidity is kept zero.

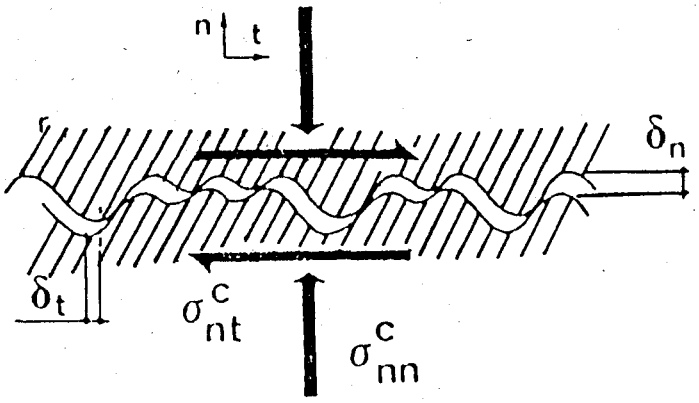

FIGURE 3.1.1.a Main variables of a crack (17)

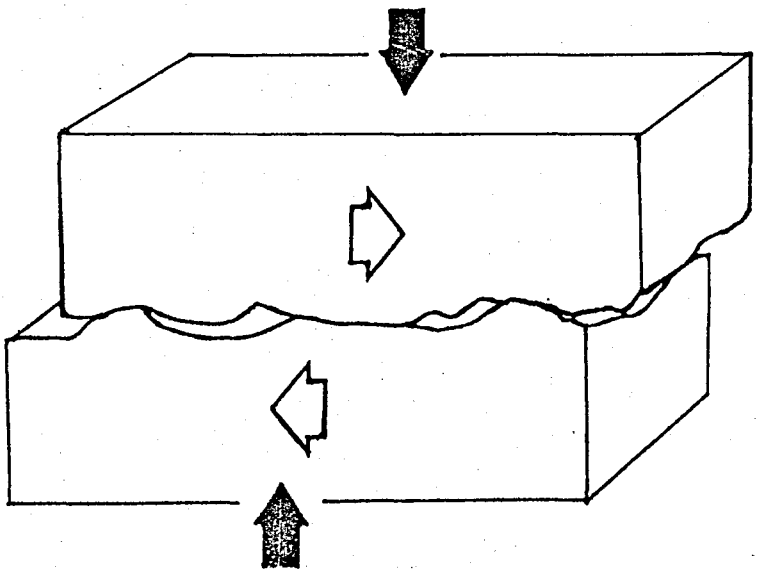

FIGURE 3.1.1.b Aggregate interlock through a crack (17)

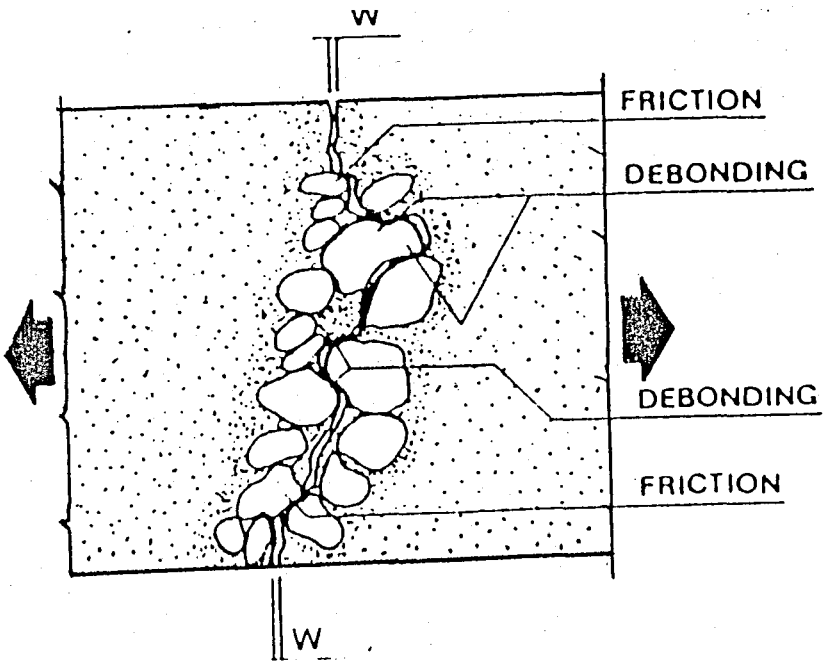

FIGURE 3.1.1.c Aggregate debonding mechanism (17)

(c) If interlocking occurs, the shear stress τ along the crack will not be zero and it is linearly related to the strain caused by the differential movement.

(d) During the unloading procedure of the structure the interlocking faces of crack and the surface deterioration will not interfere with the closing of crack. Crack closes if the normal across the crack is compressive.

The best way to handle these cracks is to adjust material laws in zones where they occur with their natural directions. The material matrice [D] can be modified easily to accomodate the initiation of the cracks in specific directions using direction cosines.

Aggregate interlock is generally associated with already formed, continuous, mostly linear through cracks, which are locally rough. A substantial interface shear transfer can only be attained if a restraining normal force is provided along the crack, either by the reinforcing steel or by the boundary restraints.

Aggregate interlock is essentially a material problem, since the behavior of a single crack is related to the characteristics of concrete such as maximum aggregate size, aggregate shape and concrete tensile strength. Cracking should be regular with mostly parallel and closely spaced cracks.

A shear slip of crack cannot occur at constant crack opening if the normal stress across the crack surface is constant. Slip is always accompanied by an increase of crack opening and if the opening is kept constant a large compressive stress is induced on the crack surface. The compressive stress must be balanced by the tensile forces in the reinforcement.

Shear displacements along diagonal tension cracks, are caused by shear forces in reinforced concrete beams. The resulting interface shear transfer by aggregate interlock is the main cause of the shear resistance in beams without web reinforcement.

Aggregate interlock problems involve so many different mechanical and geometrical parameters that analytical models must be based on sound experimental evidence. There are mainly four type of experiments for direct shear as it can be seen in Figure 3.1.2. a,b,c,d,e :

(a) at constant confinement stiffness (Figure 3.1.2.a);

(b) at variable confinement stiffness (Figure 3.1.2.b);

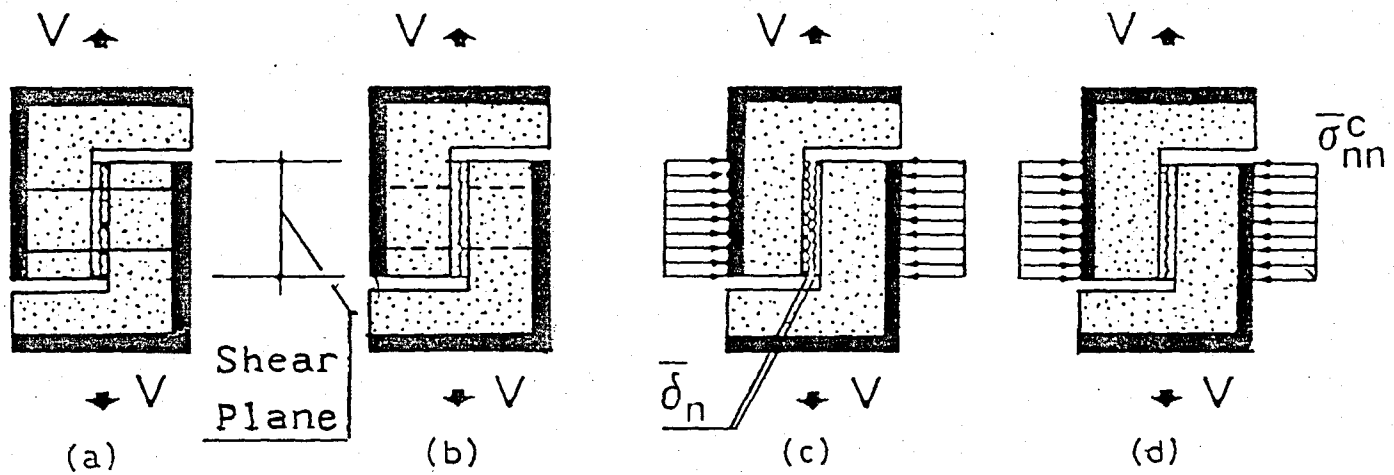

FIGURE 3.1.2 Different test types for aggregate interlock (17)

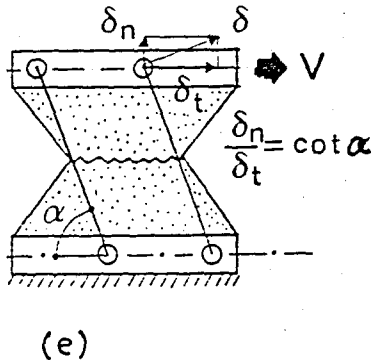

(a) At constant confinement stiffness

(b) At variable confinement stiffness

(c) At constant crack opening

(d) At constant confinement

(e) At constant crack dilatancy

(c) constant crack opening (Figure 3.1.2.c);
(d) at constant confinement (Figure 3.1.2.d);
(e) at constant crack dilatancy (Figure 3.1.2.e).

III.2. AGGREGATE INTERLOCK

The shear transfer mechanism based on aggregate interlock has been known for a long time in its behavioral aspects, owing to the many test results obtained during sixties, seventies and early eighties. According to the results of these investigations, this concept is related to either kinematic (crack opening, slip, crack dilatancy, initial crack width), mechanical (confinement across the crack plane, aggregate and matrix strengths) or morphological (overall and local roughnesses, maximum aggregate size and aggregate type i.e.rounded, crushed, light-weight).
The remarkable experimental efforts have made it possible to understand such basic concepts as crack dilatancy (i.e. the coupling between shear stress and crack opening, which also includes the coupling between normal stress and crack slip) and shear-confinement interaction. The derivation of constitutive equations for cracked concrete are improved using more realistic nonlinear finite element analysis. Actually, the formulation of suitable constitutive laws for cracked concrete became necessary after the concept of smearing the cracks over an entire element was shown to be highly suitable for finite element analysis.

Mainly there are three types of approaches which are available for finite element analysis in modellization of cracking :

(a) smeared cracking model;
(b) discrete cracking model;
(c) fracture mechanics model.

In the analysis, if overall load-deflection behavior is needed neglecting the realistic crack patterns and local stress concentrations, smeared crack approach is the best choice. In this study, smeared

crack concept is used. In general, this concept is mostly used in solving the problems of structural concrete members.

In the smeared crack concept, concrete is assumed to remain as a continuum. Gradual built-down or sudden drop of strength in the direction of tension is allowed in this concept. In this study, sudden drop of strength is assumed to use after tensile stress is exceeded.

Greatest attention has been given to the planar cracks subjected to monotonic loading, in order to formulate the incremental stiffness matrix of a crack. Generally this matrix is assumed as in the following form :

$$\begin{aligned} d\sigma^c_{nn} &= B_{nn}d\delta_n + B_{nt}d\delta_t \\ d\sigma^c_{nt} &= B_{tn}d\delta_n + B_{tt}d\delta_t \end{aligned} \qquad (3.1)$$

where B_{nn}, B_{nt}, B_{tn}, B_{tt} are crack stiffnes coefficients, which depends on δ_n ,δ_t, $\sigma_{nn}{}^c$, $\sigma_{nt}{}^c$ and other possible state parameters (Figure 3.2.1)

The crack stiffness matrix is neither symmetric nor positive definite. Thus, crack response tends to be unstable but the response is usually stabilized by the restraint provided by the reinforcement.

Because of relative scarcity of test data, much simpler and less general formulations have been adopted. Generally the functional relationships can be expressed in a direct stress-displacement form such as :

$$\sigma^c_{nn} = F_1(\delta_n,\delta_t) \quad , \quad \sigma^c_{nt} = F_2(\delta_n,\delta_t) \qquad (3.2)$$

$$\sigma^c_{nt} = F_3(\sigma^c_{nn},\delta_t) \quad , \quad \delta_n = F_4(\sigma^c_{nn},\delta_t) \qquad (3.3)$$

$$\sigma^c_{nn} = F_5(\sigma^c_{nt},\delta_n) \quad , \quad \delta_t = F_6(\sigma^c_{nt},\delta_n) \qquad (3.4)$$

The main weakness of a total deformation concept is the assumption of path-independency for the response. However, in inelastic behavior, path dependency is expected and should be accounted.

In finite element analysis, smeared crack concept can be applied to introduce the properties of crack, including the aggregate

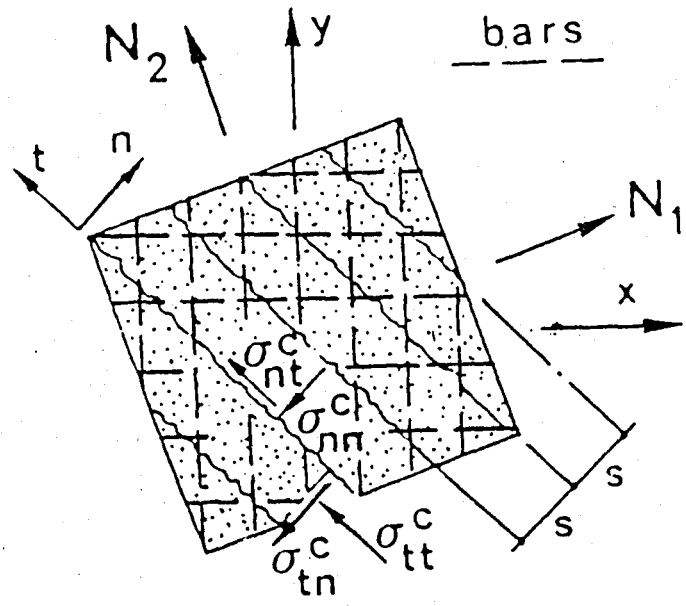

FIGURE 3.2.1 Cracked reinforced concrete (17)

interlock. Actual interface displacements are replaced with averaged strains. Thus, the constitutive laws of the cracks become the laws of a new material thus the calculation of the incremental stiffness matrix D_{cr} becomes possible. The smeared crack concept can be used in regularly cracked elements with average crack spacing 's' .

Some of the important models which can be used to develop the constitutive laws for cracked concrete, can be summarized as :

(i) Empirical models :

a) rough crack model (Bazant and Gambarova);

b) rough crack model (Gambarova and Karakoc);

c) simplified aggregate interlock relation (Walraven).

(ii) Physical crack models :

a) two-phase model (Walraven, Reinhardt, Pruijssers, Frenay);

b) contact density model (Li and Maekawa).

In this study, the "rough crack model" is used. The rough crack model is based on some general properties that are to be expected for rough and cracked surfaces. These properties can be deduced by considering a few simple micromechanical models. The interface stresses are assumed to be mostly dependent on the displacement ratio $r=\delta_t/\delta_n$ (wedge effect) for small crack widths. The general roughness is disregarded and only the local roughness is introduced and as a result of this, the number of contact points along the crack interface may be assumed as infinite and the resulting stress-displacement relations can be considered continuous and smooth.(Figure 3.2.2.a,b,c)

Basic properties of a planar but locally rough cracks are :

(a) $\delta_n<0$ that is the state of being negative crack opening and it is not possible and the normal stress σ_{nn}^c must be compressive.

(b) Full continuity in the material exists for $\delta_n=0$ (no crack).

(c) The confinement stress can not exceed the compressive strength f_c'.

(d) For $\delta_t=0$ and $\delta_n>0$, confinement stress σ_{nn}^c must be zero. Thus the crack surfaces cannot be in contact.

(e) The number of the contact points at the crack faces decreases while δ_n is increasing and δ_t is constant or increasing.

(f) The number of contact points at the crack interface increases at increasing values of δ_t while δ_n is constant or greater than zero.

(g) Crack roughness has trapezoidal asperities. As stated before, the

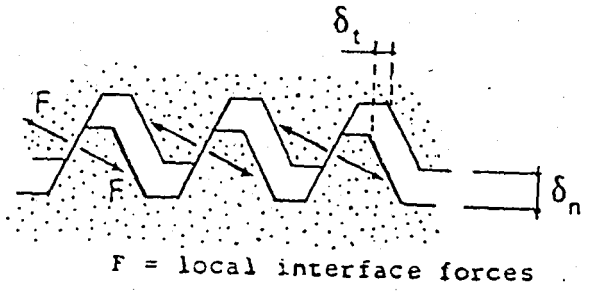

FIGURE 3.2.2.a Wedge effect (17)

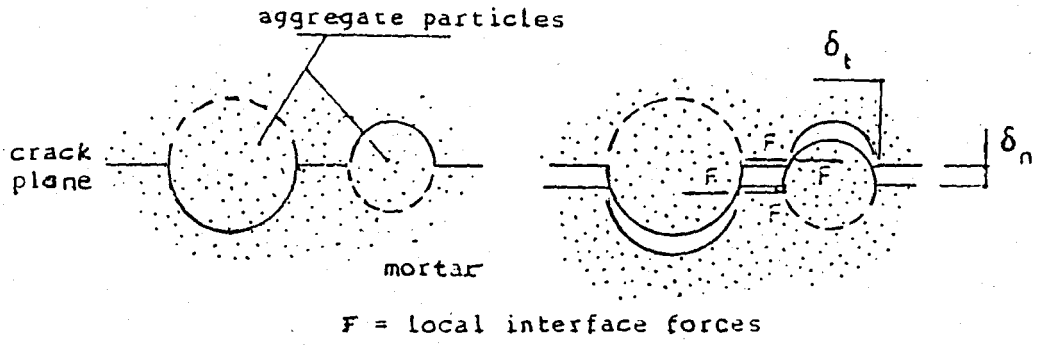

FIGURE 3.2.2.b Aggregate debonding (17)

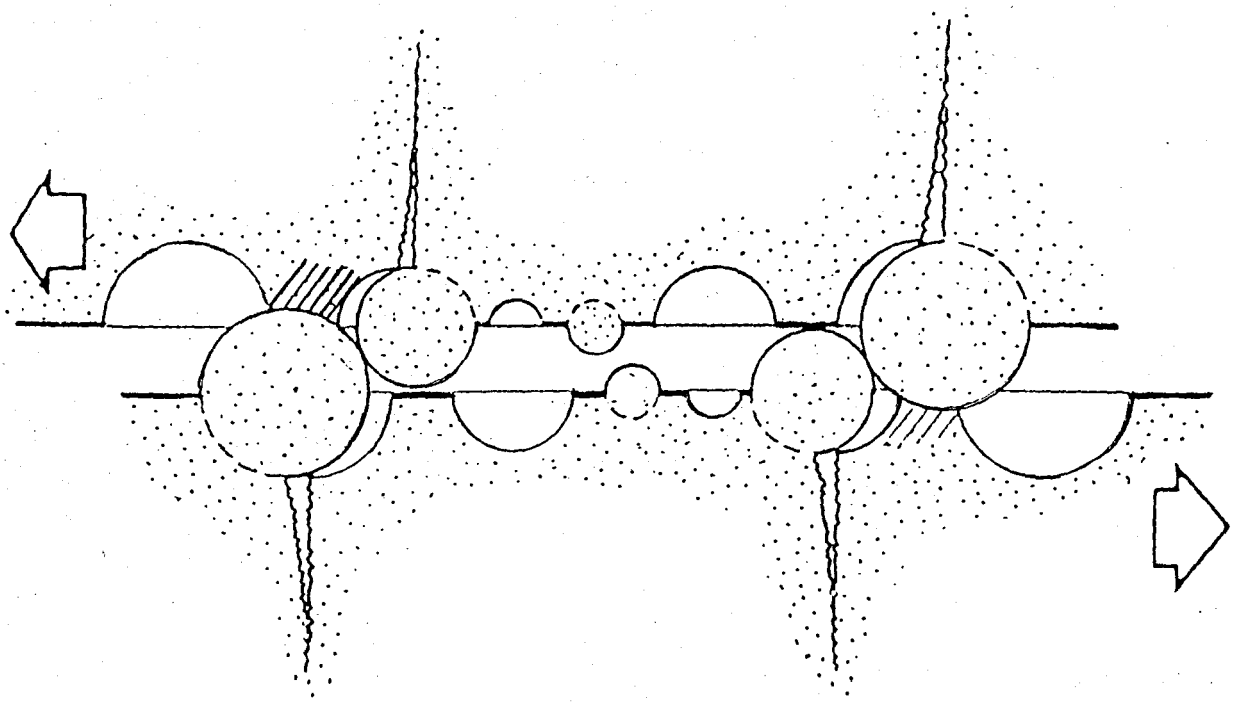

FIGURE 3.2.2.c Microcracking and crushing of concrete (17)

interface stresses are mostly related to the displacement ratio $r=\delta_t/\delta_n$. Spherical asperities cause to develop a strong wedge effect. Shear transfer requires very limited or even zero confinement at small crack openings. Crack opening prevails over crack slip when crack faces are moving apart

(h) The contact between surfaces is lost for large values of the normal crack displacement when $\delta_n > D_{max}$ where D_{max} is the maximum aggregate size in the concrete.

(i) The interface stresses are formulated as shown (17) :

$$\sigma_{nt}^c = N_1(\delta_n/d_a).N_2(r) \quad , \quad \sigma_{nn}^c = F_3(\delta_n).F_4(r\sigma_{nt}^c) \tag{3.5}$$

By optimizing the fittings of Paulay and Loeber's test data (8) with constant crack opening and infinite restraint stiffness (Figure 3.2.3.a.b.c.) and Daschner and Kupfer's test results (18) with constant confinement stress and zero restraint stiffness and by assuming for the aggregate grading by Fuller's curve, the following relations were developed :

$$\sigma_{nt}^c = \tau_0\left(1-\sqrt{\frac{2\delta_n}{D_{max}}}\right)r\frac{a_1+a_2|r|^3}{1+a_2r^4} \tag{3.6}$$

$$\sigma_{nn}^c = -0.62\frac{r}{(1+r^2)^{1/4}}\sigma_{nt} \tag{3.7}$$

where,

$$\tau_0 = 0.25f_c', r = \delta_t/\delta_n, a_1 = 2.45/\tau_0, a_2 = 2.44\left(1-\frac{4}{\tau_0}\right) \tag{3.8}$$

D_{max} is the maximum aggregate size and f_c' is the concrete cylinder strength.

The influence of the shear slip δ_t is so dominant that the contribution of the crack opening can be neglected. A new equation has derived by Karakoc(19) using this logic (Figure 3.2.4.a,b) :

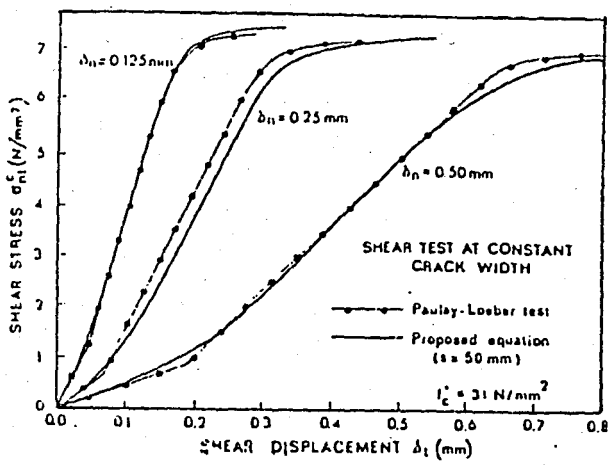

FIGURE 3.2.3.a Comparison with Paulay and Loeber's test results

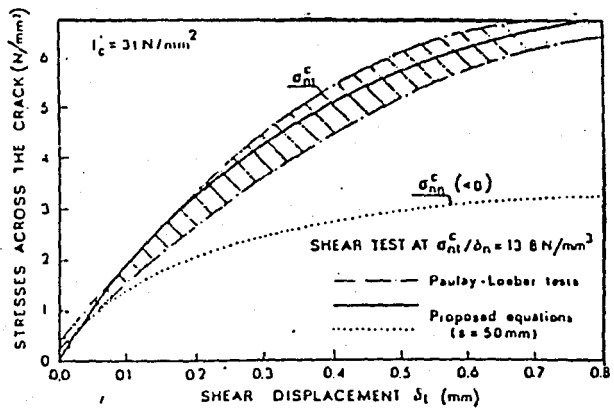

FIGURE 3.2.3.b Comparison with Paulay and Loeber's test results

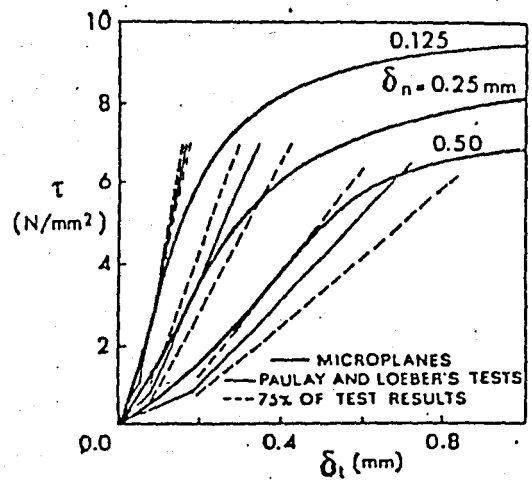

FIGURE 3.2.3.c Comparison with Paulay and Loeber's test results

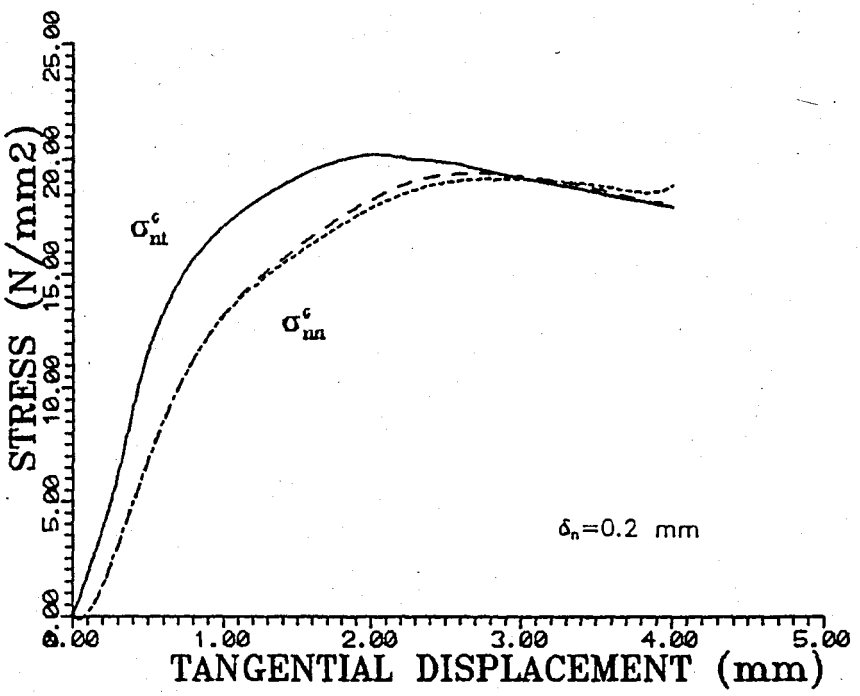

FIGURE 3.2.4.a Comparison of the Daschner and Kupfer's test results with equation 3.9 (19)

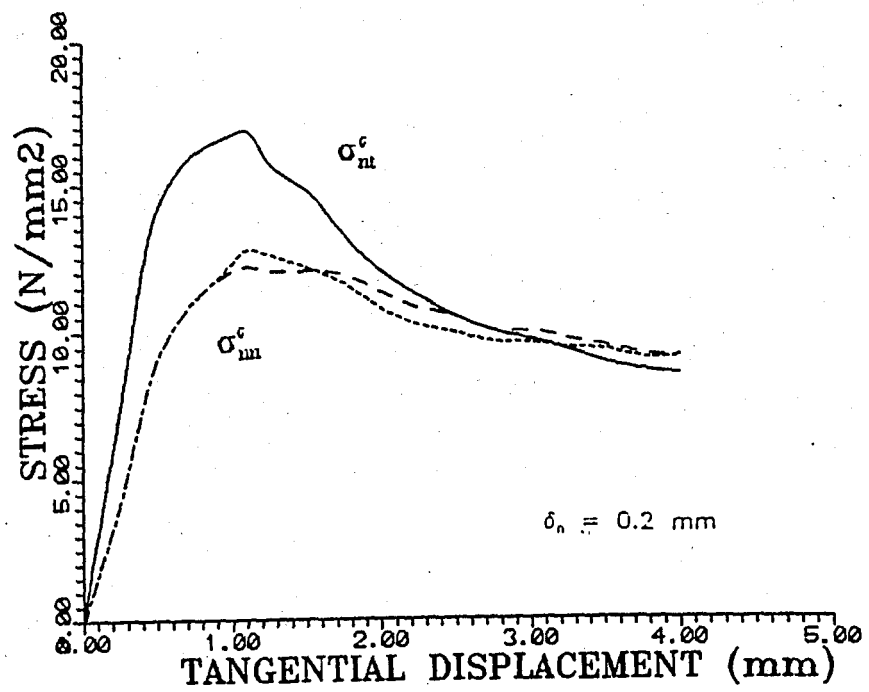

FIGURE 3.2.4.b Comparison of the Daschner and Kupfer's test results with equation 3.9 (19)

$$\sigma_{nn}^{c} = 0.55\sqrt{\delta_t}\,\sigma_{nt}^{c} \tag{3.9}$$

For the case of constant crack opening Karakoc gives the following formulations (20):

$$\sigma_{nt}^{c} = 1.82 f_{cu}^{0.80} \frac{\delta_t^{1.75}}{\delta_t^2 + 0.4\delta_t + 1.75\delta_n}\left(1 - \sqrt{\frac{4\delta_n}{D_a}}\right) \tag{3.10}$$

$$\sigma_{nn}^{c} = 0.75\delta_t^{1/4}\sigma_{nt}^{c} \tag{3.11}$$

substituting the equation (3.10) into equation (3.11) :

$$\sigma_{nn}^{c} = 1.37 f_{cu}^{0.80} \frac{\delta_t^2}{\delta_t^2 + 0.4\delta_t + 1.7\delta_n}\left(1 - \sqrt{\frac{4\delta_n}{D_a}}\right) \tag{3.12}$$

Karakoç has already shown that, for the constant crack opening case, the equations (3.10) and (3.11) can be effectively used to predict the coefficient of friction, if a frictional nature is assumed in aggregate interlock mechanism (20). The figures, from Figure 3.2.5 to Figure 3.2.10 show the comparison between equation (3.10) and test results of Daschner and Kupfer. In these tests for constant crack width case, crack width δ_n ranges from 0.05 mm. to 0.4 mm. Cube strengths of concrete specimens varies between 25 to 55 MPa. Maximum aggregate size varies between 8 mm. to 16 mm.

The formulations 3.10, 3.11, 3.12 for constant crack width case have been shown to be quite satisfactory when compared with Daschner and Kupfer's test results which have been obtained by highly developed and sophisticated experimental setup allowing the resultant of the applied shear and normal forces to pass through the centroid of the cracked concrete specimen. Therefore, no secondary stresses come into picture.

The cracked stiffness matrix can be obtained using the differentiated formulas of Delft University Report.(21)

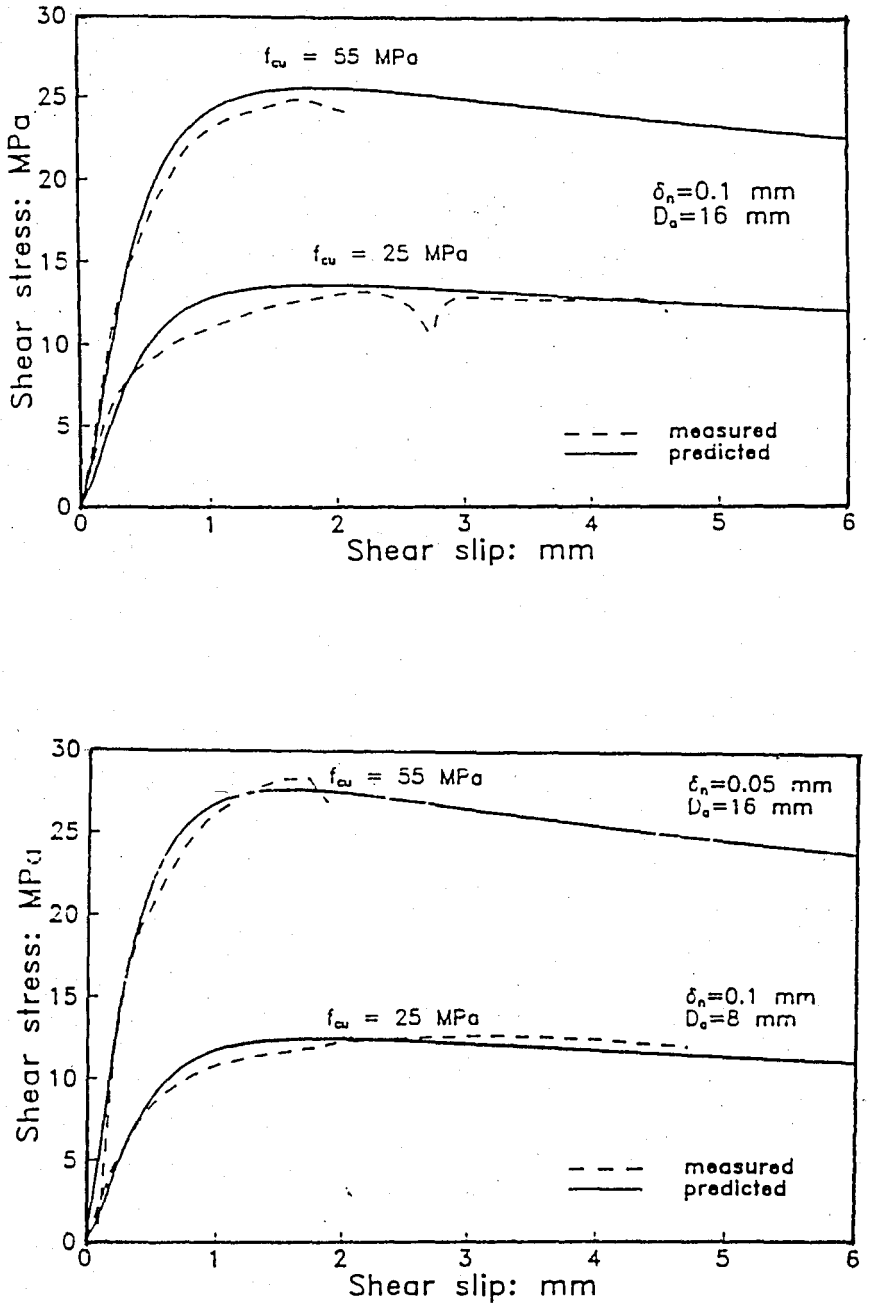

FIGURE 3.2.5 **Test results of Daschner and Kupfer (18) and predictions of the equation 3.10 (20)**

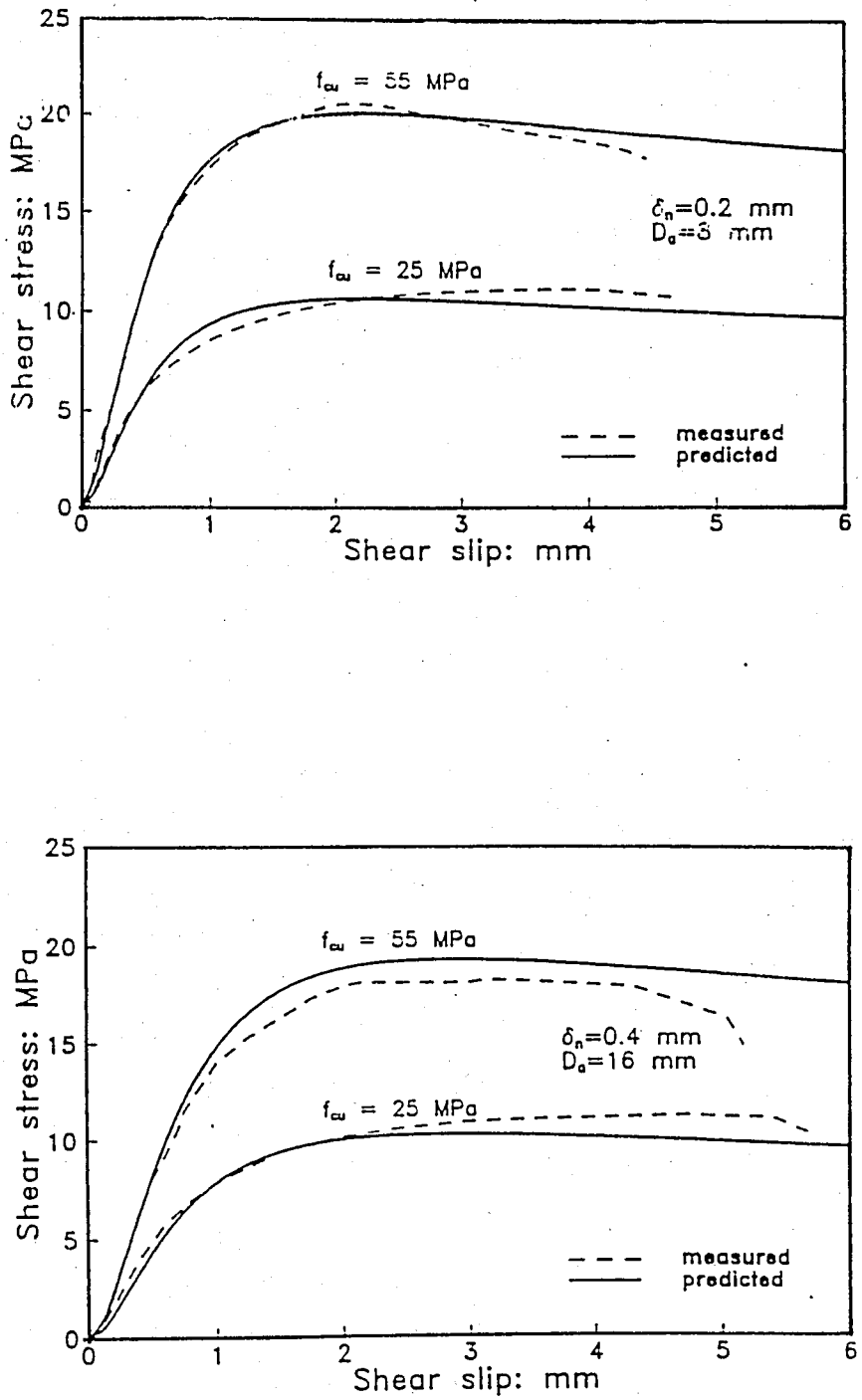

FIGURE 3.2.6 **Test results of Daschner and Kupfer (18) and predictions of the equation 3.10 (20)**

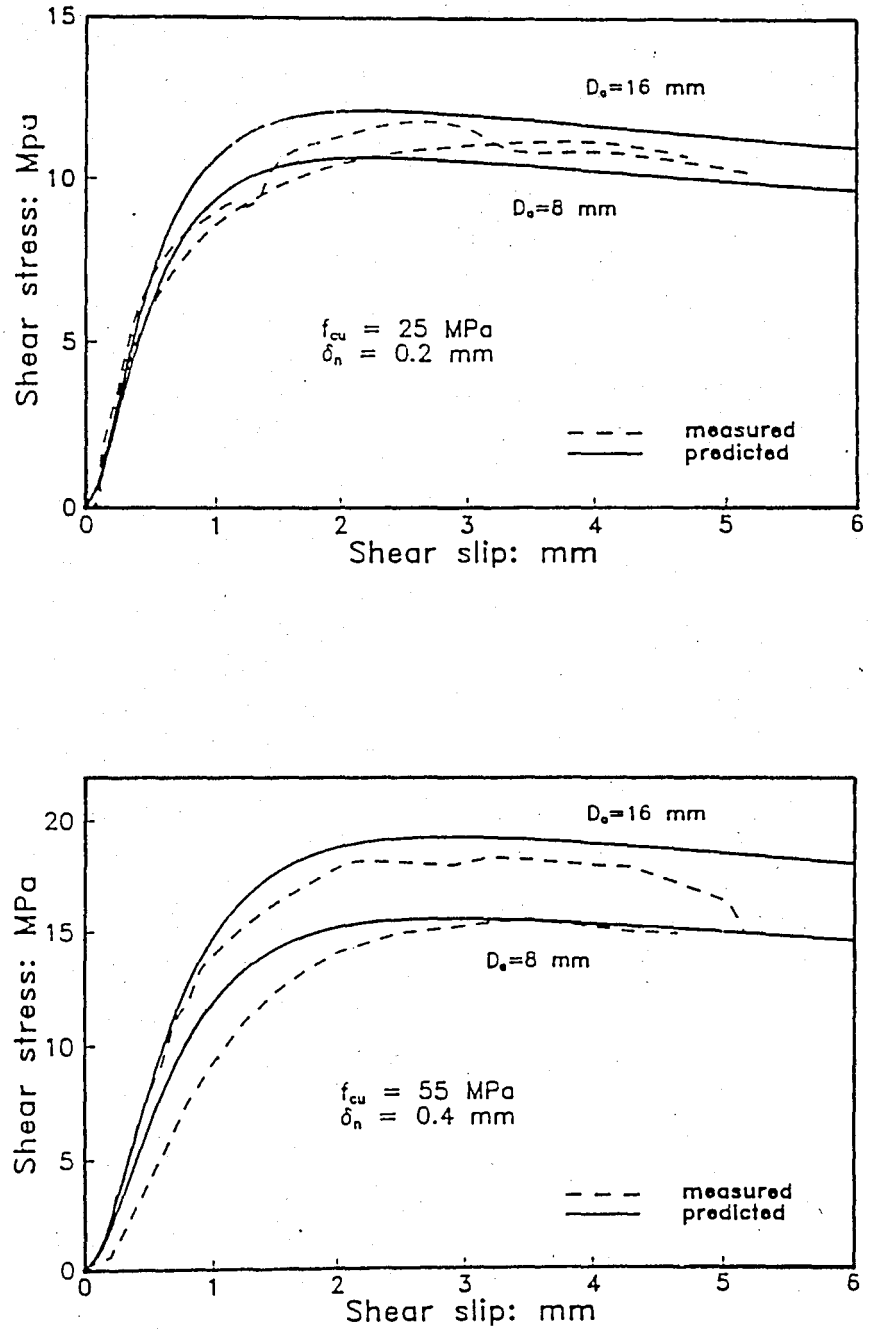

FIGURE 3.2.7 **Test results of Daschner and Kupfer (18) and predictions of the equation 3.10 (20)**

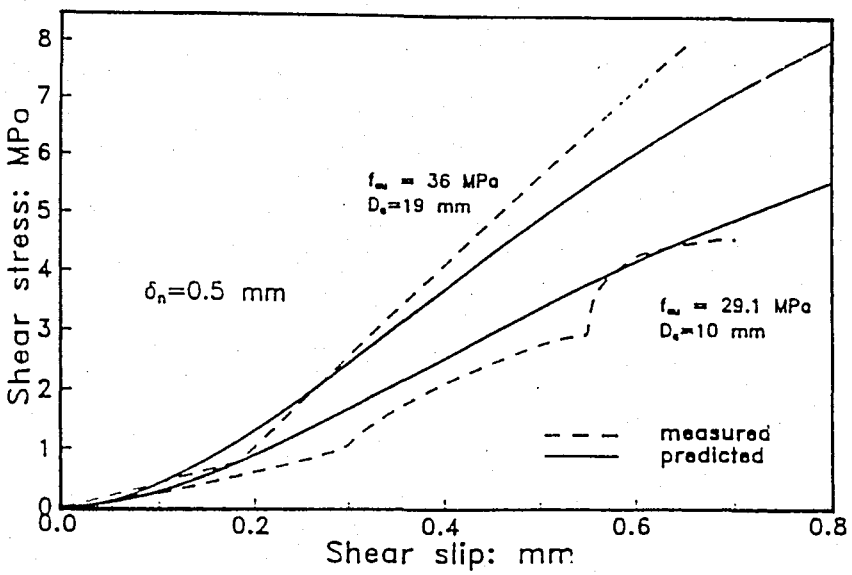

FIGURE 3.2.8 **Test results of Paulay and Loeber (18) Millard and Johnson (23) and the predictions of the equation 3.10 (20)**

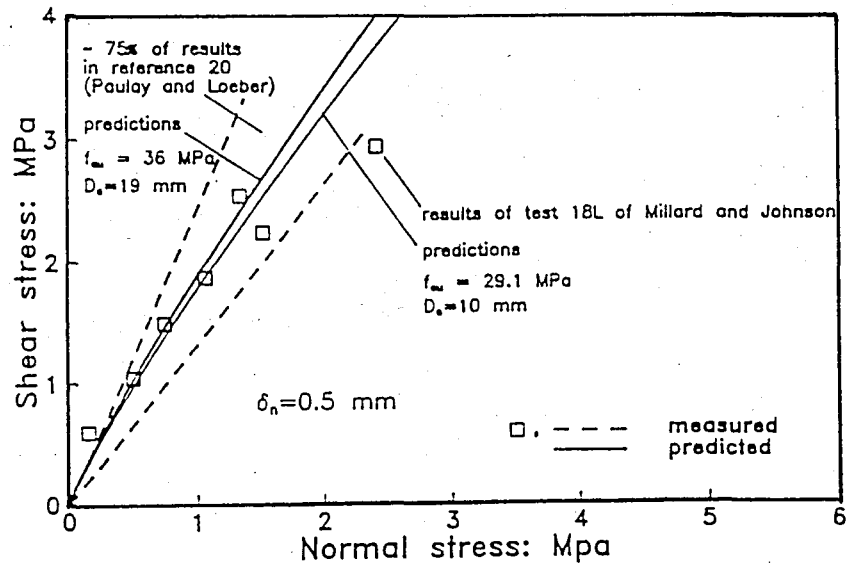

FIGURE 3.2.9 **Test results of Paulay and Loeber (18) Millard and Johnson (23) and the predictions of the equation 3.11 (20)**

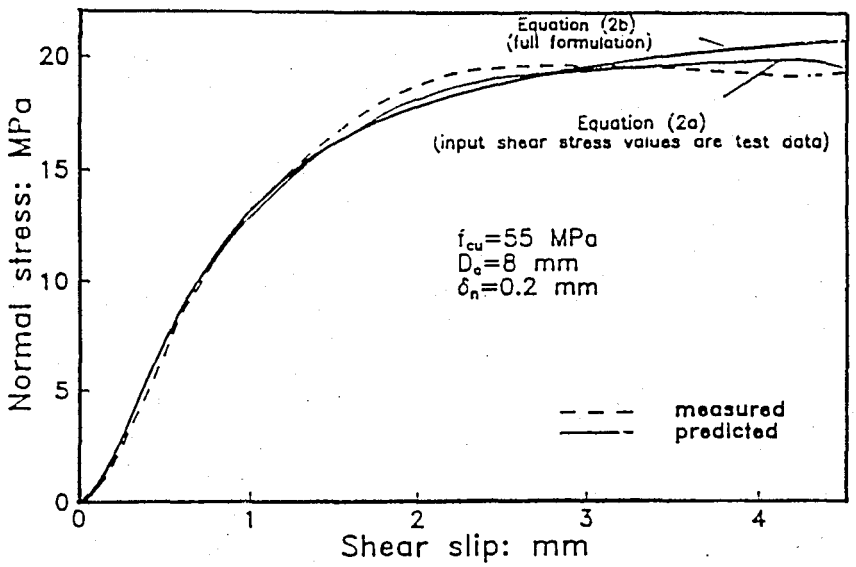

FIGURE 3.2.10 **Test results of Daschner and Kupfer (18) and the predictions of the equation 3.11, 3.12 (20)**

III.3. FINITE ELEMENT MODELLING

The cracked stiffness matrix [B] can be obtained using the equations (3.1) :

$$B_{nn} = \frac{\partial \sigma^c_{nn}}{\partial \delta_n} \tag{3.13}$$

$$B_{nt} = \frac{\partial \sigma^c_{nn}}{\partial \delta_t} \tag{3.14}$$

$$B_{tn} = \frac{\partial \sigma^c_{nt}}{\partial \delta_n} \tag{3.15}$$

$$B_{tt} = \frac{\partial \sigma^c_{nt}}{\partial \delta_t} \tag{3.16}$$

The crack stiffness matrix can be converted to the following matrix equations using the equations (3.1):

$$\begin{aligned} d\delta_n &= F_{nn}.d\sigma^c_{nn} + F_{nt}.d\sigma^c_{nt} \\ d\delta_t &= F_{tn}.d\sigma^c_{nn} + F_{tt}.d\sigma^c_{nt} \end{aligned} \tag{3.17}$$

in which the F_{ij} terms represent the elements of the flexibility matrix of the crack [F].

In the smeared crack approach, as stated before, the deformations can be considered as continuously distributed. According to this assumption, the averaged strain concept can be used in finite element modelling of cracks.

The averaged strains can be written in the following way :

$$\varepsilon_{nn}^{\alpha}=\frac{\delta_n}{s} \quad , \quad \varepsilon_{tt}^{\alpha}=0 \quad , \quad \varepsilon_{tt}^{\alpha}=0 \quad , \quad \gamma_{nt}^{\alpha}=2\varepsilon_{nt}^{\alpha}=\frac{\delta_t}{s} \qquad (3.18)$$

If the dowel action and the kinking effect of the reinforcing bars are neglected across the cracks, a new assumption can be made such as the stresses in the solid uncracked concrete between the cracks are equal to the stresses on the cracks. So, the averaged strains of the concrete element are the summation of the solid concrete strains and the strains of the crack.

$$d\varepsilon = d\varepsilon^{\alpha} + d\varepsilon^{\alpha} \qquad (3.19)$$

$$d\varepsilon^{\alpha} = F^{\alpha} d\sigma^{c} \qquad (3.20)$$

in which $[F^{cs}]$ is the incremental(tangential) flexibility matrix of uncracked solid concrete.

If perfect bond is assumed between concrete and reinforcement, the average strains of reinforcement is almost same with the cracked concrete (Figure 3.3.1):

$$d\sigma^{st} = D^{st} d\varepsilon \qquad (3.21)$$

in which superscript *st* refers to steel reinforcement. Because of occurring of cracks with inclination, transformation matrix must be used.

$$D^{st} = \sum_{i=1}^{n} T_i^T D_i^{st} T_i \qquad (3.22)$$

$$T_i = \begin{bmatrix} X & Y & 2XY \\ Y & X & -2XY \\ -XY & XY & X-Y \end{bmatrix} \qquad (3.23)$$

$$D_i^{st} = \begin{bmatrix} p_i E_s \varepsilon_i & 0 & 0 \\ 0 & 0 & 0 \\ 0 & 0 & 0 \end{bmatrix} \qquad (3.24)$$

where X=Cos β , Y=Sin β , β = angle between global axis and bar direction, p=reinforcement ratio .

Total stress-strain equation can be written as in the following form :

$$d\sigma = D.d\varepsilon \qquad D = D^c + D^s \qquad (3.25)$$

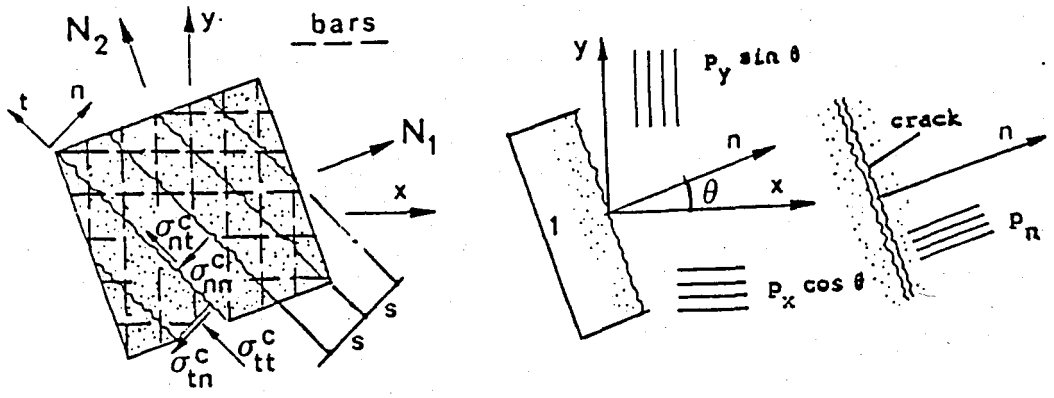

FIGURE 3.3.1. Cracked concrete and perfect bond (equivalent steel ratio) (17)

IV. SHEAR RETENTION FACTOR

In last twenty years, considerable impulse has been given to the development of non-linear calculation techniques. As stated before, the formulation for the constitutive modelling of materials, much progress has been manifested. The main aim of these studies is to develop successful constitutive models which have good balance between simplicity and accurate description of material behavior.

In plain cracked concrete, a coefficient named as shear retention factor can be used to describe the shear stiffness deterioration and introduce the contribution of aggregate interlock by decreasing the shear modulus G_c of uncracked concrete :

$$G^{cr}=\beta.G_c \qquad (4.1)$$

The development of the various formulations for shear retention factor has followed the continuous progress and an increasing sophistication of finite element analysis. Most of the formulations for the shear retention factor, although they may be so complicated, must be seen as a very simplified and empirical representation of the shear behavior of the cracked concrete, because they neglect such relevant and complex aspects as crack roughness, aggregate shape and size, concrete dilatancy, the friction between aggregate and mortar.

In the earliest period, (1970-1975) the factor β was generally given as a constant value between 0 (crack faces perfectly smooth) and 1.0 (crack faces fully locked-up) as it can be seen in Figure 4.1. In later times, two step or continuously decreasing formulations was adopted, especially after crack opening was recognized to be a major factor in reducing crack shear stiffness (Figure 4.2).

Analytical and experimental investigations with regard to the material behavior showed that the behavior depends on many factors and that the interaction between two crack faces generally cannot be characterized by only a relation between shear stress σ_{nt} and shear displacement δ_t coupled by a coefficient.

As stated before, the crack width is an important parameter which cannot be neglected. Also, for a simplified representation of the

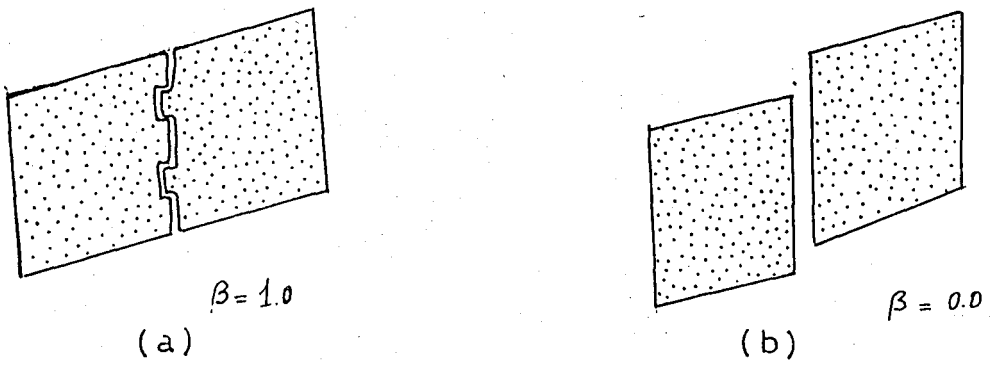

FIGURE 4.1. Two limit values for the shear retention factor(22)
(a) Crack-faces fully locked up
(b) Crack-faces perfectly smooth

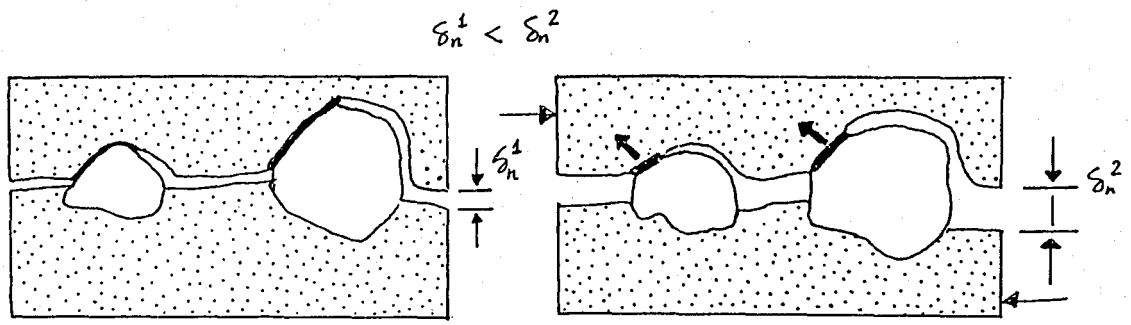

FIGURE 4.2. Simplified physical representation of aggregate interlock

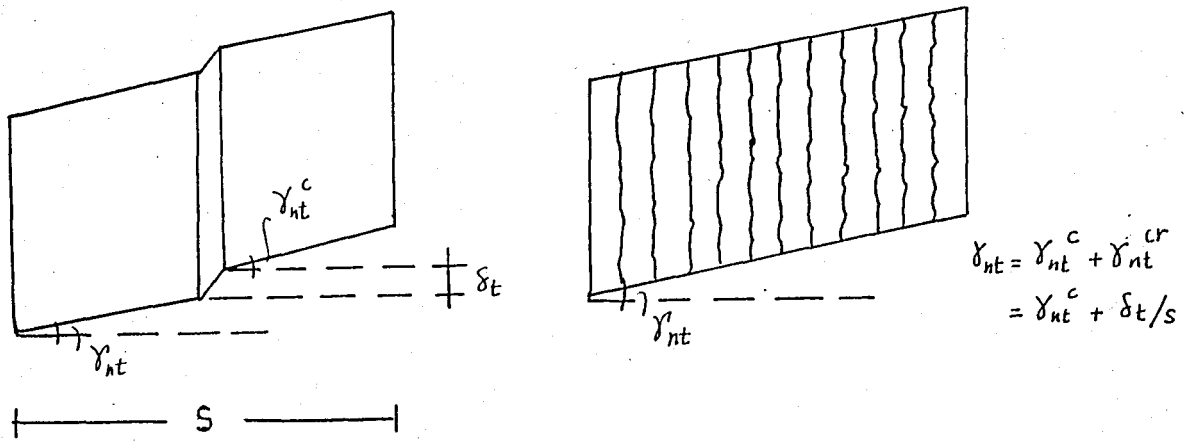

FIGURE 4.3. Total summation of the shear strains including crack and solid concrete components (22)

actual crack behavior, two important appearance should not be disregarded (Figure 4.3.)

(a) An increasing crack width should cause to a decreasing shear stiffness because the contact area becomes smaller.

(b) The wedging effect causes also to develop normal stresses.

In most formulations, the crack opening δ_n is changed by the equivalent strain $\varepsilon_{nn}^{cr} = \delta_n/s$ at right angles to the crack surfaces. Generally, the contribution of solid concrete to normal strain is neglected.

In the literature, main studies done on shear retention factor belongs to Walraven and Keuser (22), Rots and Pruijssers (17), Hanna and Mirza (17).

$$\beta = \frac{1}{1+k\varepsilon_{nn}} \tag{4.2}$$

with k=4447 and $k=F(D_a, \varepsilon_{nn}, \gamma_{nt})$. (Rots and Pruijssers)

$$\beta = \exp(-k\varepsilon_{nn}^2) \geq 0.70 \tag{4.3}$$

with k=140000 . (Hanna and Mirza)

More complex but also more rational formulations can be derived using micromechanical relations derived before. Using equations 3.1, the matrix form can be obtained as below :

$$\begin{bmatrix} \Delta\sigma_{nn} \\ \Delta\sigma_{nt} \end{bmatrix} = \begin{bmatrix} D_{11}^{\alpha} & D_{12}^{\alpha} \\ D_{21}^{\alpha} & D_{22}^{\alpha} \end{bmatrix} \begin{bmatrix} \Delta\varepsilon_{nn} \\ \Delta\gamma_{nt} \end{bmatrix} \tag{4.4}$$

with $D_{ij}^{cr} = h.B_{ij}^{cr}$.

According to the many experimental results, D_{12}^{cr} is not equal to D_{21}^{cr} which means the matrix is asymmetric and requires complicated numerical process. The aim of developing the shear retention factor is to simplify the description of the shear stiffness of cracks. So there is need to look for a further simplification in analysis.

The coefficient D_{12}^{cr} enables the calculation of the normal compressive stress σ_{nn} which is generated by parallel displacement of crack faces. It can be said that, while keeping the crack width δ_n

constant, shear and normal stresses are developed at increasing shear displacement δ_t.

The coefficient D_{21}^{cr} enables the calculation of a decrease of the shear stress σ_{nt} with increasing crack opening δ_t. The resistance to a shear displacement decreases with increasing crack width. But this can be taken into account by defining the coefficient D_{22}^{cr} as a function of the crack width δ_n. This allows us to put also D_{21}^{cr} equal to zero. Using the derivatives of Gambarova-Karakoc formulation given in Delft University Report (21) and equation 4.4 ; D_{21}^{cr},D_{22}^{cr} values are written as :

$$D_{21}^{\alpha} = \frac{1}{s}\frac{\partial \sigma_{nt}^{c}}{\partial \delta_n} = -\frac{1}{s}\frac{\sigma_{nt}^{c}}{\delta_n}\left[\frac{\delta_n}{\sqrt{2\delta_n D_{max} - 2\delta_n}} + K\right] \tag{4.5}$$

$$D_{22}^{\alpha} = \frac{1}{s}\frac{\partial \sigma_{nt}^{c}}{\partial \delta_t} = \frac{1}{s}\frac{\sigma_{nt}^{c}}{\delta_n}[K] \tag{4.6}$$

in which

$$K = \left[\frac{a_1 + 4a_2|r|^3}{a_1 + a_2|r|^3} - \frac{4a_2 r^4}{1 + a_2 r^4}\right] \tag{4.7}$$

The total strain is the summation of strains of cracked and uncracked parts of concrete between the cracks. For an uncracked section the relation between shear stress and shear strain is :

$$\gamma_{nt} = \frac{\sigma_{nt}}{G^c} = \frac{2(1+\nu_c)}{E_c}\sigma_{nt} \tag{4.8}$$

so that the total strain for the cracked concrete is (Figure 4.4.):

$$\gamma_{nt} = \gamma_{nt}^{\alpha} + \gamma_{nt}^{c} \tag{4.9}$$

The total shear strain for the cracked concrete can be written such as :

$$\gamma_{nt} = \gamma_{nt}^{\alpha} + \gamma_{nt}^{c} = \left[\frac{1}{D_{22}^{\alpha}} + \frac{2(1+\nu)}{E_c}\right]\sigma_{nt}^{\alpha} \tag{4.10}$$

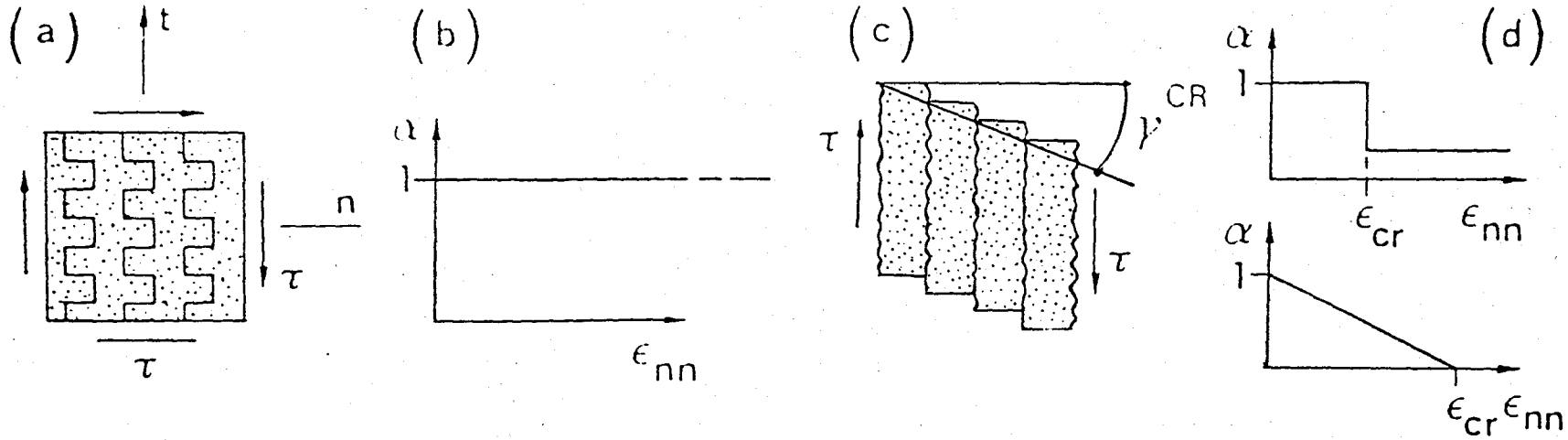

FIGURE 4.4. Shear-retention factor (17)
(a.b) Fully locked up shear stiff cracks.
(c) Two step formulations for ß.
(d) Variable formulations for ß.

The same equation can be formulated using β shear retention factor, as :

$$\gamma_{nt} = \frac{1}{\beta G}\sigma_{nt}^{c} = \frac{2(1+\nu)}{\beta E_c}\sigma_{nt}^{c} \qquad (4.11)$$

By equating the formula 4.10 to 4.11, β can be found such as :

$$\beta = \left[\frac{1}{\frac{E_c}{2(1+\nu)D_{22}^{\alpha}}+1}\right] \qquad (4.12)$$

In order to establish D_{22}^{cr}, which relates a pure shear displacement to a pure shear stress, the most feasible test type is constant crack width test.

The values for D_{22}^{cr} in the literature are mostly derived using the results of Paulay and Loeber's tests published in 1974 (8). To be realistic for the values of D_{22}^{cr}, the point which is, parallel displacement of cracks causes irreversible damage to the crack zone, cannot be disregarded. Under all kinds of loading even under monotonic loading, there must be non-particular relation between stresses and displacements along the cracks.

Millard and Johnson have concluded on this subject such as: "If a cracked specimen undergoes shear displacement without crack widening occurring, there must be a great deal of irreversible damage caused. If the crack is then widened, it might be expected that the shear and the normal stresses would be quite different from those that would result if the crack was first widened and then caused to shear "(23).

Besides, Nissen(24) has compared the test results of Walraven and Daschner in Figure 4.5.

In the lower part of diagram, for the two different crack opening paths, at the intersection point A, significant difference between shear stresses is obtained. Since the systematical investigation has not been done so far about the path dependency concept, test data on this concept is so scarce and an exact conclusion can not be made. In the Figure 4.5, the difference may be

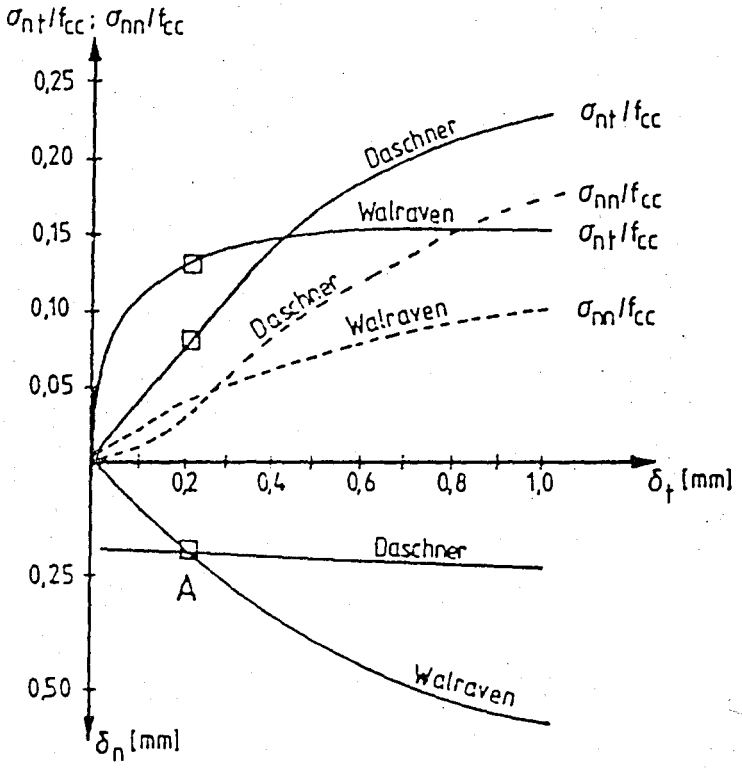

FIGURE 4.5 **Influence of the crack opening path on the stresses at equal displacements according to Nissen(24)**

due to different composition of concrete or testing equipment. So, the necessity for reformulation for the constant crack width case arises.

Karakoc (20), has proposed formulations for the constant crack width case by using test results of Daschner (9), Daschner and Kupfer (18).

The formulation is given before for the case of constant crack opening such as (20) :

$$\sigma_{nt}^{c} = 1.82 f_{cu}^{0.80} \frac{\delta_t^{1.75}}{\delta_t^2 + 0.4\delta_t + 1.75\delta_n} \left(1 - \sqrt{\frac{4\delta_n}{D_a}}\right) \tag{3.10}$$

$$\sigma_{nn}^{c} = 0.75 \delta_t^{1/4} \sigma_{nt}^{c} \tag{3.11}$$

substituting the equation (3.10) into equation (3.11) :

$$\sigma_{nn}^{c} = 1.37 f_{cu}^{0.80} \frac{\delta_t^2}{\delta_t^2 + 0.4\delta_t + 1.7\delta_n} \left(1 - \sqrt{\frac{4\delta_n}{D_a}}\right) \tag{3.12}$$

The formulations are proved very effective to predict the stresses transmitted across the cracks also for high values of shear slip 4 - 5 mm and wide range for crack widths between 0.05 to 1 mm.

Using the derivation formulas for above equations, D_{21}^{cr} and D_{22}^{cr} can be obtained such as:

$$D_{21}^{cr} = \frac{1}{s} \frac{\partial \sigma_{nt}^{c}}{\partial \delta_n} = -\frac{1}{s} \sigma_{nt}^{c} \left(\sqrt{\frac{1}{\delta_n D_{max}}} + \frac{1.7}{\delta_t^2 + 1.7\delta_n + 0.4\delta_t} \right) \tag{4.13}$$

$$D_{22}^{cr} = \frac{1}{s} \frac{\partial \sigma_{nt}^{c}}{\partial \delta_t} = \frac{1}{s} \sigma_{nt}^{c} \left(\frac{1.75}{\delta_t} - \frac{2\delta_t + 0.4}{\delta_t^2 + 1.7\delta_n + 0.4\delta_t} \right) \tag{4.14}$$

V. APPLICATION OF THE FINITE ELEMENT METHOD

The finite element method can be defined as a general method of structural analysis in which a continuous media is replaced by a finite number of elements interconnected at a finite number of nodal points. Because of abundance of literature for finite element method, only a general description is given here.

In this study, four noded rectangular plane stress element is used. The element is assumed to have two degrees of freedom at each nodal point, one vertical and one for the horizontal displacement component. (Figure 5.1)

To develop the element stiffness matrix, displacement functions which are continuous over the entire element are first selected in terms of the nodal point displacements such that any straight line before deformation remains a straight line after deformation. In this way, full compatibility is preserved between neighboring elements at their edges when the assembled structure is subjected to loads and displacements (25). The steps for the analysis are :

(a) Strains are expressed in terms of nodal point displacements d through a displacement transformation matrix G which is :

$$\{\varepsilon\} = [G]\ \{d\} \tag{5.1}$$

(b) Stresses are related to strains by a stress-strain law :

$$\{\sigma\} = [D]\ \{\varepsilon\} \tag{5.2}$$

(c) Stiffness matrix can be written such as :

$$[k] = \int [G]^T [D][G] dV \tag{5.3}$$

(d) The stiffness matrix of the entire system can be assembled using code numbering technique(25) or any other by adding the contribution of each individual element stiffness k into proper location. The resulting equation relates the external nodal point

forces P to the nodal point displacements d of the system.

$$\{P\}=[K]\{d\} \tag{5.4}$$

(e) After solving equation 5.4 for the system, by back substitution, all stress, strain, reaction force values of each element can be obtained.

There are two main categories of procedures which are purely incremental or purely iterative. Different methods of nonlinear analysis in structural engineering are based on different combinations of incremental and iterative techniques. The main idea is to control the convergence of the numerical results.

The steps for a typical iterative cycle are such as after the step (d) which is given above :

(e) computing the unbalanced loads $\{\Delta P\}$ as the vector of the applied loads plus initial nodal forces $\{P\}$;

(f) solving the structural equations $[K]\{\Delta d\}=\{\Delta P\}$ for each displacement increment $\{\Delta d\}$;

(g) adding the increments $\{\Delta d\}$ to global displacements $\{d\}$ leaved at the preceding iteration. This will give the updated form of equilibrium configuration;

(h) testing for convergence. In case of any dissatisfaction, going to step a.

The solution obtained using above procedure is named as Newton-Raphson method for solving algebraic and transcendental functions. The drawing of the method can be seen in Figure 5.2. After the convergence of load P_A, the load is increased to P_B. The related displacement d_B is sought. First order expansion of P= f(d) at the point a gives :

$$f(d_A+\Delta d_1)= f(d_A)+\Delta d_1(\frac{dP}{dd})_A \tag{5.5}$$

The derivative in the above equation is the slope of the curve at the point of A and can be defined K_A which is the stiffness of structure at A. To find Δd_1 equation 5.5 can be written

$$K_A(\Delta d_1)=P_B-P_A \tag{5.6}$$

in which $P_A = f(d_A)$ and $P_B = f(d_A + \Delta d_1)$.

The next iteration uses the tangent stiffness K_1 at point 1 and the unbalanced force $P_B - P_1$ to obtain the next correction ΔU_2. In this study, the Newton -Raphson method is used.

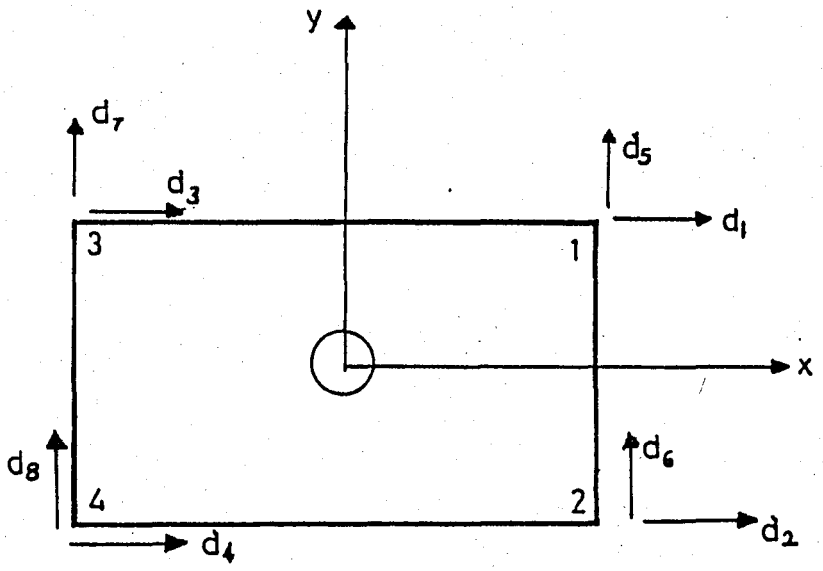

FIGURE 5.1 Four-noded rectangular plane stress element

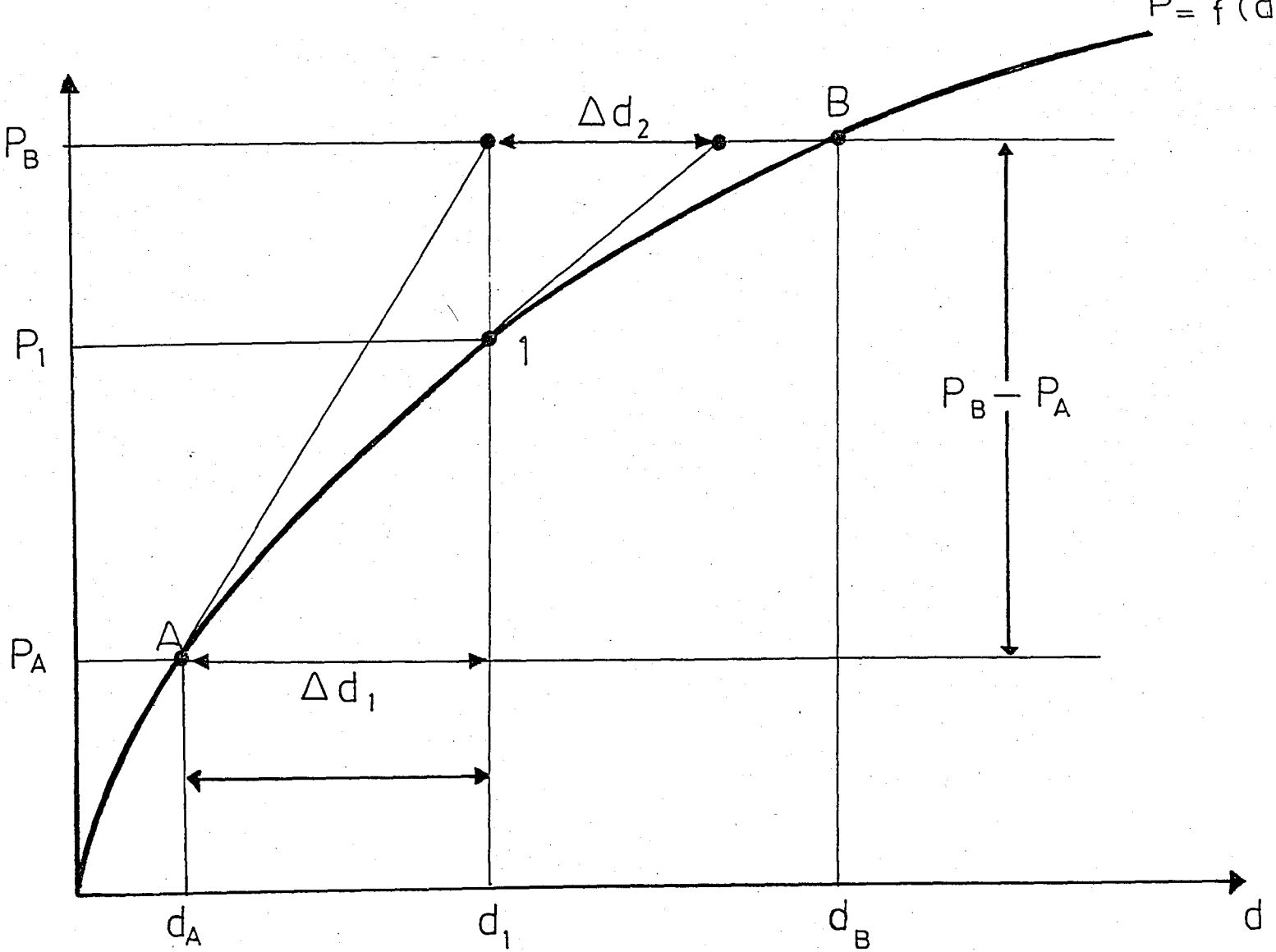

FIGURE 5.2 Typical representation of Newton-Raphson method.

VI. NUMERICAL EXAMPLES

Two simple beams without web reinforcement which are subjected to concentrated load applied at the mid span and a plain concrete prism specimen under compression are analyzed.

One of the beams was tested by Cedolin and Dei Poli (14). The geometrical information for the beam is given on the Figure 6.1. The other properties are given as :

f_c'=22.5 MPa , D_{max}=19 mm , f_y=555 MPa , 4 No.9 bars

Cedolin and Dei Poli have checked the test results with their own finite element program. They have used for aggregate interlock mechanism a constant value for G (Shear modulus). For the steel-concrete interaction, reference has been made to the idealized bond-slip curves. For G=0.1E, in which this value of G is equal approximately to β=0.16, their analysis gave the best fitting to the experimental curve with a small discrepancy but reached a higher ultimate load.

The load was applied to the computer model using an incremental iterative procedure. Because of the symmetry only one half portion of beam is analyzed. 44 concrete, 11 steel and 12 spring elements are used in analysis.

For the bond behavior between concrete and steel, an idealized local bond-slip curve is used as it can be seen on Figure 6.2. Bond is assumed as failed if local slip between concrete and steel exceeds 0.1 mm but in analysis, the failure has occurred because of yielding of steel. For steel, an ideal elastoplastic behavior is assumed as shown in Figure 6.3. An assumption is made that failure occurs at maximum strain 0.01.

The curves drawn on the Figure 6.4. represent the experimental load-deflection curve, their own analysis curve and analysis done with finite element program which is used in this study.

Although experimental values show a 32000 kgf as an ultimate value, analysis showed approximately 15000 kgf for ultimate load. Main reasons for these different behaviors between the experiment and analysis are that softening branch of concrete is not considered, concrete is assumed to have failed at ε_{cu}=0.002 value

and no information is given for K_h value for spring elements used in paper. The K_h values may not fit to each other. In analysis, Gambarova-Karakoç formulations are used instead of giving a shear retention factor. At the same time, because of capacity of the program, the fineness of the mesh size is limited.

For the second simple beam. the results of the experiment done at Structural Laboratory of Bogaziçi University on 21 May 1993, are used.

The geometrical information of test is given in Figure 6.5. The other properties are given as follows :

f_c'=24 MPa , D_{max} = 21 mm. , f_y=408.25 MPa , 2 ϕ 10 bars

Bond and steel idealizations are taken as same with the above test because of the lack of the data for these values.

The comparisons of the test results and analyses are given in Figure 6.6.

The analysis is done by changing shear stiffness characteristics. In the first analysis (1), the shear retention factor is taken as 0.25 and gave higher values. The second curve (2) uses the shear retention factor which is given by Rots. The shape of the curve and the peak value are not reasonable. Third curve is drawn using shear retention formulation proposed in this study. Although the curve shows a different behavior from experiment, it is so close to the curve 4 which is drawn by using Gambarova-Karakoç formulations.

The same criticisms done for the first example are valid also for this second group of analysis.

As a result of the second group of analyses, it can be said that the comparisons between different cases for shear retention factor are not clear enough, much more detailed studies must be done and the concept needs further study.

Third example solved with the finite element program is a plain concrete specimen tested by Niyogi (29). In Niyogi's study, various types of concrete specimens were tested by changing specific experimental parameters such as geometry of loaded area and specimen, nature of the bed supporting , supported area of the specimen, concrete properties, specimen size. Figure 6.7 shows the geometrical information of the specimen which is analyzed. Because of the lack of the load-deformation curve of the tested specimen, the results of the finite element study done on this specimen by Koksal

(28) are used for comparison. Only the experimental values for bearing and first cracking are declared such as 65 per cent and 54 per cent of the maximum compressive strength. Figure 6.8 gives a comparison of these two analysis.

The two curves shown in Figure 6.8 are very close to each other up to 40 per cent of f_c but beyond that they deviate from each other. Köksal's analysis gives bearing strength as 60 per cent of f_c and initiation of cracking as 57 per cent of f_c. The curve two gives a 62 per cent of f_c for the bearing strength and 59 per cent of f_c for the initiation of cracking

The main reason for these differences between the two curves can be stated as follows: Köksal has used constant stress triangular elements in his study and he assumed an average crack spacing "s" of 10 mm, whereas in this study, crack spacing was assumed to be five mm. and rectangular plane stress elements were used.

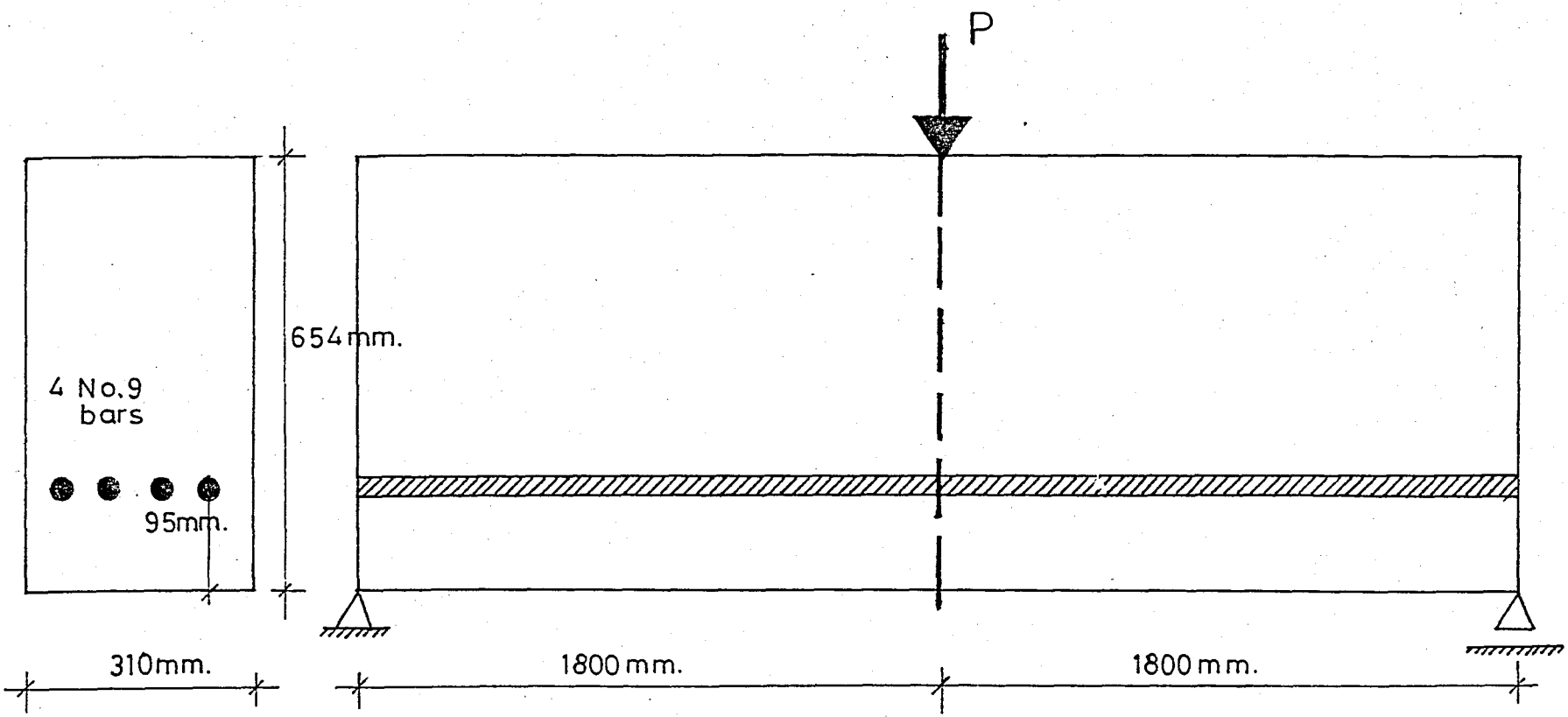

FIGURE 6.1 Geometrical information for test 1 (14)

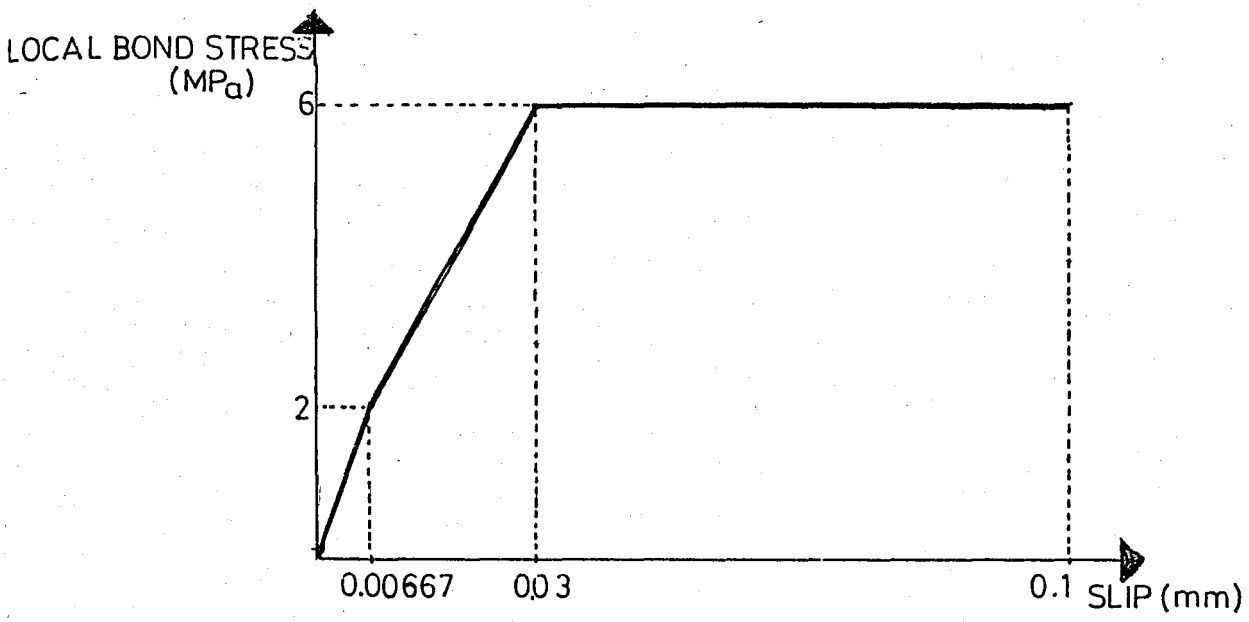

FIGURE 6.2 Idealized local bond-slip curve

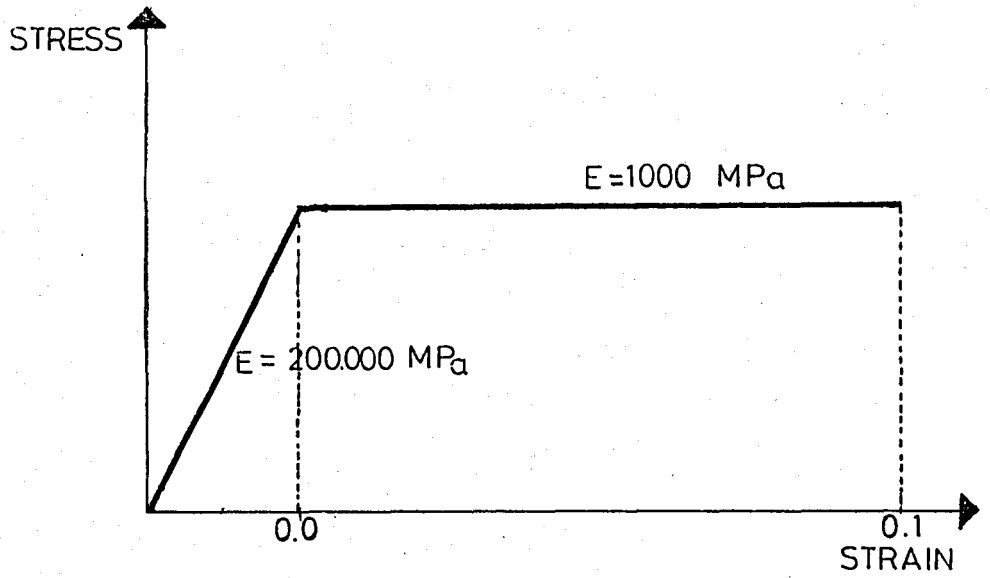

FIGURE 6.3 Idealized steel stress-strain curve

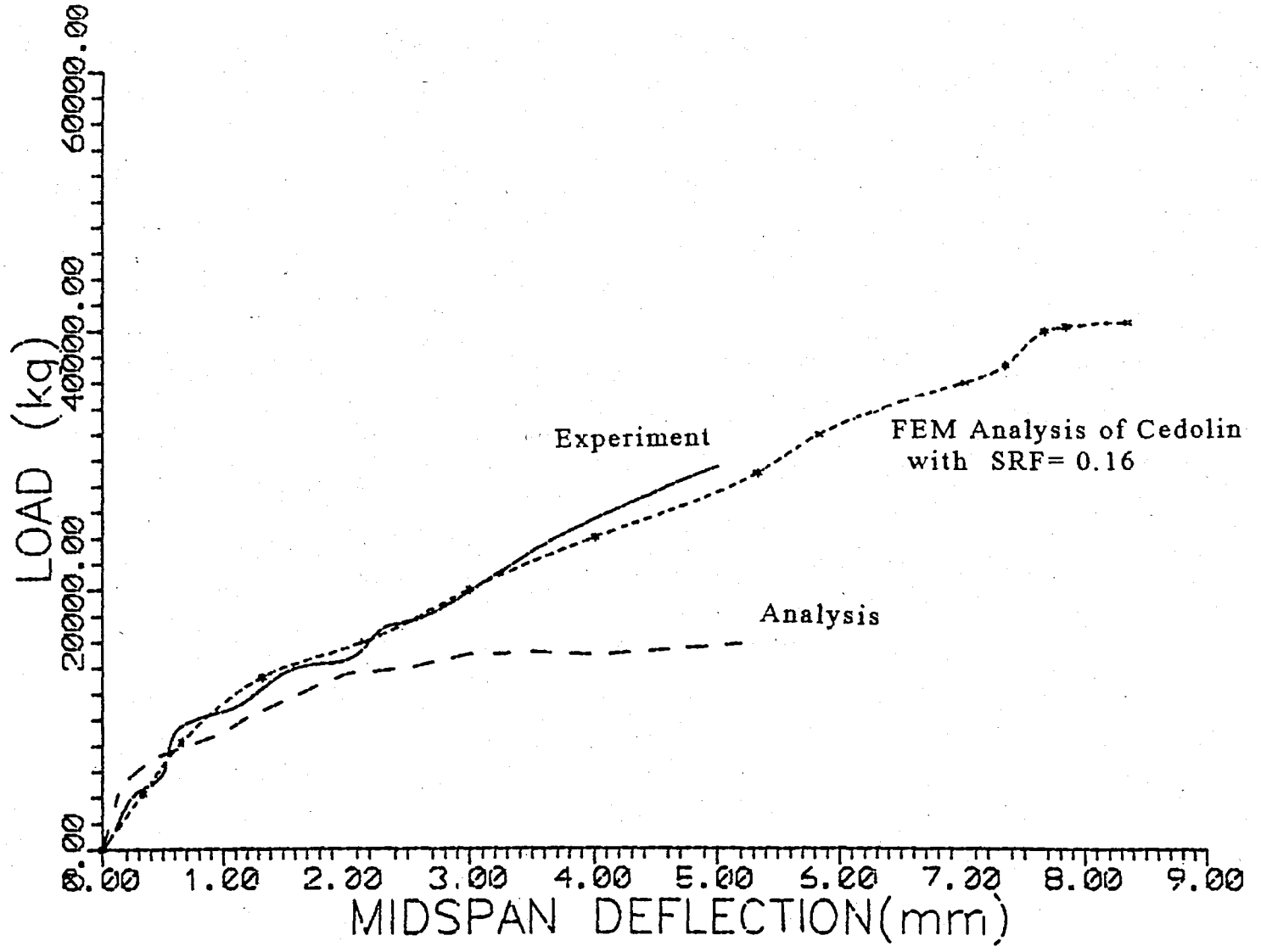

FIGURE 6.4 Load - deformation curves for test 1

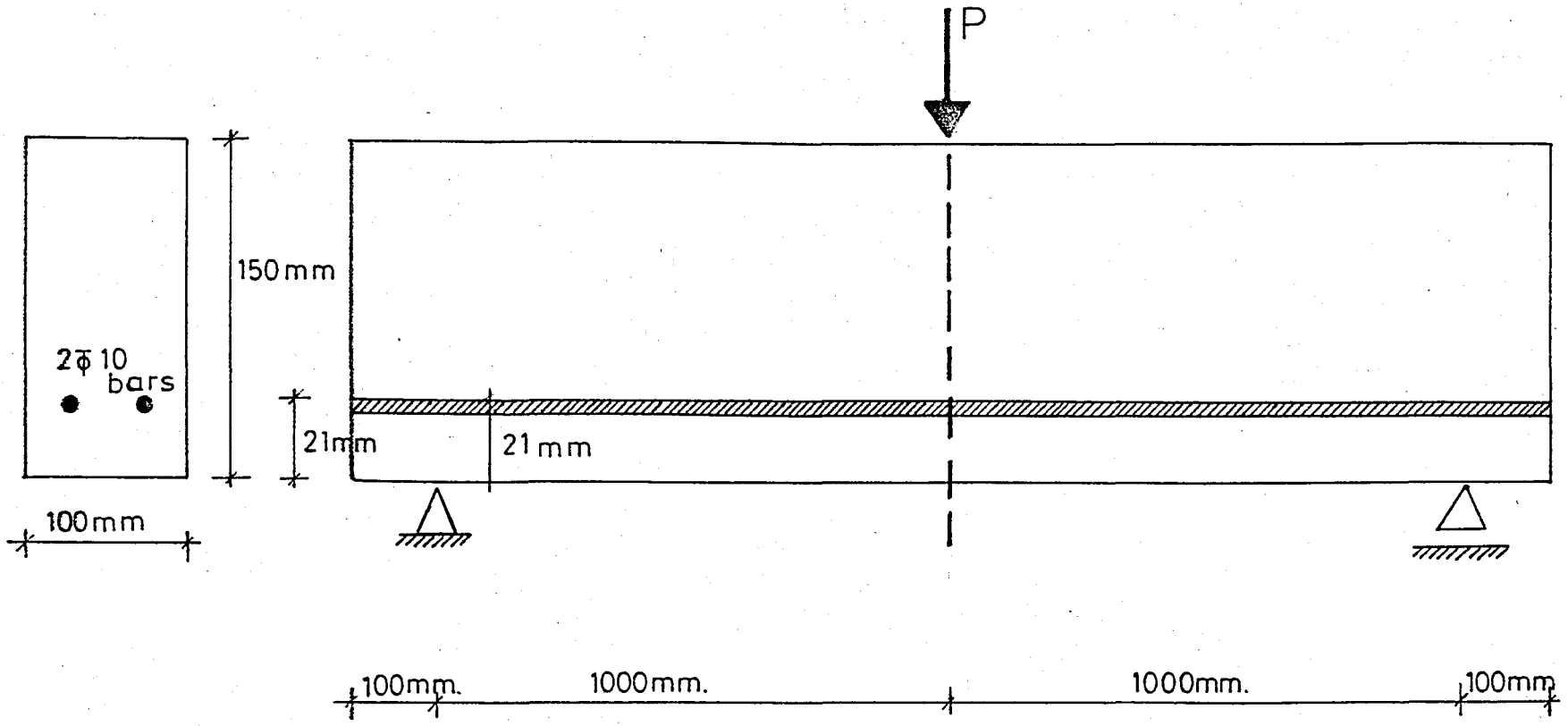

FIGURE 6.5 Geometrical information for test 2 (28)

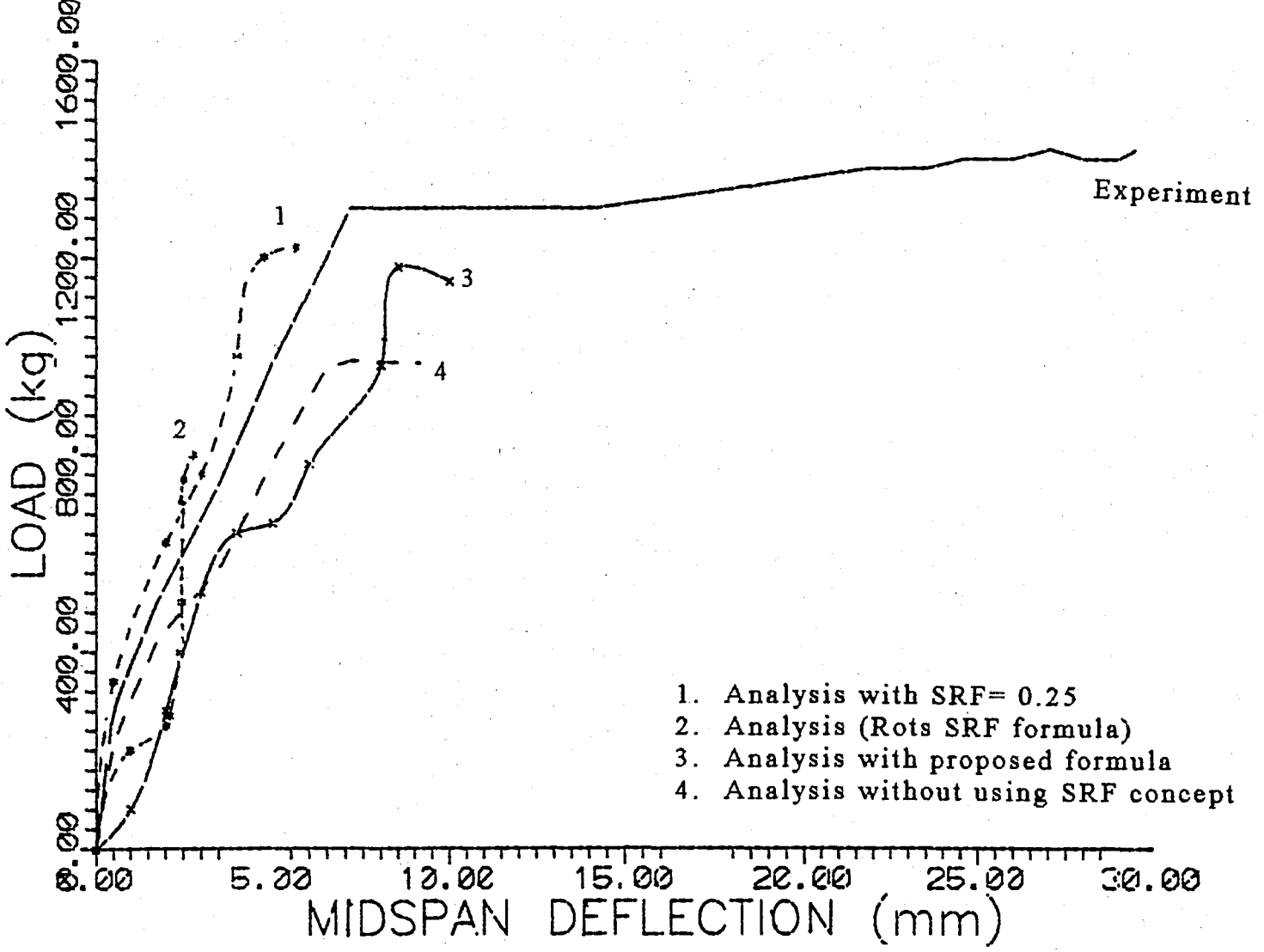

FIGURE 6.6 Load -deformation curves for test 2

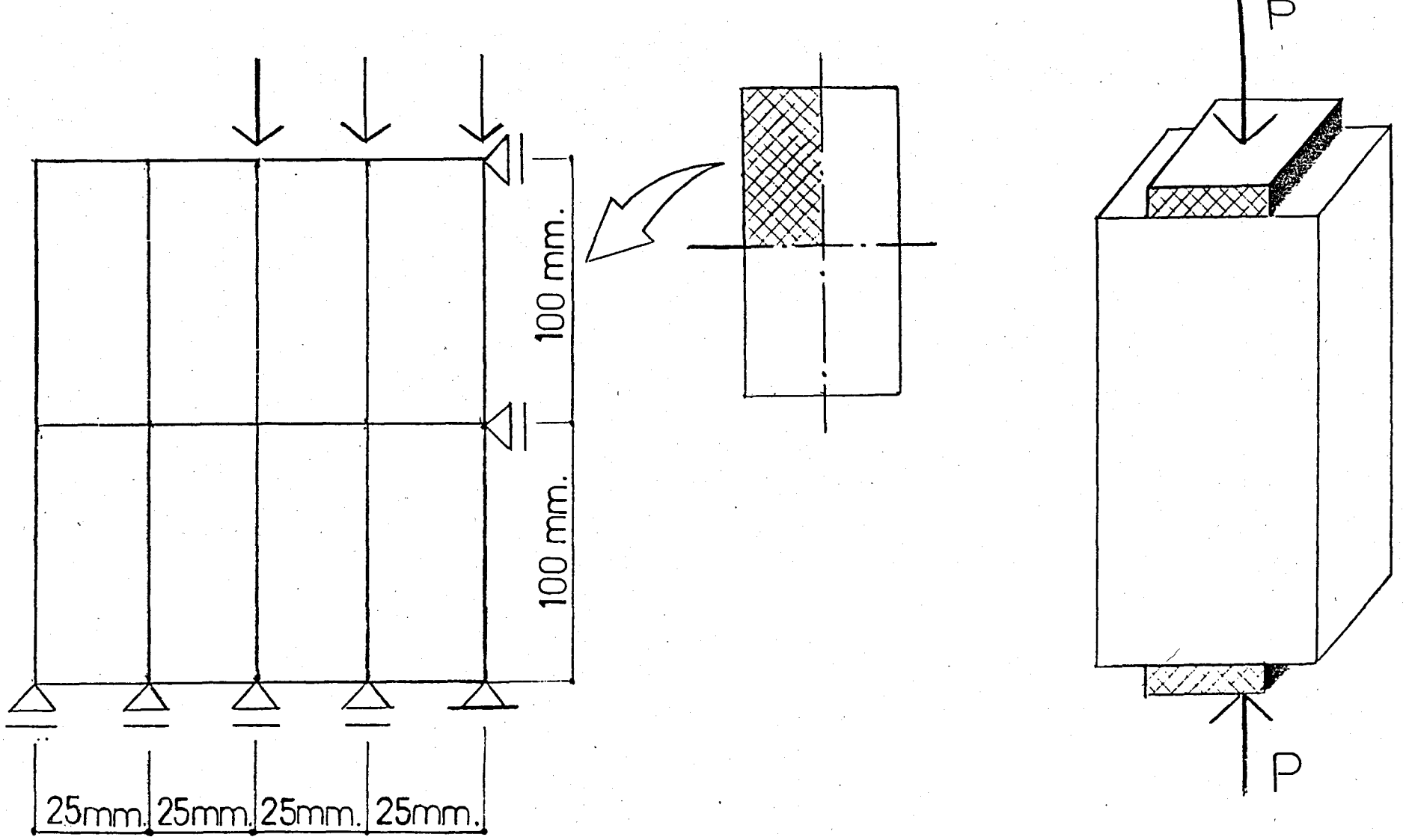

FIGURE 6.7 Geometrical information for test 3 (29)

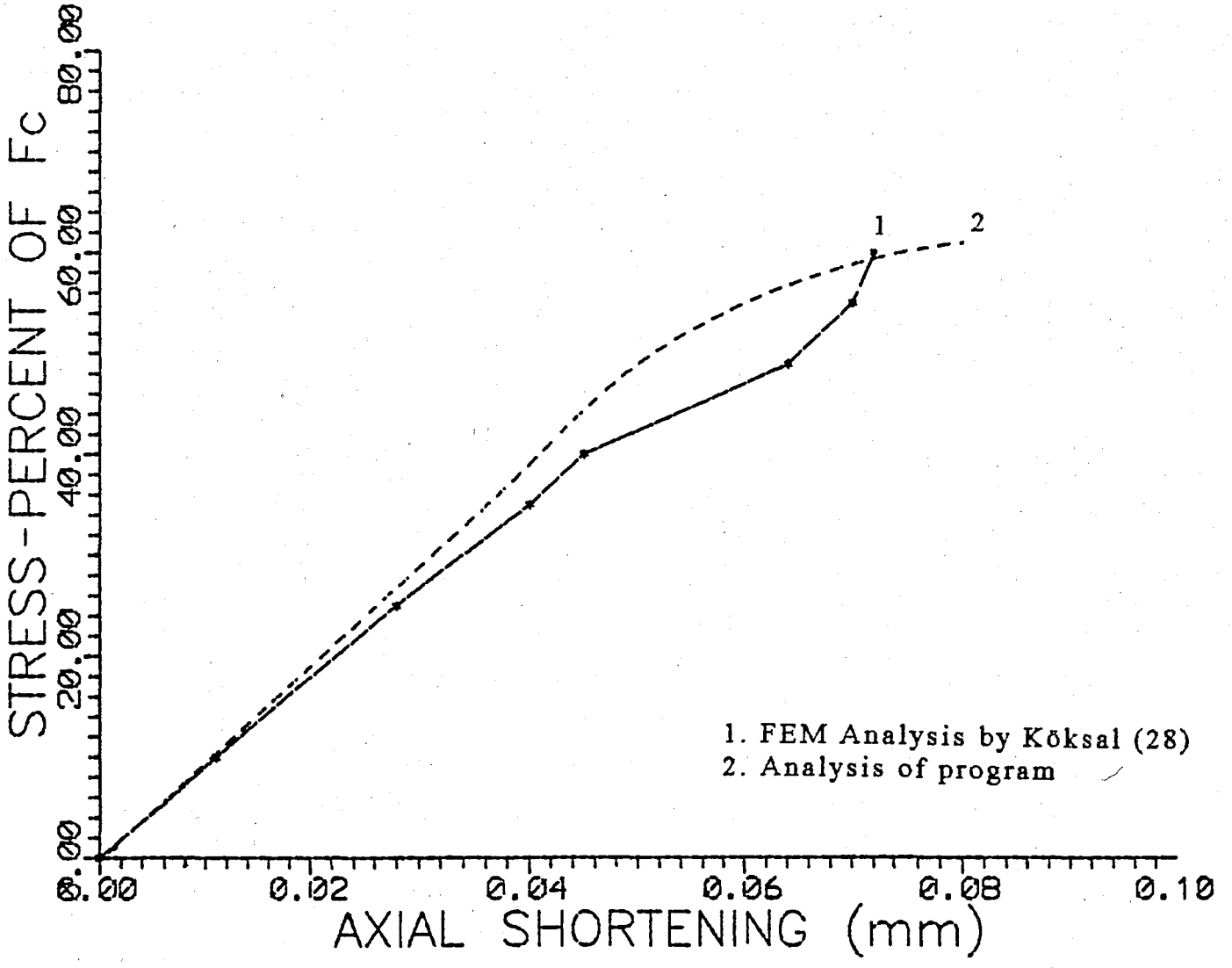

FIGURE 6.8 Stress-axial shortening curves for test 3

VII. SUMMARY AND CONCLUSIONS

The classical methods used for the analysis of reinforced concrete structures, overestimate the behavior of concrete and concrete structures. General use of uniaxial elasticity models provides very rough approximations for this complex material. So, more realistic material behavior models are needed for concrete.

The weak tensile strength of concrete is one of the reasons for the nonlinear behavior of the concrete. Consequently, after cracking the material characteristics change. The behavior of concrete after cracking depends on many factors. In microlevel, aggregate interlock has an important role on this behavior. The models developed by Gambarova- Karakoç and Karakoç are simple and easily applicable for analytical computations. The suitability of the models with the experimental results have been verified several times.

Instead of modelling the interface shear transfer mechanisms as means of transferring shear stresses along preformed cracks, a coefficient named as "shear retention factor" can be used for decreasing the shear stiffness of the section.

The derivation of the formulations for shear retention factor has been a continuous progress and required an increasing sophistication of finite element analysis. However, attention has to be paid to the fact that the models proposed for the factor must reflect the real behavior as much as possible with a preferably simple formulation. In addition to shear retention factor approach, the models proposed by Gambarova-Karakoç, Karakoç, Rots were implemented to the finite element method and comparative studies have been performed on two simply supported beams. The theoretical behavior is overestimated when a constant shear retention factor is used (Curve 1 versus experimental result given in Figure 6.6). On the other hand, both the analysis with the proposed formula (represented by curve 3) and the analysis without using shear retention factor concept (represented by curve 4 in Figure 6.6) are on the safe side and below the experimental results. Besides the last two results (curves 3 and 4) are also in close agreement with each other. This is because the formulations used for these two curves are based on the same physical

considerations and analytical models. Consequently, the proposed formula can effectively be employed instead of constant shear retention factor approach. Nevertheless much more detailed theoretical and experimental studies for this concept are needed. Simple and realistic formulations are naturally preferred.

The conclusions can be summarized as follows :

(a) The finite element program needs further improvement. Because of the limited element capacity, much finer meshes for analyses, could not be used. The fineness of mesh must be increased in order to be able to check the suitability of the program with real cases. In the future studies, much more flexibility can be provided to the program. The convergence criteria can be improved in the program.

(b) Bond between concrete and steel, is an important concept which needs further study. Especially, more clear and realistic formulations for horizontal and vertical stiffness characteristics of spring elements are needed.

(c) Although dowel action is disregarded in this study, to be able to reflect the real behavior, this mechanism must be considered. The modelling of this mechanism also needs more research work.

(d) The behavior of aggregate interlock mechanism at high compressive strengths of the concrete must be examined. This may be a good research area for further analytical and experimental studies.

Finally, no tool is perfect in itself and this is also true for finite element method of analysis. Mainly two factors should be kept in mind. First, the method is an approximate analytical procedure, whose accuracy depends on the fineness of the mesh size and structure. Secondly, the accuracy of the analytical results, referring to the actual reinforced concrete members, is strongly affected by the analytical idealization of the actual member.

APPENDIX A

The computer program developed in this study is written using Fortran language. The program solves nonlinear finite element problems of two dimensional or planar problems using rectangular plane stress element. Bar type of element for steel and spring type of element for bond are used. The program source file occupies about 36 Kb of the disk space and can run in a computer with a 640 Kb or higher.

The overall operation of the program is initiated in main program where eleven subroutines are activated. Input data are supplied by data file named as ILK.DAT . The input data needs total number of elements, concrete elements, steel elements and spring elements, total number of degree of freedom, data for each node, data for each element and data for material properties of concrete and steel. The functions of the main six subroutines are as written below.

In MODULUS subroutine, the nonlinear biaxial equations are calculated at each iteration. This subroutine checks the failure mode of concrete and update the material matrix.

STIFFNESS subroutine, calculates stiffness matrices of all elements and creates global stiffness matrix.

SOLVE subroutine solves the displacements using the GAUSS subroutine and with data send from STIFFNESS subroutine.

VALUES subroutine finds the values for the stresses and strains for every step of loading.

CRACK subroutine checks whether concrete elements is cracked. If cracking has occurred, the cracked material matrix is calculated by using Gambarova-Karakoç formulations.

```
      PROGRAM NLFEA
      DIMENSION D(50,3,3),DC(50,3,3)
      DIMENSION X(80),Y(80)
      DIMENSION DG(50,4,3,8),G(50,4,3,8)
      DIMENSION B(80,80)
      DIMENSION STRESS(50,4,3),STRAIN(50,4,3)
      DIMENSION SIGMA1(50,4),SIGMA2(50,4),ALFA(50,4)
      DIMENSION EPSNN(50),EPSTT(50),GAMANT(50)
      DIMENSION STRE1(50,4,3),STRA1(50,4,3),
     *STRE2(50,4,3),STRA2(50,4,3)
      DIMENSION DX(80),DISPL(80),SKEEP(80),BK(80),VK(80),
     *NFX(80),NFY(80),SLIP(50)
      REAL K(80,80)
      INTEGER NODE(50,8),GSP(50,2),GST(50,2),CONTROL(50),DFX(80),
     *DFY(80),NCODE(50,8)
      INTEGER NUR(80),NDR(80),NUL(80),NDL(80),NTYPE(80)
      INTEGER NL(50),NR(50),NU(50),ND(50)
      INTEGER R,REY,CEVAP,YOK,GS,E0C,EOS
      INTRINSIC ABS
      OPEN(2,FILE='ILK2.DAT',STATUS='OLD')
      OPEN(3,FILE='DISPL.OUT')
      OPEN(4,FILE='STRESS.OUT')
      READ(2,*)NUMEL,NUMCEL,NUMSTEL,NUMSPEL,NUMNOD,GS,NH
    5 READ(2,*)I,X(I),Y(I),DFX(I),DFY(I)
      IF(I.LT.NUMNOD) GO TO 5
C     READ CONCRETE ELEMENT DATA
    6 READ(2,*)I,NUR(I),NDR(I),NUL(I),NDL(I)
      NODE(I,1)=DFX(NUR(I))
      NODE(I,2)=DFX(NDR(I))
      NODE(I,3)=DFX(NUL(I))
      NODE(I,4)=DFX(NDL(I))
      NODE(I,5)=DFY(NUR(I))
      NODE(I,6)=DFY(NDR(I))
      NODE(I,7)=DFY(NUL(I))
      NODE(I,8)=DFY(NDL(I))
      IF (I.LT.NUMCEL) GO TO 6
C     READ STEEL ELEMENT DATA
    7 READ(2,*)I,NR(I),NL(I)
      GST(I,1)=DFX(NL(I))
      GST(I,2)=DFX(NR(I))
      ISL=NUMCEL+NUMSTEL
      IF(I.LT.ISL) GO TO 7
    8 READ(2,*)I,NU(I),ND(I)
      GSP(I,1)=DFX(NU(I))
      GSP(I,2)=DFX(ND(I))
      IF (I.LT.NUMEL) GO TO 8
C     READ CONCRETE ELEMENT DATA
      READ(2,*)FC,T,V,ECU,E0C
C     READ STEEL ELEMENT DATA
```

```
      READ(2,*)STAREA,STLENGTH,EOS,NOBAR,DIABAR
      DO 17 I=1,80
      BK(I)=0.0
   17 CONTINUE
      DO 1 I=1,80
      DISPL(I)=0.0
    1 CONTINUE
      R=1
      REY=1
      FG=0.0
      SUM=0.0
      SUM1=0.0
      DO 2 J=1,50
      DO 3 KL=1,4
        SIGMA1(J,KL)=0.0
        SIGMA2(J,KL)=0.0
        EPSNN(J)=0.0
        EPSTT(J)=0.0
        GAMANT(J)=0.0
    3 CONTINUE
    2 CONTINUE
      CEVAP=0
      DO 4 I=1,50
        CONTROL(I)=2
    4 CONTINUE
      DO 15 KL=1,80
        DX(KL)=0.0
        SKEEP(KL)=0.0
        VK(KL)=0.0
   15 CONTINUE
      DO 16 L=NUMCEL+NUMSTEL+1,NUMEL,1
      SLIP(L)=0.0
   16 CONTINUE
      YOK=1
      IYU=1
      CALL START(D,ALFA,DC,DX,B,STRESS,STRAIN,NUMEL,GS)
  100 CALL FIRST(D,ALFA,STRE2,STRA2,STRE1,STRA1,DG,G,K,NUMEL,E0C,V,R)
      IF(R.EQ.1) GO TO 33
      CALL MODULUS(STRAIN,SIGMA1,SIGMA2,ALFA,E0C,FC,ECU,D,
     * EPSNN,EPSTT,GAMANT,CONTROL,NUMEL)
   33 CALL STIFFNESS(K,D,DC,NUR,NDR,NUL,NDL,CONTROL,DG,G,NUMEL,
     *NUMCELÖNUMSTEL,NUMSPEL,GS,NH,T,NODE,GSP,GST,
     *STAREA,STLENGTH,NOBAR,DIABAR,X,Y,EOS,DISPL,SLIP)
      CALL SOLVE(K,B,GS,NH,CEVAP,REY,DX,DISPL,BK,VK)
      CALL VALUES(GS,NUMCEL,DX,DG,G,STRE2,STRA2,STRE1,STRA1,STRESS,
     *STRAIN,ALFA,SIGMA1,SIGMA2,NODE,CONTROL)
      CEVAP=1
      R=R+1
   55 IF(CEVAP.NE.1) GO TO 77
```

```
      CALL FIRST(D,ALFA,STRE2,STRA2,STRE1,STRA1,DG,G,K,NUMEL,E0C,V,R)
      CALL MODULUS(STRAIN,SIGMA1,SIGMA2,ALFA,E0C,FC,
     *ECU,D,EPSNN,EPSTT,GAMANT,CONTROL,NUMEL)
      CALL CRACK(CONTROL,NUMCEL,FC,DC,EPSNN,EPSTT,GAMANT,ALFA)
      DO 42 I=NUMCEL+NUMSTEL+1,NUMEL,1
      SLIP(I)=DISPL(GSP(I,1))-DISPL(GSP(I,2))
      WRITE(*,*)'SLIP VALUE:','SLIP(I)=',SLIP(I)
   42 CONTINUE
      CALL STIFFNESS(K,D,DC,NUR,NDR,NUL,NDL,CONTROL,DG,
     *G,NUMEL,NUMCEL,NUMSTEL,NUMSPEL,GS,NH,T,NODE,
     *GSP,GST,STAREA,STLENGTH,NOBAR,
     *DIABAR,X,Y,EOS,DISPL,SLIP)
      CALL NEWTON(YOK,GS,SKEEP,VK,DISPL,BK,DX,K)
      PRINT,'ILOAD=? '
      READ(5,43)ILOAD
   43 FORMAT(I6)
      FG=DISPL(16)
      IF(ABS(BK(59)).LT.(ILOAD*500.)) GO TO 77
      WRITE(6,89)'LOAD NOT CONVERGED'
   89 FORMAT(F10.1)
      CALL SOLVE(K,B,GS,NH,CEVAP,REY,DX,DISPL,BK,VK)
      CALL VALUES(GS,NUMCEL,DX,DG,G,STRE2,STRA2,STRE1,STRA1,STRESS,
     *STRAIN,ALFA,SIGMA1,SIGMA2,NODE,CONTROL)
      FA=DISPL(16)-FG
      ERT=0.05*DISPL(16)
      IF(ABS(FA).LT.ABS(ERT)) GO TO 77
      PRINT,FA,FG,DISPL(16),ERT
      YOK=YOK+1
      GO TO 55
   77 WRITE(3,*)'DISPL(I)=',DISPL(I)
      YOK=1
      CEVAP=0
      R=R+1
      CLOSE(2,STATUS='KEEP')
      CLOSE(3,STATUS='KEEP')
      CLOSE(4,STATUS='KEEP')
      IF (R.GE.500) GO TO 101
      GO TO 100
  101 STOP
      END
      SUBROUTINE MODULUS (STRMAX,S1MAXM,S2MAXM,ALFAM,EOM,FCM,
     *MAXES,Y,MEPS1,MEPS2,MGAMA,CHECK,ES)
      DIMENSION STRMAX(50,4,3),S1MAXM(50,4),S2MAXM(50,4),ALFAM(50,4)
      DIMENSION Y(50,3,3),PER(50),STMAX(50,3),S1MAX(50),S2MAX(50)
      DIMENSION ACI(50)
      REAL MEPS1(50),MEPS2(50),MGAMA(50)
      INTEGER CHECK(50),ES,EOM
      REAL MAXES
      DO 10 I=1,ES
```

```
      STMAX(I,1)=(STRMAX(I,1,1)+STRMAX(I,2,1)+STRMAX(I,3,1)+
     *STRMAX(I,4,1))/4
      STMAX(I,2)=(STRMAX(I,1,2)+STRMAX(I,2,2)+STRMAX(I,3,2)+
     *STRMAX(I,4,2))/4
      STMAX(I,3)=(STRMAX(I,1,3)+STRMAX(I,2,3)+STRMAX(I,3,3)+
     *STRMAX(I,4,3))/4
      S1MAX(I)=(S1MAXM(I,1)+S1MAXM(I,2)+S1MAXM(I,3)+S1MAXM(I,4))/4
      S2MAX(I)=(S2MAXM(I,1)+S2MAXM(I,2)+S2MAXM(I,3)+S2MAXM(I,4))/4
      ACI(I)=(ALFAM(I,1)+ALFAM(I,2)+ALFAM(I,3)+ALFAM(I,4))/4
      MEPS1(I)=(STMAX(I,1)+STMAX(I,2))/2+SQRT(((STMAX(I,1)-
     *STMAX(I,2))/2)**2+(STMAX(I,3)/2)**2)
      MEPS2(I)=(STMAX(I,1)+STMAX(I,2))/2-SQRT(((STMAX(I,1)-
     *STMAX(I,2))/2)**2+(STMAX(I,3)/2)**2)
      MGAMA(I)=SQRT(((STMAX(I,1)-STMAX(I,2))/2)**2+
     *(STMAX(I,3)/2)**2)
      IF((S1MAX(I).LE.0).AND.(S2MAX(I).LE.0)) CALL EYARDIM1(S1MAX,S2MAX,
     *FCM,SG1C,SG2C,I)
      CHECK(I)=2
      IF((S1MAX(I).GE.0).AND.(S2MAX(I).GE.0)) GO TO 100
      FREDON=S1MAX(I)/S2MAX(I)
      IF (FREDON.LT.0) GO TO 200
      EIC1=EIC(MAXES,SG1C,FCM)
      EIC2=EIC(MAXES,SG2C,FCM)
      IF((ABS(EIC1).GT.MAXES)) PRINT,'MAXIMUM COMPRESSIVE STRAIN '
      IF((ABS(EIC2).GT.MAXES)) PRINT,'MAXIMUM COMPRESSIVE STRAIN '
      IF((ABS(EIC1).LT.0.0001)) ES1=0.5*EOM
      IF(ABS(EIC1).GT.0.0001) ES1=SG1C/EIC1
      IF((ES1.GT.0.5*EOM)) ES1=0.5*EOM
      IF((ABS(EIC2).LT.0.0001)) ES2=0.0001
      IF(ABS(EIC2).GT.0.0001) ES2=SG2C/EIC2
      IF((ES2.GT.0.5*EOM)) ES2=0.5*EOM
      CALL EYY(YY11,YY12,YY13,EOM,ES1,EIC1,MEPS1,I)
      E1=YY11/((YY12+YY13)**2)
      CALL EYY(YY11,YY12,YY13,EOM,ES2,EIC2,MEPS2,I)
      E2=YY11/((YY12+YY13)**2)
      VX=0.2
      IF((S1MAX(I).LT.0).AND.(S2MAX(I).LT.0)) GO TO 300
  100 E1=EOM
      E2=EOM
      SG1C=1.83
      SG2C=1.83
      VX=0.2
      IF((S1MAX(I).GE.0).AND.(S2MAX(I).GE.0)) GO TO 300
  200 IF((S1MAX(I).LT.0).AND.(S2MAX(I).GT.0)) YORAN=S2MAX(I)/S1MAX(I)
      IF((S1MAX(I).GT.0).AND.(S2MAX(I).LT.0)) YORAN=S1MAX(I)/S2MAX(I)
      IF(S2MAX(I).GT.0) GO TO 250
      IF(YORAN.LT.-0.17) SG2C=0.65*FCM
      IF(YORAN.GE.-0.17) SG2C=(1+3.28*YORAN)/((1+YORAN)**2)*FCM
      SG1C=YORAN*SG2C
```

```
250 IF(YORAN.LT.-0.17) SG1C=0.65*FCM
    IF(YORAN.GT.-0.17) SG1C=(1+3.28*YORAN)/((1+YORAN)**2)*FCM
    IF(S1MAX(I).LT.0) GO TO 270
    VX=YVXO(S1MAX,S2MAX,FCM,I)
    EIC2=EIC(MAXES,SG2C,FCM)
    IF(ABS(EIC2).GT.MAXES) PRINT,'MAXIMUM COMPRESSIVE STRAIN'
    IF(ABS(EIC2).LT.0.0001) ES2=0.5*EOM
    IF(ABS(EIC2).GT.0.0001) ES2=SG2C/EIC2
    IF(ES2.GT.0.5*EOM) S2=0.5*EOM
    CALL EYY(YY11,YY12,YY13,EOM,ES2,EIC2,MEPS2,I)
    E2=YY11/(YY12+YY13)**2
    E1=EOM
    VX=SQRT(0.2*VX)
    IF(S2MAX(I).LT.0) GO TO 300
270 VX=YVXO(S2MAX,S1MAX,FCM,I)
    EIC1=EIC(MAXES,G1C,FCM)
    IF(ABS(EIC1).GT.MAXES) PRINT,'MAXIMUM COMPRESSIVE STRAIN'
    IF(ABS(EIC1).LT.0.0001) ES1=0.5*EOM
    IF(ABS(EIC1).GT.0.001) ES1=SG1C/EIC1
    IF(ES1.GT.0.5*EOM) ES1=0.5*EOM
    CALLEYY(YY11,YY12,YY13,EOM,ES1,EIC1,MEPS1,I)
    E1=YY11/((YY12+YY13)**2)
    E2=EOM
    VX=SQRT(0.2*VX)
300 IF (ABS(STMAX(I,1)).LT.(0.002)) STE=200000
    IF (ABS(STMAX(I,1)).GE.(0.002)) STE=50000.0
    IF (STMAX(I,1).LT.0.) STE=-200000
C    STEEL=PER(I)*STE
    IF (I.EQ.3) E1=0.0
    IF (I.EQ.4) E1=0.0
    Y(I,1,1)=E1/(1-VX*VX)
    Y(I,1,2)=VX*SQRT(ABS(E1*E2))/(1-VX*VX)
    Y(I,2,2)=E2/(1-VX*VX)
    Y(I,3,3)=(E1+E2-2*VX*SQRT(ABS(E1*E2)))/(1-VX*VX)
    Y(I,2,1)=Y(I,1,2)
    IF ((S1MAX(I).GT.7.83).OR.(S2MAX(I).GT.7.83)) CHECK(I)=1
    IF((S1MAX(I).GT.7.83).OR.(S2MAX(I).GT.7.83)) PRINT,'CRACK OPENED
   *IN THE ELEMENT NO',I
 15 CONTINUE
 10 CONTINUE
    RETURN
    END
    SUBROUTINE EYARDIM1(S1,S2,YFC,YS1C,YS2C,KI)
    DIMENSION S1(50),S2(50)
    REAL ORAN
    IF(ABS(S1(KI)).GT.(5*ABS(S2(KI)))) YS1C=YFC
    IF(ABS(S1(KI)).GT.(5*ABS(S2(KI)))) YS2C=0.0
    IF(ABS(S2(KI)).GT.(5*ABS(S2(KI)))) YS2C=YFC
    IF(ABS(S2(KI)).GT.(5*ABS(S2(KI)))) YS1C=0.0
```

```
      IF(ABS(S1(KI)).GT.(5*ABS(S2(KI)))) GO TO 34
      IF(ABS(S2(KI)).GT.(5*ABS(S2(KI)))) GO TO 34
      IF((S1(KI).EQ.0).OR.(S2(KI).EQ.0)) GO TO 34
      ORAN=S2(KI)/S1(KI)
      IF(ORAN.GT.1.0) ORAN=1/ORAN
      YS2C=(1+3.65*ORAN)/((1+ORAN)**2)*YFC
      YS1C=ORAN*YS2C
   34 RETURN
      END
      SUBROUTINE EYY(EYY11,EYY12,EYY13,YIE,YES,YEIC,YMS,IS)
      DIMENSION YMS(50)
      INTEGER YIE
      EYY11=YIE*YES*YES*YEIC*YEIC*(YEIC*YEIC-YMS(IS)*YMS(IS))
      EYY12=YIE*YEIC*YMS(IS)
      EYY13=YES*(YEIC*YEIC-2*YEIC*YMS(IS)+YMS(IS)*YMS(IS))
      RETURN
      END
      FUNCTION EIC(YCU,YS,EYFC)
      SX=YS/EYFC
      EIC=YCU*(-1.6*SX*SX*SX+2.25*SX*SX+0.35*SX)
      RETURN
      END
      SUBROUTINE START(GY,GACI,GYC,GD,GB,GSTRESS,GSTRAIN,GNE,GGS)
      DIMENSION GY(50,3,3),GYC(50,3,3)
      DIMENSION GACI(50,4)
      DIMENSION GD(80)
      DIMENSION GB(80,80)
      DIMENSION GX(50),GYY(50)
      DIMENSION GSTRESS(50,4,3),GSTRAIN(50,4,3)
      INTEGER GNE,GGS
      DO 10 I=1,50
        DO 20 J=1,3
          DO 25 K=1,3
            GY(I,J,K)=0.0
            GYC(I,J,K)=0.0
   25     CONTINUE
   20   CONTINUE
      DO 15 L=1,4
      GACI(I,L)=0.0
   15 CONTINUE
      GX(I)=0.0
      GYY(I)=0.0
   10 CONTINUE
      DO 30 I=1,50
      DO 35 J=1,4
      DO 38 K=1,3
      GSTRESS(I,J,K)=0.0
      GSTRAIN(I,J,K)=0.0
   38 CONTINUE
```

```
35 CONTINUE
30 CONTINUE
  DO 40 I=1,80
    DO 50 J=1,80
      GB(I,J)=0.0
50   CONTINUE
    GD(I)=0.0
40 CONTINUE
  RETURN
  END
  SUBROUTINE FIRST(PD,PACI,PF,PUZ,PSTRE1,PSTRA1,PDG,PG,PK,PNE,
 *PE0C,PV,PR)
  DIMENSION PD(50,3,3),PACI(50,4)
  DIMENSION PF(50,4,3),PUZ(50,4,3),PSTRE1(50,4,3),PSTRA1(50,4,3)
  DIMENSION PDG(50,4,3,8),PG(50,4,3,8),PSB(50,4,3,8)
  DIMENSION PK(80,80)
  INTEGER PNE,PR,PE0C
  IF (PR.GT.1) GO TO 12
  DO 10 I=1,PNE
    PD(I,1,1)=PE0C/(1-PV*PV)
    PD(I,1,2)=PE0C*PV/(1-PV*PV)
    PD(I,2,1)=PD(I,1,2)
    PD(I,2,2)=PD(I,1,1)
    PD(I,3,3)=PE0C/2/(1+PV)
   DO 11 J=1,4
    PACI(I,J)=0.0
11 CONTINUE
10 CONTINUE
12 DO 20 I=1,80
    DO 30 J=1,80
      PK(I,J)=0.0
30   CONTINUE
20 CONTINUE
  DO 40 I=1,50
    DO 45 J=1,4
      DO 50 K=1,3
      PF(I,J,K)=0.0
      PUZ(I,J,K)=0.0
      PSTRE1(I,J,K)=0.0
      PSTRA1(I,J,K)=0.0
50   CONTINUE
45  CONTINUE
40 CONTINUE
  DO 60 I=1,50
    DO 70 J=1,4
      DO 75 K=1,3
        DO 80 L=1,8
        PDG(I,J,K,L)=0.0
         PG(I,J,K,L)=0.0
```

```
        PSB(I,J,K,L)=0.0
80      CONTINUE
75    CONTINUE
70    CONTINUE
60 CONTINUE
  RETURN
  END
  SUBROUTINE STIFFNESS(SK,SD,SDC,SNUR,SNDR,SNUL,SNDL,SCHECK,
 *WDG,WSB,WNE,WNCE,WNSTE,WNSPE,WGS,WNH,WT,W,WSP,
 *WST,AREA,LENGTH,NOBAR,DIABAR,WX,WY,EO,SDISPL,SSLIP)
  DIMENSION SK(80,80),S(80,80),SST(80,80),SSP(80,80)
  DIMENSION SD(50,3,3),SDC(50,3,3)
  DIMENSION WDG(50,4,3,8),WSB(50,4,3,8)
  DIMENSION WX(50),WY(50),SDISPL(80),SSLIP(50)
  INTEGER SCHECK(50),W(50,8),WSP(50,2),WST(50,2)
  INTEGER WGS,WNE,WNH,WNCE,WNSTE,WNSPE,EO
  INTEGER SNUR(80),SNDR(80),SNUL(80),SNDL(80)
  INTRINSIC ABS
  REAL LENGTH
  SU=0.0
  SUM1=0.0
  I=1
  DO 34 J=1,80
    DO 35 K=1,80
      S(J,K)=0.0
      SST(J,K)=0.0
      SSP(J,K)=0.0
35  CONTINUE
34 CONTINUE
200 A1=ABS(WX(SNUR(I))-WX(SNUL(I)))/2
  B1=ABS(WY(SNUR(I))-WY(SNDR(I)))/2
  BT=B1/A1
  S(W(I,1),W(I,1))=WT/3*(SD(I,1,1)*BT+SD(I,3,3)/BT)
  S(W(I,1),W(I,2))=WT/3*(SD(I,1,1)*BT/2-SD(I,3,3)/BT)
  S(W(I,1),W(I,3))=WT/3*(-SD(I,1,1)*BT+SD(I,3,3)/(2*BT))
  S(W(I,1),W(I,4))=WT/3*(-SD(I,1,1)*BT/2-SD(I,3,3)/(2*BT))
  S(W(I,1),W(I,5))=WT/4*(SD(I,1,2)+SD(I,3,3))
  S(W(I,1),W(I,6))=WT/4*(-SD(I,1,2)+SD(I,3,3))
  S(W(I,1),W(I,7))=WT/4*(SD(I,1,2)-SD(I,3,3))
  S(W(I,1),W(I,8))=WT/4*(-SD(I,1,2)-SD(I,3,3))
  S(W(I,2),W(I,1))=S(W(I,1),W(I,2))
  S(W(I,2),W(I,2))=S(W(I,1),W(I,1))
  S(W(I,2),W(I,3))=S(W(I,1),W(I,4))
  S(W(I,2),W(I,4))=S(W(I,1),W(I,3))
  S(W(I,2),W(I,5))=S(W(I,1),W(I,7))
  S(W(I,2),W(I,6))=S(W(I,1),W(I,8))
  S(W(I,2),W(I,7))=S(W(I,1),W(I,5))
  S(W(I,2),W(I,8))=S(W(I,1),W(I,6))
  S(W(I,3),W(I,1))=S(W(I,1),W(I,3))
```

```
S(W(I,3),W(I,2))=S(W(I,2),W(I,3))
S(W(I,3),W(I,3))=S(W(I,1),W(I,1))
S(W(I,3),W(I,4))=S(W(I,1),W(I,2))
S(W(I,3),W(I,5))=S(W(I,1),W(I,6))
S(W(I,3),W(I,6))=S(W(I,1),W(I,5))
S(W(I,3),W(I,7))=S(W(I,1),W(I,8))
S(W(I,3),W(I,8))=S(W(I,1),W(I,7))
S(W(I,4),W(I,1))=S(W(I,1),W(I,4))
S(W(I,4),W(I,2))=S(W(I,2),W(I,4))
S(W(I,4),W(I,3))=S(W(I,3),W(I,4))
S(W(I,4),W(I,4))=S(W(I,1),W(I,1))
S(W(I,4),W(I,5))=S(W(I,1),W(I,8))
S(W(I,4),W(I,6))=S(W(I,1),W(I,7))
S(W(I,4),W(I,7))=S(W(I,1),W(I,6))
S(W(I,4),W(I,8))=S(W(I,1),W(I,5))
S(W(I,5),W(I,1))=S(W(I,1),W(I,5))
S(W(I,5),W(I,2))=S(W(I,2),W(I,5))
S(W(I,5),W(I,3))=S(W(I,3),W(I,5))
S(W(I,5),W(I,4))=S(W(I,4),W(I,5))
S(W(I,5),W(I,5))=WT/3*(SD(I,2,2)/BT+SD(I,3,3)*BT)
S(W(I,5),W(I,6))=WT/3*(-SD(I,2,2)/BT+SD(I,3,3)*BT/2)
S(W(I,5),W(I,7))=WT/3*(SD(I,2,2)/(2*BT)-SD(I,3,3)*BT)
S(W(I,5),W(I,8))=WT/3*(-SD(I,2,2)/(2*BT)-SD(I,3,3)*BT/2)
S(W(I,6),W(I,1))=S(W(I,1),W(I,6))
S(W(I,6),W(I,2))=S(W(I,2),W(I,6))
S(W(I,6),W(I,3))=S(W(I,3),W(I,6))
S(W(I,6),W(I,4))=S(W(I,4),W(I,6))
S(W(I,6),W(I,5))=S(W(I,5),W(I,6))
S(W(I,6),W(I,6))=S(W(I,5),W(I,5))
S(W(I,6),W(I,7))=S(W(I,5),W(I,8))
S(W(I,6),W(I,8))=S(W(I,5),W(I,7))
S(W(I,7),W(I,1))=S(W(I,1),W(I,7))
S(W(I,7),W(I,2))=S(W(I,2),W(I,7))
S(W(I,7),W(I,3))=S(W(I,3),W(I,7))
S(W(I,7),W(I,4))=S(W(I,4),W(I,7))
S(W(I,7),W(I,5))=S(W(I,5),W(I,7))
S(W(I,7),W(I,6))=S(W(I,6),W(I,7))
S(W(I,7),W(I,7))=S(W(I,5),W(I,5))
S(W(I,7),W(I,8))=S(W(I,5),W(I,6))
S(W(I,8),W(I,1))=S(W(I,1),W(I,8))
S(W(I,8),W(I,2))=S(W(I,2),W(I,8))
S(W(I,8),W(I,3))=S(W(I,3),W(I,8))
S(W(I,8),W(I,4))=S(W(I,4),W(I,8))
S(W(I,8),W(I,5))=S(W(I,5),W(I,8))
S(W(I,8),W(I,6))=S(W(I,6),W(I,8))
S(W(I,8),W(I,7))=S(W(I,7),W(I,8))
S(W(I,8),W(I,8))=S(W(I,5),W(I,5))
DO 145  J=1,4
IF (J.EQ.1) THEN
```

```
KSI=1.0
ITA=1.0
 ELSEIF (J.EQ.2) THEN
 KSI=1.0
 ITA=-1.0
  ELSEIF (J.EQ.3) THEN
  KSI=-1.0
  ITA=1.0
   ELSE
   KSI=-1.0
   ITA=-1.0
ENDIF
WDG(I,J,1,1)=(SD(I,1,1)*B1*(1+ITA))/(4*A1*B1)
WDG(I,J,1,2)=(SD(I,1,1)*B1*(1-ITA))/(4*A1*B1)
WDG(I,J,1,3)=(-SD(I,1,1)*B1*(1+ITA))/(4*A1*B1)
WDG(I,J,1,4)=(-SD(I,1,1)*B1*(1-ITA))/(4*A1*B1)
WDG(I,J,1,5)=(SD(I,1,2)*A1*(1+KSI))/(4*A1*B1)
WDG(I,J,1,6)=(-SD(I,1,2)*A1*(1+KSI))/(4*A1*B1)
WDG(I,J,1,7)=(SD(I,1,2)*A1*(1-KSI))/(4*A1*B1)
WDG(I,J,1,8)=(-SD(I,1,2)*A1*(1-KSI))/(4*A1*B1)
WDG(I,J,2,1)=(SD(I,1,2)*B1*(1+ITA))/(4*A1*B1)
WDG(I,J,2,2)=(SD(I,1,2)*B1*(1-ITA))/(4*A1*B1)
WDG(I,J,2,3)=(-SD(I,1,2)*B1*(1+ITA))/(4*A1*B1)
WDG(I,J,2,4)=(-SD(I,1,2)*B1*(1-ITA))/(4*A1*B1)
WDG(I,J,2,5)=(SD(I,2,2)*A1*(1+KSI))/(4*A1*B1)
WDG(I,J,2,6)=(-SD(I,2,2)*A1*(1+KSI))/(4*A1*B1)
WDG(I,J,2,7)=(SD(I,2,2)*A1*(1-KSI))/(4*A1*B1)
WDG(I,J,2,8)=(-SD(I,2,2)*A1*(1-KSI))/(4*A1*B1)
WDG(I,J,3,1)=(SD(I,3,3)*A1*(1+KSI))/(4*A1*B1)
WDG(I,J,3,2)=(-SD(I,3,3)*A1*(1+KSI))/(4*A1*B1)
WDG(I,J,3,3)=(SD(I,3,3)*A1*(1-KSI))/(4*A1*B1)
WDG(I,J,3,4)=(-SD(I,3,3)*A1*(1-KSI))/(4*A1*B1)
WDG(I,J,3,5)=(SD(I,3,3)*B1*(1+ITA))/(4*A1*B1)
WDG(I,J,3,6)=(SD(I,3,3)*B1*(1-ITA))/(4*A1*B1)
WDG(I,J,3,7)=(-SD(I,3,3)*B1*(1+ITA))/(4*A1*B1)
WDG(I,J,3,8)=(-SD(I,3,3)*B1*(1-ITA))/(4*A1*B1)
WSB(I,J,1,1)=B1*(1+ITA)/(4*A1*B1)
WSB(I,J,1,2)=B1*(1-ITA)/(4*A1*B1)
WSB(I,J,1,3)=-B1*(1+ITA)/(4*A1*B1)
WSB(I,J,1,4)=-B1*(1-ITA)/(4*A1*B1)
WSB(I,J,1,5)=0.0
WSB(I,J,1,6)=0.0
WSB(I,J,1,7)=0.0
WSB(I,J,1,8)=0.0
WSB(I,J,2,1)=0.0
WSB(I,J,2,2)=0.0
WSB(I,J,2,3)=0.0
WSB(I,J,2,4)=0.0
WSB(I,J,2,5)=A1*(1+KSI)/(4*A1*B1)
```

```
      WSB(I,J,2,6)=-A1*(1+KSI)/(4*A1*B1)
      WSB(I,J,2,7)=A1*(1-KSI)/(4*A1*B1)
      WSB(I,J,2,8)=-A1*(1-KSI)/(4*A1*B1)
      WSB(I,J,3,1)=A1*(1+KSI)/(4*A1*B1)
      WSB(I,J,3,2)=-A1*(1+KSI)/(4*A1*B1)
      WSB(I,J,3,3)=A1*(1-KSI)/(4*A1*B1)
      WSB(I,J,3,4)=-A1*(1-KSI)/(4*A1*B1)
      WSB(I,J,3,5)=B1*(1+ITA)/(4*A1*B1)
      WSB(I,J,3,6)=B1*(1-ITA)/(4*A1*B1)
      WSB(I,J,3,7)=-B1*(1+ITA)/(4*A1*B1)
      WSB(I,J,3,8)=-B1*(1-ITA)/(4*A1*B1)
  145 CONTINUE
  100 S(W(I,1),W(I,1))=WT/12*(4*SDC(I,1,1)*BT+3*SDC(I,1,3)+
     *3*SDC(I,3,1)+4*SDC(I,3,3)/BT)+S(W(I,1),W(I,1))
      S(W(I,1),W(I,2))= WT/12*(2*SDC(I,1,1)*BT-3*SDC(I,1,3)+
     *3*SDC(I,3,1)-4*SDC(I,3,3)/BT)+S(W(I,1),W(I,2))
      S(W(I,1),W(I,3))= WT/12*(-4*SDC(I,1,1)*BT+3*SDC(I,1,3)-
     *3*SDC(I,3,1)+2*SDC(I,3,3)/BT)+S(W(I,1),W(I,3))
      S(W(I,1),W(I,4))= WT/12*(-2*SDC(I,1,1)*BT-3*SDC(I,1,3)-
     *3*SDC(I,3,1)-2*SDC(I,3,3)/BT)+S(W(I,1),W(I,4))
      S(W(I,1),W(I,5))= WT/12*(4*SDC(I,1,3)*BT+3*SDC(I,3,3))+
     *S(W(I,1),W(I,5))
      S(W(I,1),W(I,6))= WT/12*(2*SDC(I,1,3)*BT+3*SDC(I,3,3))+
     *S(W(I,1),W(I,6))
      S(W(I,1),W(I,7))= WT/12*(-4*SDC(I,1,3)*BT-3*SDC(I,3,3))+
     *S(W(I,1),W(I,7))
      S(W(I,1),W(I,8))= WT/12*(-2*SDC(I,1,3)*BT-3*SDC(I,3,3))+
     *S(W(I,1),W(I,8))
      S(W(I,2),W(I,1))=WT/12*(2*SDC(I,1,1)*BT+3*SDC(I,1,3)-
     *3*SDC(I,3,1)-4*SDC(I,3,3)/BT)+S(W(I,2),W(I,1))
      S(W(I,2),W(I,2))= WT/12*(4*SDC(I,1,1)*BT-3*SDC(I,1,3)-
     *3*SDC(I,3,1)+4*SDC(I,3,3)/BT)+S(W(I,2),W(I,2))
      S(W(I,2),W(I,3))= WT/12*(-2*SDC(I,1,1)*BT+3*SDC(I,1,3)+
     *3*SDC(I,3,1)-2*SDC(I,3,3)/BT)+S(W(I,2),W(I,3))
      S(W(I,2),W(I,4))= WT/12*(-4*SDC(I,1,1)*BT-3*SDC(I,1,3)+
     *3*SDC(I,3,1)+2*SDC(I,3,3)/BT)+S(W(I,2),W(I,4))
      S(W(I,2),W(I,5))= WT/12*(2*SDC(I,1,3)*BT-3*SDC(I,3,3))+
     *S(W(I,2),W(I,5))
      S(W(I,2),W(I,6))= WT/12*(4*SDC(I,1,3)*BT-3*SDC(I,3,3))+
     *S(W(I,2),W(I,6))
      S(W(I,2),W(I,7))= WT/12*(-2*SDC(I,1,3)*BT+3*SDC(I,3,3))+
     *S(W(I,2),W(I,7))
      S(W(I,2),W(I,8))= WT/12*(-4*SDC(I,1,3)*BT+3*SDC(I,3,3))+
     *S(W(I,2),W(I,8))
      S(W(I,3),W(I,1))=WT/12*(-4*SDC(I,1,1)*BT-3*SDC(I,1,3)+
     *3*SDC(I,3,1)+2*SDC(I,3,3)/BT)+S(W(I,3),W(I,1))
      S(W(I,3),W(I,2))= WT/12*(-2*SDC(I,1,1)*BT+3*SDC(I,1,3)+
     *3*SDC(I,3,1)-2*SDC(I,3,3)/BT)+S(W(I,3),W(I,2))
      S(W(I,3),W(I,3))= WT/12*(4*SDC(I,1,1)*BT-3*SDC(I,1,3)-
```

```
*3*SDC(I,3,1)+4*SDC(I,3,3)/BT)+S(W(I,3),W(I,3))
 S(W(I,3),W(I,4))= WT/12*(2*SDC(I,1,1)*BT+3*SDC(I,1,3)-
*3*SDC(I,3,1)-4*SDC(I,3,3)/BT)+S(W(I,3),W(I,4))
 S(W(I,3),W(I,5))= WT/12*(-4*SDC(I,1,3)*BT+3*SDC(I,3,3))+
*S(W(I,3),W(I,5))
 S(W(I,3),W(I,6))= WT/12*(-2*SDC(I,1,3)*BT+3*SDC(I,3,3))+
*S(W(I,3),W(I,6))
 S(W(I,3),W(I,7))= WT/12*(4*SDC(I,1,3)*BT-3*SDC(I,3,3))+
*S(W(I,3),W(I,7))
 S(W(I,3),W(I,8))= WT/12*(2*SDC(I,1,3)*BT-3*SDC(I,3,3))+
*S(W(I,3),W(I,8))
 S(W(I,4),W(I,1))=WT/12*(-2*SDC(I,1,1)*BT-3*SDC(I,1,3)-
*3*SDC(I,3,1)-2*SDC(I,3,3)/BT)+S(W(I,4),W(I,1))
 S(W(I,4),W(I,2))= WT/12*(-4*SDC(I,1,1)*BT+3*SDC(I,1,3)-
*3*SDC(I,3,1)+2*SDC(I,3,3)/BT)+S(W(I,4),W(I,2))
 S(W(I,4),W(I,3))= WT/12*(2*SDC(I,1,1)*BT-3*SDC(I,1,3)+
*3*SDC(I,3,1)-4*SDC(I,3,3)/BT)+S(W(I,4),W(I,3))
 S(W(I,4),W(I,4))= WT/12*(4*SDC(I,1,1)*BT+3*SDC(I,1,3)+
*3*SDC(I,3,1)+4*SDC(I,3,3)/BT)+S(W(I,4),W(I,4))
 S(W(I,4),W(I,5))= WT/12*(-2*SDC(I,1,3)*BT-3*SDC(I,3,3))+
*S(W(I,4),W(I,5))
 S(W(I,4),W(I,6))= WT/12*(-4*SDC(I,1,3)*BT-3*SDC(I,3,3))+
*S(W(I,4),W(I,6))
 S(W(I,4),W(I,7))= WT/12*(2*SDC(I,1,3)*BT+3*SDC(I,3,3))+
*S(W(I,4),W(I,7))
 S(W(I,4),W(I,8))= WT/12*(4*SDC(I,1,3)*BT+3*SDC(I,3,3))+
*S(W(I,4),W(I,8))
 S(W(I,5),W(I,1))=WT/12*(4*SDC(I,3,1)*BT+3*SDC(I,3,3))+
*S(W(I,5),W(I,1))
 S(W(I,5),W(I,2))=WT/12*(2*SDC(I,3,1)*BT-3*SDC(I,3,3))+
*S(W(I,5),W(I,2))
 S(W(I,5),W(I,3))=WT/12*(-4*SDC(I,3,1)*BT+3*SDC(I,3,3))+
*S(W(I,5),W(I,3))
 S(W(I,5),W(I,4))=WT/12*(-2*SDC(I,3,1)*BT-3*SDC(I,3,3))+
*S(W(I,5),W(I,4))
 S(W(I,5),W(I,5))=WT/12*(4*SDC(I,3,3)*BT)+S(W(I,5),W(I,5))
 S(W(I,5),W(I,6))=WT/12*(2*SDC(I,3,3)*BT)+S(W(I,5),W(I,6))
 S(W(I,5),W(I,7))=WT/12*(-4*SDC(I,3,3)*BT)+S(W(I,5),W(I,7))
 S(W(I,5),W(I,8))=WT/12*(-2*SDC(I,3,3)*BT)+S(W(I,5),W(I,8))
 S(W(I,6),W(I,1))=WT/12*(2*SDC(I,3,1)*BT+3*SDC(I,3,3))+
*S(W(I,6),W(I,1))
 S(W(I,6),W(I,2))=WT/12*(4*SDC(I,3,1)*BT-3*SDC(I,3,3))+
*S(W(I,6),W(I,2))
 S(W(I,6),W(I,3))=WT/12*(-2*SDC(I,3,1)*BT+3*SDC(I,3,3))+
*S(W(I,6),W(I,3))
 S(W(I,6),W(I,4))=WT/12*(-4*SDC(I,3,1)*BT-3*SDC(I,3,3))+
*S(W(I,6),W(I,4))
 S(W(I,6),W(I,5))=WT/12*(2*SDC(I,3,3)*BT)+S(W(I,6),W(I,5))
 S(W(I,6),W(I,6))=WT/12*(4*SDC(I,3,3)*BT)+S(W(I,6),W(I,6))
```

```
S(W(I,6),W(I,7))=WT/12*(-2*SDC(I,3,3)*BT)+S(W(I,6),W(I,7))
S(W(I,6),W(I,8))=WT/12*(-4*SDC(I,3,3)*BT)+S(W(I,6),W(I,8))
S(W(I,7),W(I,1))=WT/12*(-4*SDC(I,3,1)*BT-3*SDC(I,3,3))+
*S(W(I,7),W(I,1))
S(W(I,7),W(I,2))=WT/12*(-2*SDC(I,3,1)*BT+3*SDC(I,3,3))+
*S(W(I,7),W(I,2))
S(W(I,7),W(I,3))=WT/12*(4*SDC(I,3,1)*BT-3*SDC(I,3,3))+
*S(W(I,7),W(I,3))
S(W(I,7),W(I,4))=WT/12*(2*SDC(I,3,1)*BT+3*SDC(I,3,3))+
*S(W(I,7),W(I,4))
S(W(I,7),W(I,5))=WT/12*(-4*SDC(I,3,3)*BT)+S(W(I,7),W(I,5))
S(W(I,7),W(I,6))=WT/12*(-2*SDC(I,3,3)*BT)+S(W(I,7),W(I,6))
S(W(I,7),W(I,7))=WT/12*(4*SDC(I,3,3)*BT)+S(W(I,7),W(I,7))
S(W(I,7),W(I,8))=WT/12*(2*SDC(I,3,3)*BT)+S(W(I,7),W(I,8))
S(W(I,8),W(I,1))=WT/12*(-2*SDC(I,3,1)*BT-3*SDC(I,3,3))+
*S(W(I,8),W(I,1))
S(W(I,8),W(I,2))=WT/12*(-4*SDC(I,3,1)*BT+3*SDC(I,3,3))+
*S(W(I,8),W(I,2))
S(W(I,8),W(I,3))=WT/12*(2*SDC(I,3,1)*BT-3*SDC(I,3,3))+
*S(W(I,8),W(I,3))
S(W(I,8),W(I,4))=WT/12*(4*SDC(I,3,1)*BT+3*SDC(I,3,3))+
*S(W(I,8),W(I,4))
S(W(I,8),W(I,5))=WT/12*(-2*SDC(I,3,3)*BT)+S(W(I,8),W(I,5))
S(W(I,8),W(I,6))=WT/12*(-4*SDC(I,3,3)*BT)+S(W(I,8),W(I,6))
S(W(I,8),W(I,7))=WT/12*(2*SDC(I,3,3)*BT)+S(W(I,8),W(I,7))
S(W(I,8),W(I,8))=WT/12*(4*SDC(I,3,3)*BT)+S(W(I,8),W(I,8))
DO 146  J=1,4
IF (J.EQ.1) THEN
KSI=1.0
ITA=1.0
 ELSEIF (J.EQ.2) THEN
 KSI=1.0
 ITA=-1.0
  ELSEIF (J.EQ.3) THEN
  KSI=-1.0
  ITA=1.0
   ELSE
   KSI=-1.0
   ITA=-1.0
ENDIF
WDG(I,J,1,1)=(SDC(I,1,1)*B1*(1+ITA)+SDC(I,1,3)*A1*(1+KSI))/
*(4*A1*B1)+WDG(I,J,1,1)
WDG(I,J,1,2)=(SDC(I,1,1)*B1*(1-ITA)-SDC(I,1,3)*A1*(1+KSI))/
*(4*A1*B1)+WDG(I,J,1,2)
WDG(I,J,1,3)=(-SDC(I,1,1)*B1*(1+ITA)+SDC(I,1,3)*A1*(1-KSI))/
*(4*A1*B1)+WDG(I,J,1,3)
WDG(I,J,1,4)=(-SDC(I,1,1)*B1*(1-ITA)-SDC(I,1,3)*A1*(1-KSI))/
*(4*A1*B1)+WDG(I,J,1,4)
WDG(I,J,1,5)=(SDC(I,1,3)*B1*(1+ITA))/(4*A1*B1)+WDG(I,J,1,5)
```

```
      WDG(I,J,1,6)=(SDC(I,1,3)*B1*(1-ITA))/(4*A1*B1)+WDG(I,J,1,6)
      WDG(I,J,1,7)=(-SDC(I,1,3)*B1*(1+ITA))/(4*A1*B1)+WDG(I,J,1,7)
      WDG(I,J,1,8)=(-SDC(I,1,3)*B1*(1-ITA))/(4*A1*B1)+WDG(I,J,1,8)
      WDG(I,J,2,1)=0.0+WDG(I,J,2,1)
      WDG(I,J,2,2)=0.0+WDG(I,J,2,2)
      WDG(I,J,2,3)=0.0+WDG(I,J,2,3)
      WDG(I,J,2,4)=0.0+WDG(I,J,2,4)
      WDG(I,J,2,5)=0.0+WDG(I,J,2,5)
      WDG(I,J,2,6)=0.0+WDG(I,J,2,6)
      WDG(I,J,2,7)=0.0+WDG(I,J,2,7)
      WDG(I,J,2,8)=0.0+WDG(I,J,2,8)
      WDG(I,J,3,1)=(SDC(I,3,1)*B1*(1+ITA)+SDC(I,3,3)*A1*(1+KSI))/
     *(4*A1*B1)+WDG(I,J,3,1)
      WDG(I,J,3,2)=(SDC(I,3,1)*B1*(1-ITA)-SDC(I,3,3)*A1*(1+KSI))/
     *(4*A1*B1)+WDG(I,J,3,2)
      WDG(I,J,3,3)=(-SDC(I,3,1)*B1*(1+ITA)+SDC(I,3,3)*A1*(1-KSI))/
     *(4*A1*B1)+WDG(I,J,3,3)
      WDG(I,J,3,4)=(-SDC(I,3,1)*B1*(1-ITA)-SDC(I,3,3)*A1*(1-KSI))/
     *(4*A1*B1)+WDG(I,J,3,4)
      WDG(I,J,3,5)=(SDC(I,3,3)*B1*(1+ITA))/(4*A1*B1)+WDG(I,J,3,5)
      WDG(I,J,3,6)=(SDC(I,3,3)*B1*(1-ITA))/(4*A1*B1)+WDG(I,J,3,6)
      WDG(I,J,3,7)=(-SDC(I,3,3)*B1*(1+ITA))/(4*A1*B1)+WDG(I,J,3,7)
      WDG(I,J,3,8)=(-SDC(I,3,3)*B1*(1-ITA))/(4*A1*B1)+WDG(I,J,3,8)
      IF (SCHECK(I).EQ.2) GO TO 150
      WSB(I,J,1,1)=B1*(1+ITA)/(4*A1*B1)+WSB(I,J,1,1)
      WSB(I,J,1,2)=B1*(1-ITA)/(4*A1*B1)+WSB(I,J,1,2)
      WSB(I,J,1,3)=-B1*(1+ITA)/(4*A1*B1)+WSB(I,J,1,3)
      WSB(I,J,1,4)=-B1*(1-ITA)/(4*A1*B1)+WSB(I,J,1,4)
      WSB(I,J,1,5)=0.0+WSB(I,J,1,5)
      WSB(I,J,1,6)=0.0+WSB(I,J,1,6)
      WSB(I,J,1,7)=0.0+WSB(I,J,1,7)
      WSB(I,J,1,8)=0.0+WSB(I,J,1,8)
      WSB(I,J,2,1)=0.0+WSB(I,J,2,1)
      WSB(I,J,2,2)=0.0+WSB(I,J,2,2)
      WSB(I,J,2,3)=0.0+WSB(I,J,2,3)
      WSB(I,J,2,4)=0.0+WSB(I,J,2,4)
      WSB(I,J,2,5)=A1*(1+KSI)/(4*A1*B1)+WSB(I,J,2,5)
      WSB(I,J,2,6)=-A1*(1+KSI)/(4*A1*B1)+WSB(I,J,2,6)
      WSB(I,J,2,7)=A1*(1-KSI)/(4*A1*B1)+WSB(I,J,2,7)
      WSB(I,J,2,8)=-A1*(1-KSI)/(4*A1*B1)+WSB(I,J,2,8)
      WSB(I,J,3,1)=A1*(1+KSI)/(4*A1*B1)+WSB(I,J,3,1)
      WSB(I,J,3,2)=-A1*(1+KSI)/(4*A1*B1)+WSB(I,J,3,2)
      WSB(I,J,3,3)=A1*(1-KSI)/(4*A1*B1)+WSB(I,J,3,3)
      WSB(I,J,3,4)=-A1*(1-KSI)/(4*A1*B1)+WSB(I,J,3,4)
      WSB(I,J,3,5)=B1*(1+ITA)/(4*A1*B1)+WSB(I,J,3,5)
      WSB(I,J,3,6)=B1*(1-ITA)/(4*A1*B1)+WSB(I,J,3,6)
      WSB(I,J,3,7)=-B1*(1+ITA)/(4*A1*B1)+WSB(I,J,3,7)
      WSB(I,J,3,8)=-B1*(1-ITA)/(4*A1*B1)+WSB(I,J,3,8)
146 CONTINUE
```

```
      KK=I+WNCE
      K1=WNCE+WNSTE
      IF (KK.GT.K1) GO TO 142
      SST(WST(KK,1),WST(KK,1))=(AREA*EO)/LENGTH
      SST(WST(KK,1),WST(KK,2))=-(AREA*EO)/LENGTH
      SST(WST(KK,2),WST(KK,1))=-(AREA*EO)/LENGTH
      SST(WST(KK,2),WST(KK,2))=(AREA*EO)/LENGTH
  142 L=I+WNCE+WNSTE
      IF (L.GT.WNE) GO TO 150
      SSLIP(L)=SDISPL(WSP(L,1))-SDISPL(WSP(L,2))
      IF (ABS(SSLIP(L)).LE.0.00667) THEN
      SSP(WSP(L,1),WSP(L,1))=0.3*3.1416*DIABAR*NOBAR*LENGTH
      ELSEIF (ABS(SSLIP(L)).LE.0.03) THEN
      SSP(WSP(L,1),WSP(L,1))=0.128*3.1416*DIABAR*NOBAR*LENGTH
      ELSEIF (ABS(SSLIP(L)).LE.0.1) THEN
      SSP(WSP(L,1),WSP(L,1))=0.001*3.1416*DIABAR*NOBAR*LENGTH
      ELSE
      WRITE(*,*)'BOND FAILED IN THE ELEMENT',L
      SSP(WSP(L,1),WSP(L,1))=0.0
      ENDIF
      SSP(WSP(L,1),WSP(L,2))=0.0
      SSP(WSP(L,2),WSP(L,1))=0.0
      SSP(WSP(L,2),WSP(L,2))=1000000
  150 DO 11 J=1,WGS
        DO 12 K=1,WGS
          SK(J,K)=SK(J,K)+S(J,K)+SSP(J,K)+SST(J,K)
          S(J,K)=0.0
          SSP(J,K)=0.0
          SST(J,K)=0.0
   12   CONTINUE
   11 CONTINUE
      I=I+1
      IF (I.LE.WNCE) GO TO 200
      RETURN
      END
      SUBROUTINE
      SOLVE(DK,DDG,DGS,DNH,DCEVAP,DREY,D2,DDISPL,DBK,DVK)
      DIMENSION DK(80,80),DDG(80,80)
      DIMENSION D2(80),DDISPL(80),DBK(80),DVK(80)
      DIMENSION DHK(80,80)
      INTEGER DGS,DNH,DCEVAP,DREY
      DO 10 I=DNH+1,DGS
        DO 20 J=DNH+1,DGS
          DHK(I-DNH,J-DNH)=DK(I,J)
   20   CONTINUE
   10 CONTINUE
      IF (DCEVAP.EQ.0) DREY=DREY+1
      IF (DCEVAP.GE.1) GO TO 30
   11 WRITE(*,*)'ENTER NDOF NUMBER AND LOAD INCREMENT
```

```
  READ(*,*)I,DBK(I)
  WRITE(*,*)'ENTER 1 FOR MORE NODAL FORCE OR 0 NO MORE'
  READ(*,*)NUMG
  IF (NUMG.EQ.1) GO TO 11
30 DO 50 I=1,DGS
    DO 60 J=1,DGS
      DDG(I,J)=0.0
60   CONTINUE
50 CONTINUE
  DO 70 I=DNH+1,DGS
    DDG(I-DNH,1)=DBK(I)
70 CONTINUE
  IJK=DGS-DNH
  CALL GAUSS(DHK,IJK,IJK,DDG,IJK,1)
  DO 80 I=1,DGS-DNH
    DDISPL(I+DNH)=DDG(I,1)+DDISPL(I+DNH)
    D2(I+DNH)=DDG(I,1)
80 CONTINUE
  TUY=0.0
  DO 55 I=1,DNH
      DDISPL(I)=0.0
55 CONTINUE
  DO 90 I=1,DGS
    DO 95 J=1,DGS
      TUY=TUY+DK(I,J)*D2(J)
95   CONTINUE
    DVK(I)=TUY
    TUY=0.0
90 CONTINUE
  RETURN
  END
  SUBROUTINE VALUES(RGS,RNCE,RD,RDG,RSB,RF,RUZ,RSTRE1,RSTRA1,
 *RSTRESS,RSTRAIN,RALFA,RSIGMA1,RSIGMA2,RG,RCHECK)
  DIMENSION RD(80)
  DIMENSION RDG(50,4,3,8),RSB(50,4,3,8)
  DIMENSION RF(50,4,3),RUZ(50,4,3),RSTRE1(50,4,3),RSTRA1(50,4,3)
  DIMENSION RSTRESS(50,4,3),RSTRAIN(50,4,3),RALFA(50,4)
  DIMENSION RSIGMA1(50,4),RSIGMA2(50,4)
  INTEGER RG(50,8)
  INTEGER RCHECK(50)
  INTEGER RGS,RNCE
  RS1=0.0
  PI=22/7
  RS2=0.0
  DO 10 J=1,RNCE
    DO 20 L=1,4
      DO 25 I=1,3
        DO 30 K=1,8
          RS1=RS1+RDG(J,L,I,K)*RD(RG(J,K))
```

```
        RS2=RS2+RSB(J,L,I,K)*RD(RG(J,K))
30     CONTINUE
       RF(J,L,I)=RS1
       RUZ(J,L,I)=RS2
       RS1=0.0
       RS2=0.0
25    CONTINUE
20  CONTINUE
10 CONTINUE
  DO 40 I=1,RNCE
  DO 45 J=1,4
  CO=COS(-RALFA(I,J)*PI/180)
  SI=SIN(-RALFA(I,J)*PI/180)
  RSTRE1(I,J,1)=CO**2*RF(I,J,1)+SI**2*RF(I,J,2)+2*CO*SI*RF(I,J,3)
  RSTRE1(I,J,2)=SI**2*RF(I,J,1)+CO**2*RF(I,J,2)-2*CO*SI*RF(I,J,3)
  RSTRE1(I,J,3)=-CO*SI*RF(I,J,1)+CO*SI*RF(I,J,2)+(CO**2-SI**2)*
 *RF(I,J,3)
  RSTRA1(I,J,1)=CO**2*RUZ(I,J,1)+SI**2*RUZ(I,J,2)+CO*SI*RUZ(I,J,3)
  RSTRA1(I,J,2)=SI**2*RUZ(I,J,1)+CO**2*RUZ(I,J,2)-CO*SI*RUZ(I,J,3)
  RSTRA1(I,J,3)=-2*CO*SI*RUZ(I,J,1)+2*CO*SI*RUZ(I,J,2)+
 *(CO**2-SI**2)*(RUZ(I,J,3))
45 CONTINUE
40 CONTINUE
  DO 50 I=1,RNCE
    DO 55  L=1,4
     DO 60 J=1,3
       RSTRESS(I,L,J)=RSTRESS(I,L,J)+RSTRE1(I,L,J)
       RSTRAIN(I,L,J)=RSTRAIN(I,L,J)+RSTRA1(I,L,J)
60    CONTINUE
55   CONTINUE
50 CONTINUE
  DO 70 I=1,RNCE
  DO 75 K=1,4
   T1=((RSTRESS(I,K,1)-RSTRESS(I,K,2))/2)**2
   T2=(RSTRESS(I,K,3)**2)
   TX=SQRT(T1+T2)
   RSIGMA1(I,K)=(RSTRESS(I,K,1)+RSTRESS(I,K,2))/2+TX
   RSIGMA2(I,K)=(RSTRESS(I,K,1)+RSTRESS(I,K,2))/2-TX
   IF (RCHECK(I).EQ.1) GO TO 70
   IF (RSTRESS(I,K,1).EQ.RSTRESS(I,K,2)) RALFA(I,K)=90
   IF (RSTRESS(I,K,1).EQ.RSTRESS(I,K,2)) GO TO 70
   RALFA(I,K)=ATAN(2*RSTRESS(I,K,3)/(RSTRESS(I,K,1)-RSTRESS(I,K,2)))
   RALFA(I,K)=-RALFA(I,K)*180/PI
  WRITE(4,*)RSTRESS(I,1,1),RSTRESS(I,1,2),RSTRESS(I,1,3),ALFA(I,1)
  WRITE(4,*)RSTRESS(I,2,1),RSTRESS(I,2,2),RSTRESS(I,2,3),ALFA(I,2)
  WRITE(4,*)RSTRESS(I,3,1),RSTRESS(I,3,2),RSTRESS(I,3,3),ALFA(I,3)
  WRITE(4,*)RSTRESS(I,4,1),RSTRESS(I,4,2),RSTRESS(I,4,3),ALFA(I,4)
75 CONTINUE
70 CONTINUE
```

```
      RETURN
      END
      SUBROUTINE CRACK(CCHECK,CNCE,CFC,CDC,CEPSNN,CEPSTT,
     *CGAMANT,CAL)
      DIMENSION CEPSNN(50),CEPSTT(50),CGAMANT(50)
      DIMENSION D21CR(50),D22CR(50),CD21CR(50),CD22CR(50)
      DIMENSION CDC(50,3,3),CT(3,3),CARP(3,3),CAL(50)
      INTEGER CCHECK(50)
      INTEGER CNCE
      REAL L,H1,H2,H3,H4
      SMEAR=50
      TOP=0.25*CFC
      DMAX=19
      A1=2.45/TOP
      A2=2.44*(1-4/TOP)
      DO 10 I=1,CNCE
      IF (CCHECK(I).EQ.2) GO TO 10
      DELTAN=CEPSNN(I)*SMEAR
      IF (DELTAN.LT.0.0) GO TO 10
      DELTAT=CGAMANT(I)*SMEAR*2
      IF (DELTAN.LE.0.0) PRINT,'NEGATIVE OPENING'
      IF (DELTAN.LT.(0.05)) CCHECK(I)=2
      IF (DELTAN.LT.(0.05)) GO TO 10
      L=DELTAT/DELTAN
      G1=TOP*(1-SQRT(2*DELTAN/DMAX))
      G2=L
      G3=A1+A2*L*L*ABS(L)
      G4=1+A2*L*L*L*L
      FT=G1*G2*G3/G4
      H1=-0.62*L
      H2=FT
      H3=SQRT(DELTAN)
      H4=SQRT(SQRT(1+L*L))
      FN=H1*H2*H3/H4
      DSET=(4*A2*L*L*L*L)/DELTAN/(1+A2*L*L*L*L)
      PRINT,'SIGMANN  SIGMANT',FN,FT
      PRINT,'DELTAT  DELTAN',DELTAT,DELTAN
      CDC(I,3,3)=FT*(1./DELTAT+3*A2*L*L/ABS(DELTAN)/(A1+A2*L*L*
     *ABS(L))-4*A2*L*L*L/DELTAN/(1+A2*L*L*L*L))
      CDC(I,3,1)=FT*(-1./SQRT(2.*DELTAN*DMAX)*(1.-2.*DELTAN/DMAX)-1./
     *DELTAN-3*A2*ABS(L*L*L)/DELTAN/(A1+A2*ABS(L*L*L))+DSET)
      CDC(I,1,3)=FN*(1/DELTAT+CDC(I,3,3)/FT-0.5*DELTAT/(DELTAN**2)/
     *(1+L*L))
      CDC(I,1,1)=FN*(-1/DELTAN+CDC(I,3,1)/FT+0.5/SQRT(DELTAN)+
     *0.5*L*L/DELTAN/(1+L*L))
   10 CONTINUE
      RETURN
      END
      SUBROUTINE NEWTON(TYOK,TGS,TSKEEP,TVK,TDISPL,TBK,TD,TK)
```

```
  DIMENSION TSKEEP(80),TVK(80),TDISPL(80),TBK(80),TD(80)
  DIMENSION TK(80,80)
  DIMENSION TSK(80)
  INTEGER TYOK,TGS
  DO 6 I=1,80
    TSK(I)=0.0
 6 CONTINUE
  IF (TYOK.GT.1) GO TO 21
  DO 20 I=1,TGS
    TSKEEP(I)=TSKEEP(I)+TVK(I)
20 CONTINUE
21 SUY=0.0
  DO 50 I=1,TGS
    DO 60 J=1,TGS
     SUY=SUY+TK(I,J)*TDISPL(J)
60   CONTINUE
    TSK(I)=SUY
    SUY=0.0
50 CONTINUE
  DO 88 I=1,TGS
    TBK(I)=TSKEEP(I)-TSK(I)
88 CONTINUE
  RETURN
  END
  SUBROUTINE GAUSS(UA,N,NP,UB,M,MP)
  DIMENSION UA(80,80),UB(80,80),IPIV(80),INDXR(80),INDXC(80)
  DO 11 J=1,N
    IPIV(J)=0
11 CONTINUE
  DO 22 I=1,N
    BIG=0.0
    DO 13 J=1,N
      IF (IPIV(J).NE.1) THEN
        DO 12 K=1,N
          IF (IPIV(K).EQ.0) THEN
            IF (ABS(UA(J,K)).GE.BIG) THEN
              BIG=ABS(UA(J,K))
              IROW=J
              ICOL=K
            ENDIF
          ELSE IF (IPIV(K).GT.1) THEN
            PAUSE 'SINGULAR MATRIX'
          ENDIF
12        CONTINUE
      ENDIF
13   CONTINUE
  IPIV(ICOL)=IPIV(ICOL)+1
  IF (IROW.NE.ICOL) THEN
    DO 14 L=1,N
```

```
      DUM=UA(IROW,L)
      UA(IROW,L)=UA(ICOL,L)
      UA(ICOL,L)=DUM
14   CONTINUE
     DO 15 L=1,M
      DUM=UB(IROW,L)
      UB(IROW,L)=UB(ICOL,L)
      UB(ICOL,L)=DUM
15   CONTINUE
  ENDIF
  INDXR(I)=IROW
  INDXC(I)=ICOL
  IF (UA(ICOL,ICOL).EQ.0.0) PAUSE 'SINGULAR MATRIX'
  PIVINV=1/UA(ICOL,ICOL)
  UA(ICOL,ICOL)=1.0
  DO 16 L=1,N
    UA(ICOL,L)=UA(ICOL,L)*PIVINV
16 CONTINUE
  DO 17 L=1,M
    UB(ICOL,L)=UB(ICOL,L)*PIVINV
17 CONTINUE
  DO 21 LL=1,N
    IF (LL.NE.ICOL) THEN
      DUM=UA(LL,ICOL)
      UA(LL,ICOL)=0.0
      DO 18 L=1,N
        UA(LL,L)=UA(LL,L)-UA(ICOL,L)*DUM
18     CONTINUE
      DO 19 L=1,M
        UB(LL,L)=UB(LL,L)-UB(ICOL,L)*DUM
19     CONTINUE
    ENDIF
21 CONTINUE
22 CONTINUE
  DO 24 L=N,1,-1
    IF (INDXR(L).NE.INDXC(L)) THEN
      DO 23 K=1,N
        DUM=UA(K,INDXR(L))
        UA(K,INDXR(L))=UA(K,INDXC(L))
        UA(K,INDXC(L))=DUM
23     CONTINUE
    ENDIF
24 CONTINUE
  RETURN
  END
  FUNCTION YVXO(V1,V2,VFC,MI)
  DIMENSION V1(50),V2(50)
  YVXO=0.2+0.6*((V2(MI)/VFC)**2)**2+0.4*((V1(MI)/(1-0.8*V2(MI)*
 *0.1))**2)**2
```

```
RETURN
END
```

REFERENCES

1. Kupfer, H. B. and Gerstle, K. H., "Behavior of Concrete Under Biaxial Stresses, " *Journal of the Engineering Mechanics Division* , ASCE, Vol.99, No. em4, Proc. paper 9917, pp.852-866, August 1973.

2. Darwin, D. and Pecknold, D.A. , " Nonlinear Biaxial Stress-Strain Law for Concrete," *Journal of the Engineering Mechanics Division* , ASCE, Vol. 103, No. EM2, Proc. paper 12839, pp. 229-240, April 1977.

3. Cedolin, L. , Crutzen, R. J. and Dei Poli, S., " Triaxial Stress-Strain Relationship for Concrete", *Journal of the Engineering Mechanics Division*, ASCE, Vol.103, No.EM3, pp 423-439, 1977.

4. Fardis, M.N. and Büyüköztürk, O.," Shear Transfer Model for Reinforced Concrete," *Journal of the Engineering Mechanics Division*, ASCE, Vol.105, No.EM2, April 1979

5. Bazant, Z.P. and Gambarova, P.G.," Rough Cracks in Reinforced Concrete," *Journal of the Structural Engineering* ASCE, Vol.106, No ST4, Proc. paper 15330, pp.819-842, April 1980.

6. Gambarova, P.G. and Karakoç, C.,"A New Approach to the Analysis of the Confinement Role in Regularly Cracked Concrete Elements,"*Transactions 7th SMIRT Conference*, Vol. H, Paper H5/7, Chicago, pp. 251-261, August 1983.

7. Walraven, J.C., "Fundamental Analysis of Aggregate Interlock,"*Journal of the Structural Engineering*, ASCE, Vol. 107, No. 11, pp 2245-2271, November 1981.

8. Paulay, T. and Loeber, P.J., "Shear in Reinforcement Concrete, Shear in Reinforced Concrete, *Special Publications. SP-42* , ACI, Vol.1, Detroit, 1974.

9. Daschner, F., "Schubkraftubertragung in Rissen von Normal und Lichtbeton, *Bericht Erstattet, Institut fur Bauingenieurwesen, Lehrstuhl fur Massivbau*, Technische Universitat München, München, 1980.

10. Ngo, D. and Scordelis, A.C., "Finite Element Analysis of Reinforced Concrete Beams," *Journal of A.C.I.*, Vol. 64, No. 3, pp. 152-163, March 1967.

11. Cervenka, V., " Inelastic Finite Element Analysis of Reinforced Concrete Panels," Ph. D. dissertation, University of Colorado, Dep.of Civil Engineering, Boulder.

12. Valliopan, S. and Doolan, T.F., "Nonlinear Analysis of Reinforced Concrete," *Journal of Structural Division* , ASCE, Vol. 100, No. ST5, pp.885-897, April 1972.

13. Yüzügüllü, O., " Finite Element Approach for the Prediction of Inelastic Behavior of Shear Wall-Frame Systems,"Ph. D. dissertation, University of Illinois at Urbana-Champaign, Dep. of Civil Engineering, 1972.

14. Cedolin, L. and Dei Poli, S., " Finite Element Studies of Shear Critical R/C Beams," *Journal of the Engineering Mechanics Division*, ASCE, Vol.103, No.EM3, Proc.paper 12968, pp.395-410, June 1977.

15. Hognestad, E., " A Study of Combined bending and axial load in reinforced concrete members," *Bulletin No. 399 Engineering Experiment Station*, University of Illinois, Urbana, Illinois, Vol. 49, No. 22, November 1951.

16. Saenz, I., " Discussion of Equation for the Stress-Strain Curve of Concrete," Desai and Krishnan, *Proceedings of American*

Concrete Institute, Vol. 61, No.9, pp. 1229-1235, September 1964.

17. Gambarova, P.G. and Di Prisco, M.,"Interface Behavior" *Bulletin d'Information No. 210, Contribution to the 28th Plenary Session of CEB*, CEB-GTG 22, September 1991.

18. Daschner, F. and Kupfer, H., "Versuche zur Schubkraft-ubertragung in Rissen von Normal and Leichtbeton, B*auingenieur*, No. 57, pp. 51-55, 1983.

19. Karakoç, C., "On Aggregate Interlock ," *Bulletin of Technical University of Istanbul*,Vol.40, pp.705-722, 1987.

20. Karakoç, C., "Shear Transfer in Plain Concrete : tests for specimens for the constant crack width case," To be published.

21. Feenstra, P.H., " Numerical Simulation and Stability Analysis of Crack Dilatancy Models," *TNO Institute for Building Materials and Structures-Computational Mechanics, Project No. TNO 7241000*, Delft University of Technology, 1989.

22. Walraven, J.C. and Keuser, W., " The shear retention factor as a compromise between numerical simplicity and realistic material behavior," *Darmstadt Concrete, Annual Journal on Concrete and Concrete Structures*, Vol.2, pp. 221-234, 1987.

23. Millard, S.G. and Johnson R.P., " Shear tranfer across cracks in reinforced concrete due to aggregate interlock and dowel action, *Magazine of Concrete Research*, Vol.36, No.126, pp.9-21, 1984.

24. Nissen, I., " Rissverzahnung des betons - Gegenseitige Rissuferverschiebungen undubertragene Krafte,"Ph. D. Thesis, Technical University of Munchen,1987.

25. Tezcan, S.S., " Finite Element Method," Lecture Notes, Department of Civil Engineering, Bogaziçi University.

26. Bangash, M.Y.H., *Concrete and Concrete Structures : Numerical Modelling and Applications*, London: Elsevier Applied Science, 1989.

27. Dei Poli, S., Gambarova, P. G. and Karakoç, C., "Aggregate Interlock Role in R/C Thin Webbed Beams in Shear," *Journal of the Structural Engineering*, ASCE Vol.113, No.1,Proc. Paper 21139, pp.1-19, Jan. 1987.

28. Köksal, O., " Nonlinear Finite Element Analysis of Reinforced Concrete Structures, " M.S. Thesis , Bogaziçi University, 1992.

29. Niyogi, S.K., " Concrete Bearing Strength - Support, Mix, Size, Effect, " *Journal of the Structural Division,* ASCE, Vol. 100, No. ST8, Proc. paper 10765, pp. 1685-1702, August 1974.